INSTITUTO SUPERIOR DE ENGENHARIA DO PORTO
MESTRADO EM ENGENHARIA QUÍMICA

DESENVOLVIMENTO DE UMA TECNOLOGIA HÍBRIDA DE REMEDIAÇÃO PARA A REMOÇÃO DE PFAS DE MATRIZES AQUÁTICAS

ANA SOFIA DA CUNHA PINTO
Julho de 2023

POLITÉCNICO
DO PORTO

DEVELOPMENT OF A HYBRID REMEDIATION TECHNOLOGY FOR THE REMOVAL OF PFAS FROM AQUATIC MATRICES

Ana Sofia da Cunha Pinto

External supervisor

PhD Maria Fátima Carvalho (researcher at CIIMAR)

PhD Diogo Alexandrino (researcher at CIIMAR)

Internal supervisor

Professor Olga Matos de Freitas (ISEP)

Professor Valentina Fernandes Domingues (ISEP)

Julho 2023

Dissertation Submitted as partial requirement for obtaining the degree of Master's in Chemical Engineering, area of specialization Energy and Biorefinery

Acknowledgments

Words can never express my deep gratitude to my family. Thank you for being my rock and support in all circumstances, for instilling in me the best values and teaching me the true meaning of what love is. Thank you for always played a key role in teaching me to be the best version of myself every day. I love you all more than words can say.

To the sisters that life has given me, Sarinha, Nena and Cat, the sincerest thank you! Little do you know what your support, the belly-pounding laughter, the moments we created, and your affection did for me. Thank you for all the doors that never closed when I needed your lap and advice the most over so many years. Your love and support mean more to me than you can ever imagine.

To João, thank you for all the love, respect, and care, for making my dreams yours too. Thank you for all the encouragement in difficult moments and for every bottle opened to celebrate the smallest success. To you, for always being the one in the front row cheering and for being the best friend and boyfriend.

To Nuh, Rafa and Aninha, thank you for never making distance an obstacle, for hundreds of miles not shaking this bond. Thank you for being present on one more stage and making it so special. For being the reason to love Lisbon.

To Xavi, Mari and Rafa, thank you! The smallest detail did not go unnoticed on this path. Thank you for making this journey so beautiful, for showing me every day that I was ready for this challenge. Thank you for always having the right words at the right moments.

Finally, I must thank my dear ISEP and CIIMAR for welcoming me in this stage of my path and showing me that I am on the right track. I also thank all the material and space made available allowing me to do this work. To my supervisors Diogo, Fátima and to engineers Valentina and Olga thanks for all the support. Thanks to the rest of my colleagues at ECOBIOTEC, this small laboratory with such a big heart. This research was conducted in the scope of the project Xenohybrid, funded by Fundação Amélia da Silva de Mello. This work was also supported by the Strategic Funding UIDB/04423/2020 and UIDP/04423/2020, through national funds provided by Fundação para a Ciência e Tecnologia and European Regional Development Fund.

And thank you to those who, unfortunately, will never be able to read this thesis.

Resumo

Atualmente, muitas substâncias são uma ameaça e ecológica e para a saúde humana. Entre estes poluentes há uma preocupação relativamente aos PFAS devido à sua persistência e bioacumulação. Os PFAS, são utilizados em muitos produtos de consumo e têm sido encontrados em ecossistemas aquáticos. Uma vez que estes ecossistemas são um habitat para uma variedade de criaturas e um abastecimento de água potável para o Homem, isto representa um problema ecológico substancial.

Este estudo teve como objetivo desenvolver uma tecnologia de remediação híbrida para a remoção de PFAS de matrizes aquáticas utilizando nanofotocatálise e biorremediação. Foram testadas várias estirpes quanto à sua capacidade de degradar compostos fluorados, a fim de criar um consórcio com um potencial para degradar os PFAS resultantes do tratamento por nanofotocatálise. A estirpe COL5 apresentou uma defluorinação completa do fluoroacetato de sódio, tal como a estirpe F11, mas para o composto fluorobenzeno, ambos a uma concentração de 50 mgL^{-1}. A estirpe 3EE foi capaz de defluorinar 17% do composto epoxiconazole a 5 mgL^{-1} e a estirpe DPS8 desflorou 20% da paroxetina a 1 mgL^{-1}. Tentou-se avaliar a biocompatibilidade entre as estirpes que apresentaram os melhores desempenhos de defluorinação, mas, devido à contaminação, não foi possível concluir. A nanofotocatálise foi realizada com nanopartículas de TiO_2 e ZnO a uma concentração de 1 gL^{-1}. Esses ensaios foram realizados em uma solução de água desionizada contendo ácido perfluorohexanóico e noutra solução com trifloxistrobina, ambas na concentração de 1 mgL^{-1}. Verificou-se, por potenciometria, que o tratamento com nanopartículas de ZnO levou à defluorinação de 27% da trifloxistrobina em 6 horas. Por outro lado, o tratamento do ácido perfluorohexanóico e da trifloxistrobina (1 mgL^{-1}) pelo consórcio sintético não resultou em biodegradação. Finalmente, quando a tecnologia foi testada em conjunto, o consórcio sintético foi capaz de defluorinar uma pequena percentagem de trifloxistrobina (4,7%).

Em conclusão, embora tenham sido encontradas estirpes capazes de degradar compostos fluorados, não foram capazes de defluorinar PFAS quando incluídos num consórcio sintético. A nanofotocatálise por nanopartículas de ZnO, por outro lado, mostrou um potencial de degradação da trifloxistrobina. Ao juntar estas duas tecnologias, obteve-se uma percentagem de defluorinação de cerca de 30%.

Palavras-chave: Ambiente aquático, Poluição, PFAS, consórcio, Nanofotocatálise, Biodegradação.

Abstract

Today, many substances pose a serious threat to human and ecological health. Due to their persistence, bioaccumulation, and possible negative consequences, PFAS have emerged as particularly worrying among these pollutants. PFAS, have been widely found in aquatic ecosystems. Since these ecosystems are an essential habitat for a wide variety of creatures and a crucial supply of drinking water for human societies, this poses a substantial ecological problem.

This study aimed to develop a hybrid remediation technology for the removal of PFAS from aquatic matrices using nanophotocatalysis and bioremediation. Several strains were tested for their capabilities of degrading fluorinated compounds to create a consortium with potential do degrade PFAS resultant from the nanophotocatalysis treatment. Strain COL5 showed complete defluorination of sodium fluoroacetate, as did strain F11 but for the compound fluorobenzene, both at a concentration of 50 mgL^{-1}. Strain 3EE was able to defluorinate 17% of the compound epoxiconazole at 5 mgL^{-1}, and strain DPS8 defluorinated 20% of paroxetine at 1 mgL^{-1}. Biocompatibility between the strains showing the best defluorination performances was studied, but due to contamination, it was not possible to verify compatibility between them. The nanophotocatalysis experiments were performed with TiO_2 and ZnO nanoparticles at a concentration of 1 gL^{-1}. These assays were performed in deionized water containing perfluorohexanoic acid or trifloxystrobin, both at a concentration of 10 and 1 mgL^{-1}. It was verified by potentiometry, that the treatment with ZnO nanoparticles led to the defluorination of 27% of trifloxystrobin in 6 hours. On the other hand, treatment of perfluorohexanoic acid and trifloxystrobin (1 mgL^{-1}) by the synthetic consortium resulted in no biodegradation. Finally, when the technology was tested together, the synthetic consortium was capable of defluorinating a small percentage of trifloxystrobin (4.7%).

In conclusion, although strains capable of degrading fluorinated compounds were found, they were not able to degrade PFAS when included in a synthetic consortium. Nano-photocatalysis by ZnO nanoparticles, on the other hand, showed a potential degradation of trifloxystrobin. By combining these two technologies, a defluorination percentage of about 30% was obtained.

Keywords: Aquatic environment, Pollution, PFAS, consortium, Nanophotocatalysis, Biodegradation.

Contents

Chapter 1 - Introduction 1
1.1. Context 1
1.2. Motivations 7
1.3. CIIMAR 7
1.4. Organization of the Dissertation 8

Chapter 2 – State of art 11
2.1. The new and traditional PFAS definition, properties, and compounds in study . 11
2.1.1. Perfluorohexanoic acid 14
2.1.2. Trifloxystrobin 15
2.2. Environmental dynamics of PFAS 15
2.3. Ecotoxicity of PFAS 18
2.4. European and national regulations of PFAS 19
2.4.1. European Union's Water Framework Directive 20
2.4.2. PFAS under Registration Evaluation Authorization and Restriction of Chemicals (REACH) 21
2.4.2. Portugal regulation 22
2.5. PFAS remediation technologies 23
2.5.1. Separation techniques for PFAS contaminated water 23
2.5.2. Removal techniques for PFAS contaminated water 26
2.6. Main goals 27

Chapter 3 – Materials and Methods 29
3.1. Framework of adopted methodologies 29
3.1.1. Pre-Selection of the bacterial strains for the assembly of a degrading consortium 29
3.1.2. Assessment of the catabolic viability of the pre-selected bacterial strains ... 29
3.1.3. Biocompatibility assays 31
3.1.4. Assembly of a degrading bacterial consortium and evaluation of its efficiency 32
3.1.5. Nanophotocatalytic assays 33
3.1.6. Biodegradation of trifloxystrobin or perfluorohexanoic acid spiked water treated by nanophotocatalysis 33
3.2. Analytical methods 34

Chapter 4 – Results and Discussion 37

4.1. Selection of prospective bacterial strains for the construction of a degrading consortium 37
Sodium fluoroacetate 37
Fluorobenzene 39
Paroxetine 40
Epoxiconazole 42
4.2. Analysis of species compatibilities 43
4.3. Technology Deployment 44
4.3.1. Nanophotocatalysis treatment 44
4.3.2. Bioremediation treatment 45
4.3.3. Implementation of hybrid technology 47

Chapter 5 – Conclusion and Suggestions for Future Work 49

Bibliographic References 51

Appendices 67
A. Liquid and solid culture media preparation 67
B. Assessment of the catabolic viability of the pre-selected bacterial strains 68
B.1. Sodium Fluoroacetate 68
B.2. Fluorobenzene 75
B.3. Paroxetine 81
B.4. Epoxiconazole 86
C. Hybrid technology deployment 89
C.1. Nanotechnology treatment 89
C.2. Bioremediation treatment 94
C.3. Implementation of hybrid technology 101

Illustration index

Figure 2.1: Examples of substances that are, and are not, PFAS based on the new definition [22]……..……13

Figure 2.2: Emission of and exposure to PFAS during their lifecycle. Adapted from [44]……...16

Figure 3.1: Procedure performed for the inoculation of the strains used throughout the work…….29

Figure 3.2: Procedure for the realization of assays of viability……..……..31

Figure 3.3: Procedure for the realization of biocompatibility assay……..……32

Figure 3.4: Synthetic bacterial consortium building procedure……..…..32

Figure 4.1: Results of sodium fluoroacetate biodegradation by the several bacterial strains tested in this study. Results are the average of duplicate samples and standard deviation is represented. The % of defluorination is represented by the bars and OD measurement is represented by the line…….…….38

Figure 4.2: Results of fluorobenzene biodegradation by the several bacterial strains tested in this study. Results are the average of duplicate samples and standard deviation is represented. The % of defluorination is represented by the bars and OD measurement is represented by the line……..39

Figure 4.3: Results of paroxetine biodegradation by the several bacterial strains tested in this study. Results are the average of duplicate samples and standard deviation is represented. The % of defluorination is represented by the bars and OD measurement is represented by the line……..……41

Figure 4.4: Results of epoxiconazole biodegradation by the several bacterial strains tested in this study. Results are the average of duplicate samples and standard deviation is represented. The % of defluorination is represented by the bars and OD measurement is represented by the line……..42

Figure 4.5: Efficiency of the constructed consortium to degrade the compounds perfluorohexanoic acid and trifloxystrobin. The % of defluorination is represented by the bars and OD measurement is represented by the line……..45

Figure 4.6: Biodegradation of the tenfold-diluted effluent containing trifloxystrobin (theoretical concentration of 1 mgL^{-1}), after the photocatalytic treatment with ZnO nanoparticles. The % of defluorination is represented by the bars and OD measurement is represented by the datapoints……..……...……..47

Figure B.1: Calibration curve obtain using the values in Table B.1 and the corresponding straight-line equation……..……68

Figure B.2: Calibration curve obtained using the values in Table B.5 and the corresponding straight-line equation……..……..72

Figure B.3: Calibration curve obtained using the values in Table B.9 and the corresponding straight-line equation……..……76

Figure B.4: Calibration curve obtained using the values in Table B.13 and the corresponding straight-line equation……..……..78

Figure B.5: Calibration curve obtained using the values in Table B.16 and the corresponding straight-line equation……..……..82

Figure B.6: Calibration curve obtained using the values in Table B.20 and the corresponding straight-line equation……86

Figure C.1: Calibration curve obtained using the values in Table C.1 and the corresponding straight-line equation……90

Figure C.2: Calibration curve obtained using the values in Table C.8 and the corresponding straight-line equation……..……..95

Figure C.3: Calibration curve obtained using the values in Table C.19 and the corresponding straight-line equation……..101

Figure C.4: Calibration curve obtained using the values in Table C.19 and the corresponding straight-line equation…….……..……105

Table index

Table 3.1: Species used throughout the study, the used culture media, environmental source, and tested degraded compound……...….28

Table 4.1: Data obtained from fluoride potentiometry for the analysis of the degradation capability of nanophotocatalysis technology…….…..44

Table A.1: Nutrient composition of the culture media used to grow the preselected strains…….……..67

Table B.1: Concentration values and potential difference of standards for the viability assay concerning the compound sodium fluoroacetate……...…….68

Tabela B.2: Potential difference of each strain and the values obtained in the calculation of free fluoride for the moment T0 of the first sodium fluoroacetate assay……..….69

Table B.3: Potential difference of each strain and the values obtained in the calculation of free fluoride for the moment T8 of the first sodium fluoroacetate assay……..…….70

Table B.4: Potential difference of each strain and the values obtained in the calculation of free fluoride for the moment T14 of the first sodium fluoroacetate assay…….....71

Table B.5. Concentration values and potential difference of standards for the second viability assay concerning the compound sodium fluoroacetate……...71

Table B.6: Potential difference of each strain and the values obtained in the calculation of free fluoride for the moment T0 of the second sodium fluoroacetate assay……..72

Table B.7: Potential difference of each strain and the values obtained in the calculation of free fluoride for the moment T8 of the second sodium fluoroacetate assay……..73

Table B.8: Potential difference of each strain and the values obtained in the calculation of free fluoride for the moment T15 of the second sodium fluoroacetate assay……....73

Table B.9: OD values after 8 and 14 days, the average of these values and the associated standard deviation for the sodium fluoroacetate assay…….……74

Table B.10: % of defluorination values after 8 and 14 days, the average of these values and the associated standard deviation for the sodium fluoroacetate assay……...….75

Table B.11: Concentration values and potential difference of standards for the first viability assay concerning the compound fluorobenzene…….……75

Table B.12: Potential difference of each strain and the values obtained in the calculation of free fluoride for the moment T0 of the first fluorobenzene assay…….76

Table B.13: Potential difference of each strain and the values obtained in the calculation of free fluoride for the moment T8 of the first fluorobenzene assay…….77

Table B.14: Potential difference of each strain and the values obtained in the calculation of free fluoride for the moment T14 of the first fluorobenzene assay…….……..78

Table B.15: Concentration values and potential difference of standards for the second viability assay concerning the compound fluorobenzene……78

Table B.16: Potential difference of each strain and the values obtained in the calculation of free fluoride for the moment T0 of the second fluorobenzene assay……..…..79

Table B.17: Potential difference of each strain and the values obtained in the calculation of free fluoride for the moment T8 of the second fluorobenzene assay…….……79

Table B.18: Potential difference of each strain and the values obtained in the calculation of free fluoride for the moment T14 of the second fluorobenzene assay……...…80

Table B.19: OD values after 8 and 14 days, the average of these values and the associated standard deviation for the fluorobenzene assay……....80

Table B.20: % of defluorination values after 8 and 14 days, the average of these values and the associated standard deviation for the fluorobenzene assay…….…..81

Table B.21: Concentration values and potential difference of standards for the viability assay concerning the compound paroxetine. ……..…….81

Table B.22: Potential difference of each strain and the values obtained in the calculation of free fluoride for the moment T0 of the paroxetine assay…….……..82

Table B.23: Potential difference of each strain and the values obtained in the calculation of free fluoride for the moment T8 of the paroxetine assay……..….83

Table B.24: Potential difference of each strain and the values obtained in the calculation of free fluoride for the moment T21 of the paroxetine assay…….……84

Table B.25: OD values after 8 and 21 days, the average of these values and the associated standard deviation for the paroxetine assay…….……85

Table B.26: % of defluorination values after 8 and 21 days, the average of these values and the associated standard deviation for the paroxetine assay…….85

Table B.27: Concentration values and potential difference of standards for the viability assay concerning the compound epoxiconazole……..…….86

Table B.28: Potential difference of each strain and the values obtained in the calculation of free fluoride for the moment T0 of the epoxiconazole assay……87

Table B.29: Potential difference of each strain and the values obtained in the calculation of free fluoride for the moment T14 of the epoxiconazole assay……..87

Table B.30: Potential difference of each strain and the values obtained in the calculation of free fluoride for the moment T21 of the epoxiconazole assay……..…88

Table B.31: OD values after 14 and 21 days, the average of these values and the associated standard deviation for the epoxiconazole assay……...….89

Table B.32: % of defluorination values after 14 and 21 days, the average of these values and the associated standard deviation for the epoxiconazole assay…….……89

Table C.1: Concentration values and potential difference of standards for the relative to the nanophotocatalytic treatment……...……..90

Table C.2: Potential difference and the values obtained in the calculation of free fluoride at the beginning of the assay and 6 hours later for the ZnO nanoparticle in the control samples……....91

Table C.3: Potential difference, values obtained in the calculation of free fluoride and % defluorination at the beginning of the test and 6 hours later by the ZnO nanoparticle on the perfluorohexanoic acid compound…….……91

Table C.4: Potential difference, values obtained in the calculation of free fluoride and % defluorination at the beginning of the test and 6 hours later by the ZnO nanoparticle on the trifloxystrobin compound……..……92

Table C.5: Potential difference and the values obtained in the calculation of free fluoride at the beginning of the assay and 6 hours later for the TiO_2 nanoparticle in the control samples……93

Table C.6: Potential difference, values obtained in the calculation of free fluoride and % defluorination at the beginning of the test and 6 hours later by the TiO_2 nanoparticle on the perfluorohexanoic acid compound…….93

Table C.7: Potential difference, values obtained in the calculation of free fluoride and % defluorination at the beginning of the test and 6 hours later by the TiO_2 nanoparticle on the trifloxystrobin compound……...……94

Table C.8: Concentration values and potential difference of standards for the relative to the bioremediation treatment……95

Table C.9: Potential difference for each replicate and the values obtained in the calculation of free fluoride for the time of trial start (T0) in the bioremediation trial for the perfluorohexanoic acid compound…….96

Table C.10: Potential difference for each replicate and the values obtained in the calculation of free fluoride, and % defluorination for the time (T7) in the bioremediation trial for the perfluorohexanoic acid compound…….96

Table C.11: Potential difference for each replicate and the values obtained in the calculation of free fluoride, and % defluorination for the time (T14) in the bioremediation trial for the perfluorohexanoic acid compound…….……97

Table C.12: Potential difference for each replicate and the values obtained in the calculation of free fluoride, and % defluorination for the time (T20) in the bioremediation trial for the perfluorohexanoic acid compound…….97

Table C.13: OD values after 7, 14 and 20 days, the average of these values and the associated standard deviation for the bioremediation assay for the perfluorohexanoic acid compound……..……..97

Table C.14: % of defluorination values after 7, 14 and 20 days, the average of these values and the associated standard deviation for the bioremediation assay for the perfluorohexanoic acid compound……...……98

Table C.15: Potential difference for each replicate and the values obtained in the calculation of free fluoride for the time of trial start (T0) in the bioremediation trial for the trifloxystrobin compound……..…….98

Table C.16: Potential difference for each replicate and the values obtained in the calculation of free fluoride, and % defluorination for the time (T7) in the bioremediation trial for the trifloxystrobin compound……..……99

Table C.17: Potential difference for each replicate and the values obtained in the calculation of free fluoride, and % defluorination for the time (T14) in the bioremediation trial for the trifloxystrobin compound……..……..100

Table C.18: Potential difference for each replicate and the values obtained in the calculation of free fluoride, and % defluorination for the time (T20) in the bioremediation trial for the trifloxystrobin compound……..……..100

Table C.19: OD values after 7, 14 and 20 the average of these values and the associated standard deviation for the hybrid technology assay for the trifloxystrobin compound..100

Table C.20: % of defluorination values after 7, 14 and 20 the average of these values and the associated standard deviation for the hybrid technology assay for the trifloxystrobin compound……..100

Table C.21: Concentration values and potential difference of standards for the relative to the hybrid technology……...……..101

Table C.22: Potential difference for each replicate and the values obtained in the calculation of free fluoride for the time of test start (T0) in the hybrid assay……..……102

Table C.23: Potential difference for each replicate and the values obtained in the calculation of free fluoride, and % of defluorination for the time (T7) in the hybrid assay……...……102

Table C.24: Potential difference for each replicate and the values obtained in the calculation of free fluoride, and % of defluorination for the time (T14) in the hybrid assay…….……..103

Table C.25: Potential difference for each replicate and the values obtained in the calculation of free fluoride, and % of defluorination for the time (T20) in the hybrid assay…….……..103

Table C.26: OD values after 7, 14 and 20 days, the average of these values and the associated standard deviation for the hybrid assay……..……..104

Table C.27: % of defluorination values after 7, 14 and 20 days, the average of these values and the associated standard deviation for the hybrid assay……..……104

Table C.28: Concentration values and potential difference of the standards compared to the assay to check for biological degradation and resistance of the consortium in the water samples…….……104

Table C.29: Potential difference for each replicate of each assay (consortium resistance and non-biological degradation) and the values obtained in the calculation of free fluoride for the moment of the beginning of the assay (T0)…….……105

Table C.30: Potential difference for each replicate of each assay (consortium resistance and non-biological degradation), the values obtained in the calculation of free fluoride and % of fluorination for the moment (T8)……...……..106

Table C.31: Potential difference for each replicate of each assay (consortium resistance and non-biological degradation), the values obtained in the calculation of free fluoride and % of fluorination for the moment (T14)……..……107

Table C.32: Potential difference for each replicate of each assay (consortium resistance and non-biological degradation), the values obtained in the calculation of free fluoride and % of fluorination for the moment (T21)…….……..107

Table C.33: OD values for the assay of consortium resistance and non-biological degradation after 8, 14 and 21 days……...….107

Abbreviations List

AC Activated Carbon

AFFF Aqueous Film Forming Foam

AOP Advanced Oxidation Process

ARP Advanced Reduction Process

CE Circular economy

CIIMAR Interdisciplinary Centre of Marine Environmental Research

EP Emerging Pollutants

EPO Epoxiconazole

EQSD Environmental Quality Standards Directive

GAC Granular Activated Carbon

GWD Groundwater Directive

HFPO-DA Hexafluoropropylene Oxide Dimer Acid

IPPC Pollution Prevention and Control

ISE Ion Selective Electrode

IXR Ion Exchange Resin

NB Nutrient Broth

NF Nanofiltration

OC Organochlorine

OECD Organization for Economic Co-operation and Development

PBDE Polybrominated Diphenyl Ether

PCA Plate Count Agar

PCB Polychlorinated Biphenyls

PFAAS Perfluoroalkyl Acids

PFAS Per- and Polyfluoroalkyl Substances

PFC Perfluorinated Compounds

PFCA Perfluoroalkyl Carboxylic Acids

PFHxS Perfluorohexane Sulfonic Acid

PFOA Perfluorooctanoic acid

PFOS Perfluorooctane Sulfonic Acid

PFSA Perfluoroalkane sulfonic

PLC Polymers of Low Concern

POP Persistent Organic Pollutants

R2A Reasoner's 2A

REACH Registration Evaluation Authorization and Restriction of Chemicals

RO Reverse Osmosis

SVHC Substances of Very High Concern

UN United Nations

WFD Water Framework Directive

WWTP Waste Water Treatment Plant

Chapter 1 - Introduction

This chapter presents the context of the study, the motivation, the institution where it was conducted, the objectives and the structure of the thesis.

1.1. Context

The introduction of harmful substances and products into the environment causes significant damage to living organisms and natural systems. Contamination and pollution are two terms commonly used to describe the presence of these substances in the environment and their adverse effects. However, it is important to distinguish between the two. According to the literature, pollution is a result of human activities that introduce substances or energy into the environment in ways that have detrimental effects. These effects can be immediate or long-term, and they can affect both the natural environment and human society. Pollution can take various forms, such as air pollution, water pollution, soil pollution, noise pollution, and many others. Contamination, on the other hand, is the outcome of pollution and represents the abnormal concentration of chemicals or contaminants in the environment. Contamination can occur as a result of various human activities, such as industrial processes, improper waste disposal, or accidental spills [1].

Environmental pollution is not a recent phenomenon, but it remains the greatest threat to human and environmental health [2]. Pollution can be caused by natural (earthquakes, floods, cyclones [3]) or human causes (population growth, nature of modern technology, industrial development, agricultural development, transportation, and the disposal of waste[3]) , and most pollution is due to human actions that cause the decline or degradation of the quality of the natural environment and can take many forms [2].

Population growth in urban areas requires a proportional increase in the exploitation of the resources necessary for the life of human beings, putting health, ecology, and human sustenance at risk. The unavoidable outcome of a counter-ecological pattern of productive expansion is the ecological crisis. The nature of modern technology leads to the production of synthetic and non-biodegradable substances, such as plastics, chemical fertilizers, chemical products and by-products, synthetic detergents, synthetic fibers, automobile, the petrochemical industries (and other environmentally damaging industries), and the “throwaway culture” (the act of discarding something after just one

single usage) [3]. The development of agriculture brought solutions to society's problems, but it has also brought problems. To solve the issue of the growing demand for food due to the increase in population, modern and advanced scientific techniques have developed, which include an increase in the production and use of chemical fertilizers, expansion of irrigation facilities, etc. However, the use of these solutions is creating dangerous environmental problems of serious concern. The conversion of forest land into agricultural holdings accelerates the rate of soil erosion due to the substantial increase in land productivity through intensive cultivation, increased use of machinery and modern scientific techniques, application of chemical fertilizers, pesticides (insecticides and herbicides and fungicides, some of them fluorinated aromatic compounds), increased frequency and irrigation area increase of agricultural fields. Industrialization produces a variety of unwelcome byproducts from industries in addition to the useful outputs, including industrial waste, polluted water, toxic fumes, precipitated chemicals, and aerosols, which have the potential to cause harm into the environment by polluting the air, water, land, and soil. The concentration of pollutants released by manufacturers into the air, water, and land has increased in industrialized nations to the point where the environment has been severely compromised, putting human society in significant danger [3].

For human health and wellbeing across the globe, access to clean drinking water is crucial [4]. Water pollution is a systematic problem in today's world, with our waters being flooded by two main types of pollution: chemicals and waste. Chemical pollution is alarming for health, environmental, and economic reasons. This type of pollution occurs due to human activities, such as the use of fertilizers in agricultural fields, leading to the runoff of chemicals into waterways and consequently ending up in the oceans [5]. An example of a consequence due to chemical contamination is the increased concentration of chemicals, such as nitrogen and phosphorus, on the ocean shore promoting the growth of algae blooms, which can be toxic to wildlife and harmful to humans. The negative health and environmental effects caused by algae blooms harm local fisheries and tourist industries [5].

Trash in the water encompasses some manufactured products most of them plastic. The most common types of plastic waste include shopping bags and beverage bottles, along with cigarette butts, bottle caps, food wrappers, and fishing gear. Plastic waste is

particularly problematic as a pollutant because it is so long-lasting and poses dangers to both humans and animals since animals can become entangled and injured in the debris, and mistake items like plastic bags for food. Small organisms feed on small pieces of broken plastic, called microplastics, and absorb the chemicals from the plastic into their tissues. These microplastics have already been detected in several marine species, including plankton and whales [5]. At the same time small organisms consume microplastics, these organisms serve as food for larger animals and the toxic chemicals consequently become part of their tissues. In this way, microplastic pollution migrates up the food chain in succession, eventually becoming part of the food that humans consume [5].

Regardless of the type of contaminants, anthropogenic contamination of water sources can lead to devastating consequences, which may include:

- Loss of biodiversity: As contaminants enter the water, they can harm or even kill aquatic life, such as fish, invertebrates, and other organisms. This loss of biodiversity can create an imbalance in the ecosystem, leading to a reduction in the food chain and an increase in certain types of species, such as algae or bacteria. This, in turn, can lead to the collapse of the entire ecosystem, impacting not only aquatic life but also the many animals that depend on it for their survival [6].
- Habitat destruction: Many aquatic species rely on specific water conditions, such as temperature and oxygen levels, to survive. When water pollution alters these conditions, it can lead to habitat loss and a decline in species populations. This can have a cascading effect, leading to the loss of entire ecosystems and the services they provide, such as flood protection, water purification, and nutrient cycling [6].
- Food insecurity: Food insecurity is a significant problem in many parts of the world, with an estimated 690 million people suffering from chronic hunger in 2019 [7]. Water pollution is one of the factors that contribute to food insecurity, particularly in low-income communities that rely on agriculture and fishing for their livelihoods. Water contamination and pollution can significantly interfere with food security, both in terms of the quantity and quality of food produced. Crops can uptake dangerous elements including heavy metals, pesticides, and industrial chemicals when irrigation water is polluted [8]. These pollutants may build up in plant tissues, which may have an impact on crop development, quality, and growth. On the other

hand, Aquaculture and fisheries, which are important for the supply of food for the world, can also be badly impacted by water pollution. Fish, shellfish, and other aquatic species are particularly sensitive to the quality of the water used for their rearing [7]. Fish yields can be decreased by pollution, and it can also damage fish health and potentially cause large-scale fish deaths. Fish tissues may get contaminated over time, rendering them unsafe for ingestion and harming local fishing economies.

- Economic costs: Nutrient pollution can have negative economic effects on organizations, tourism, and recreational fishing [9] The tourist sector loses close to a billion dollars annually as a result of water bodies that have been impacted by nutrient pollution and hazardous algal blooms, mostly via losses in fishing and boating activities [9].

The circular economy (CE) model presents an innovative chance for creative thinking and synergy among waste management, corporate reengineering, daily life, and society. The circular model of resources has to be established in a comprehensive way that is recognized globally. Our earth is being suffocated by materialism and throwaway goods while also being overworked [10]. To address the problem of ecosystem degradation due to water pollution, it is essential to reduce the number of contaminants entering our waterways. This can be done through better waste management practices, such as recycling, composting, and proper disposal of household waste. In addition, industries must adopt more sustainable practices, such as using less harmful chemicals and implementing treatment processes to remove contaminants from waste waters. Governments can also play a role by implementing regulations and providing incentives for businesses to adopt sustainable practices [6]. The prevention of waterborne diseases is essential, and it can be achieved through a range of measures, such as proper sanitation and hygiene practices, adequate wastewater treatment, and safe drinking water sources. Improved sanitation practices, such as building latrines and using proper handwashing techniques, can significantly reduce the spread of waterborne diseases. Additionally, wastewater treatment facilities can remove contaminants from wastewater, preventing them from entering water sources and spreading disease. Access to safe drinking water sources, such as treated tap water, can also help prevent the spread of waterborne diseases [8].

Aquatic ecosystems are affected by a variety of pollutants that can have a significant impact on water quality and the health of organisms inhabiting these environments. It is important to note that the presence of these pollutants can vary depending on the geographic location, the human activities present, and the specific characteristics of each aquatic ecosystem. Therefore, detailed analysis of local conditions is fundamental to identify priority pollutants and implement effective environmental management strategies. However, the pollutants most frequently found in aquatic ecosystems include:

- Inorganic nutrients: A natural component of aquatic ecosystems, nitrogen and phosphorus are nutrients that promote the growth of algae and aquatic plants, which in turn offer food and habitat for fish, shellfish, and other smaller aquatic species [11]. However, the advent of intense agricultural production techniques [12-13] has resulted in an overabundance of nitrogen and phosphorus in water supplies, which causes algae to develop more quickly than the ecosystems can support [11]. Enormous algal blooms have the potential to drastically restrict or completely remove oxygen from the water, which can lead to fish illnesses and the demise of enormous numbers of fish. The high levels of toxins and bacterial growth produced by some algal blooms can make people sick if they come in touch with polluted water, eat infected fish or shellfish, or drink contaminated water [11].
- Emerging pollutants (EPs): EPs are a group of chemicals that are of growing concern due to their presence in various water bodies at concentrations ranging from micrograms to milligrams per liter [14]. These pollutants can be either organic or inorganic in nature. Organic pollutants include pharmaceutical compounds, personal care substances, endocrine disruptors, hormones, and chemicals from industries, while inorganic pollutants mainly consist of heavy metals. The accumulation of EPs in wastewater is a global issue that has recently gained attention from policymakers and researchers due to the potential risks they pose to human health and the ecosystem [14]. EPs are receiving considerable attention for their treatment, as they have the potential to cause adverse effects on human health and the environment. The widespread occurrence of EPs has raised awareness about the associated human health and environmental concerns. Some of the risks posed by EPs include long-term environmental toxicity, endocrine disruption, increased antibiotic resistance, and their accumulation in the food chain. In certain cases, EPs have been released into the environment for extended periods without being detected until new

detection methods were introduced. Notable classes of EPs include metals, nano compounds, pesticides, pharmaceuticals, and cosmetic products [14].

- Legacy pollutants: Oil and other hazardous material spills harm the ecosystem and put both aquatic life and human activities at danger. These pollutants pose a risk of fire and explosion in addition to interfering with leisure activities on beaches and in waterways. During spills, businesses that use water for desalination or cooling may need to close. Normal vessel operations might have to be suspended for cleanup activities using booms and skimmers [15]. As little as one part per billion dissolved oils can be harmful to aquatic life. Spills may physically contaminate an area, suffocate it, build up, and taint it, all of which have long-lasting repercussions on the ecology. Oil slicks may suffocate and pollute the ecosystem as they drift and reach the shoreline [15]. For instance, oil might cause mangroves to have air-breathing roots that are obstructed. Additionally, oil has the ability to penetrate into sediments, polluting worms, and crab burrows, where it can linger for years and cause further harm to aquatic life. Waterbirds in particular are particularly susceptible to oil spills because their feathers become tarnished. Birds can become poisoned by eating prey that has been tainted with oil or by ingesting oil from their feathers [15].
- Persistent Organic Pollutants (POP's): Persistent organic pollutants are considered silent killers due to their bio-accumulative and long persistent nature. These are present everywhere in our environment including plants, animals, and human beings [16]. The sources of POPs are direct applications of pesticides in the environment, industrial wastes and by products of industrial processes [17] agriculture, forestry, horticulture, industries, municipal, medical activities [16]. Additionally, some natural sources such as volcanic activities and vegetation fires are also responsible for adding these pollutants into our ecosystem [17]. Persistent organic pollutants include polybrominated diphenyl ethers (PBDEs), per- and polyfluoroalkyl substances (PFAS), polychlorinated biphenyls (PCBs), and organochlorine (OC) pesticides [18]. These are responsible for various lethal diseases and environmental problems. The different diseases due to POPs are diabetes, obesity, endocrine disturbance, cancer, cardiovascular, reproductive, and environmental problems [16]. These have tendencies of bioaccumulation in living organisms with slow metabolism. That is why these pollutants exist for long time in our body [17]. The

scientists, Governments and NGOs are very much concerned with POPs pollution and hazards [16].

1.2. Motivations

This dissertation work addresses the topic of developing a hybrid remediation technology for the removal of PFAS from contaminated aquatic matrices. PFAS contamination is a global concern due to their wide distribution and persistence in the environment. The presence of these compounds in aquatic matrices, such as rivers, lakes, and aquifers, represents a significant challenge to public health and environmental management. The lack of effective and sustainable methods for removing PFAS from contaminated waters is a critical gap that needs to be addressed.

While there are remediation technologies available to treat PFAS contamination, many of them have limitations in terms of efficiency, cost, and environmental sustainability. This research will contribute to the academic field by developing and evaluating an innovative hybrid remediation technology that combines physical-chemical and biological treatment approaches to improve the effectiveness and cost-effectiveness of PFAS removal from aquatic matrices.

The technology proposed in this dissertation has the potential to provide an efficient, sustainable, and low-cost solution for PFAS removal, contributing to the remediation of contaminated waterways. Furthermore, the research can be applied in industrial and government sectors involved in contaminated water management.

1.3. CIIMAR

Interdisciplinary Centre of Marine and Environmental Research (CIIMAR) is a leading research and advanced training institution of the University of Porto that works at the frontier of Ocean Knowledge and Innovation located in Matosinhos. As a non-governmental and non-profit organization, CIIMAR is an R&D institution with individual and collective members from the University of Porto, Polytechnic of Porto, and private entities.

CIIMAR's mission is to promote transdisciplinary research, technological development, and training, contributing to advances in scientific knowledge and

sustainability of the marine and coastal environments. This institution promotes a joint approach to the oceans and coastal zones, leading to the understanding and knowledge of the biological, physical, and chemical dynamics of these environments and the impact of natural and human activities, with the aim of unraveling the links between these processes, as well as understanding the functioning of oceans, ecosystems, and responses to global change. CIIMAR fields of expertise cover three key research domains: Global Changes and Ecosystem Services, Aquaculture and Seafood Quality and Marine Biotechnology, addressing important economic and societal challenges and contributing to achieving United Nations (UN) Sustainable Development Goals.

CIIMAR promotes innovative solutions and products in response to current economic and social challenges. It includes new medicines, marine products for industrial and medicinal needs, preparedness and mitigation of oil spills and other Environmental pollution: causes, effects, and the remediation, environmental monitoring and risk assessment, preservation of ecosystem services, ocean and coastal management, and ocean literacy.

1.4. Organization of the Dissertation

The first chapter focuses on a brief introduction to some key concepts to the development of this work, as well as the presentation of the workplace and motivation.

Chapter 2 provides a comprehensive literature review of the state of the art on PFAS. It begins with an introduction, followed by an in-depth exploration of various aspects related to PFAS. The review covers the definition and characteristics of PFAS, their sources of contamination, environmental impacts, toxicity, regulatory frameworks, and remediation technologies available. This chapter aims to establish a solid foundation of knowledge on PFAS and identify any gaps in existing research.

Chapter 3 focuses on the methodologies employed in this dissertation. It starts with an introduction and then proceeds to explain the step-by-step procedures followed in the research. The methodologies covered include the pre-selection of bacterial strains for the assembly of a degrading consortium, the assessment of catabolic viability of the pre-selected bacterial strains, fluoride analysis, biocompatibility assays, assembly of a degrading bacterial consortium, and evaluation of its efficiency, as well as

nanophotocatalytic treatments. Each methodology is described in detail, providing clarity on the experimental procedures and techniques utilized.

In Chapter 4, the results obtained from the research are presented and discussed. This chapter begins with an introduction to provide context for the results. The obtained results are then presented for each methodology outlined in Chapter 2, such as the pre-selection of bacterial strains, assessment of catabolic viability, fluoride analysis, biocompatibility assays, assembly of a degrading bacterial consortium, evaluation of its efficiency, and nanophotocatalytic treatments. The results are thoroughly analyzed and discussed, highlighting any significant findings, trends, or patterns observed. This chapter serves to interpret the data and provide valuable insights into the research outcomes.

The fifth chapter focuses on drawing conclusions based on the findings presented in Chapter 3. It begins with a summary of the main results obtained and proceeds to derive meaningful conclusions from the research. Additionally, this chapter suggests potential future approaches or avenues for further investigation within the research topic. By doing so, it provides a platform for building upon the current study and offers suggestions for future research directions.

The bibliographic references mentions all the sources referenced throughout the thesis. It includes academic papers, books, reports, and any other relevant materials consulted during the research process.

The appendices section includes supplementary information that supports the main body of the thesis. It consists of various appendices labeled alphabetically. These appendices provide additional details, data, and resources that are essential for a thorough understanding of the research.

Chapter 2 – State of art

2.1. The new and traditional PFAS definition, properties, and compounds in study

PFAS where traditionally defined as a significant group of contaminants consisting of approximately 5000 human-made chemicals [19]. The traditional PFAS are composed of an aliphatic carbon backbone with hydrogen atoms replaced by fluorine, making them highly stable in the environment [20-21]. Although in 2021, the Organization for Economic Co-operation and Development (OECD) defined PFAS as fluorinated substances that contain at least one fully fluorinated methyl or methylene carbon atom (without any H/Cl/Br/I atom attached to it) [22]. This definition acknowledges the broad range of PFAS that exist and the potential risks that they pose to human health and the environment [22]. In 2018, unlike the traditional definition, OECD revised the classification of PFASs by include additional substances including side-chain aromatics [23].

The PFAS can be categorized into polymers and non-polymers [19]. Traditional non-polymer PFAS include perfluoroalkyl substances with fully fluorinated alkyl chains and polyfluoroalkyl substances with partly fluorinated alkyl chains containing at least one fluorine atom [24]. Perfluoroalkyl substances consist of various subgroups with a structure composed of a perfluoroalkyl chain tail containing multiple carbon-fluorine bonds and a charged functional group head [24]. This functional group is typically a carboxylic or sulfonic acid, although other forms are also observed. Perfluoroalkyl acids (PFAAS), a subgroup of PFAS, are the most commonly found compounds in the environment [25-26]. They are considered terminal PFAS as they do not naturally degrade further. Perfluoroalkyl carboxylic acids (PFCA) and perfluoroalkane sulfonic acids (PFSA) are the main types of PFAAs detected in various matrices. Polyfluoroalkyl substances, on the other hand, are non-polymer PFAS that are not fully fluorinated. They contain a carbon chain with at least one carbon atom attached to a non-fluorine atom, such as hydrogen or oxygen [25-26]. The non-fluorine bonds in polyfluoroalkyl substances are susceptible to degradation under environmental conditions, leading to the formation of fully fluorinated PFAA. Therefore, polyfluoroalkyl substances are considered precursors of PFAA [26-27].

PFAS polymers are large molecules formed by combining repeating units with carbon and fluorine bonds. These polymers can be fully or partially fluorinated and do not possess a functional group. PFAS polymers include fluoropolymers, polymeric perfluoropolyethers, and side-chain fluorinated polymers. Side-chain fluorinated polymers can degrade into fully fluorinated PFAS, making them precursors of PFAAs [26].

By updating the definition to include all organic molecules containing, at least, a perfluorinated moiety, the OECD aimed to provide more comprehensive guidance for the management and regulation of these substances, including recommendations for testing, assessment, and the identification and management of potential sources of exposure [22]. The revised definition was also developed with the aim of making it easy for experts and non-experts alike to distinguish between PFAS and non-PFAS. Figure .1 provides examples of substances that are and are not considered PFAS, and with the updated definition captures the diverse range of PFAS, which includes small molecules, complex aromatics with a perfluorinated methyl/methylene group on the side chain(s), and diverse polymers [22].

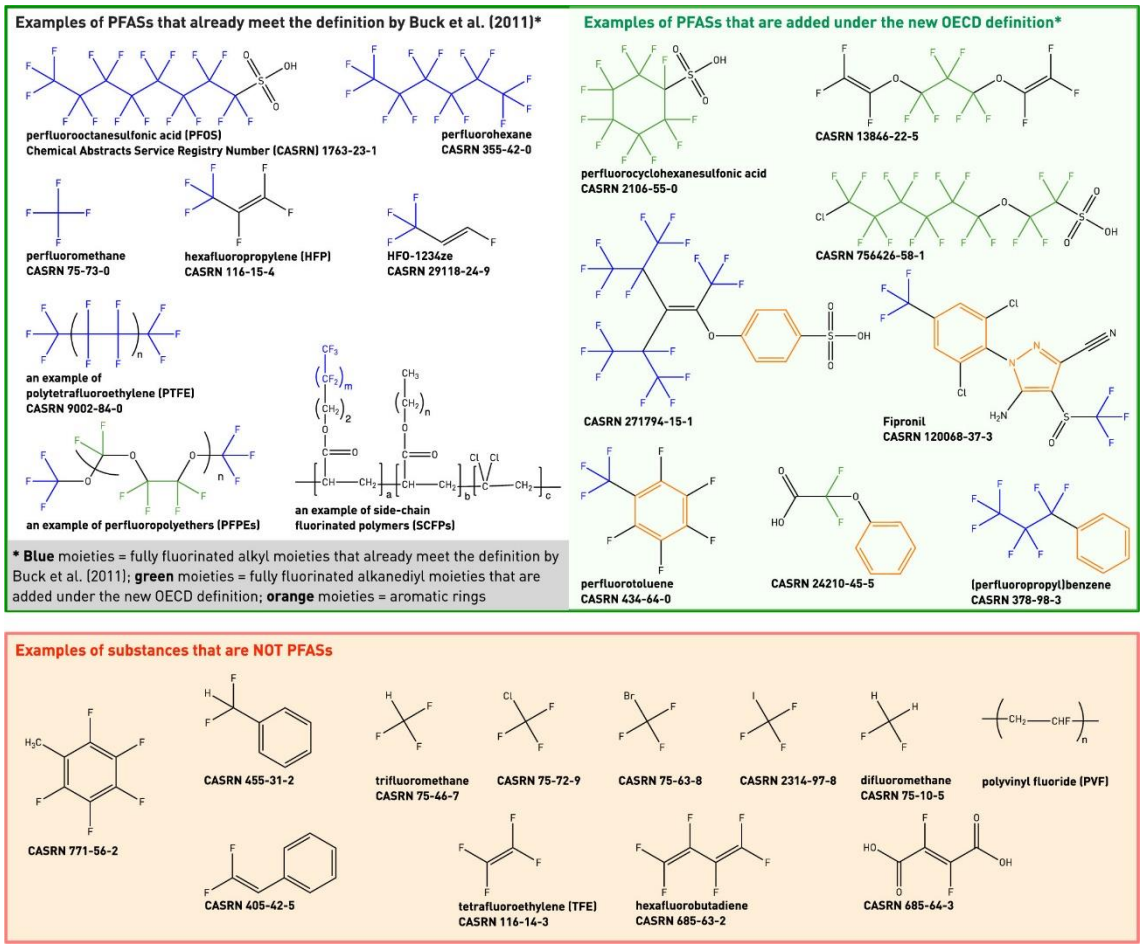

Figure 2.1: Examples of substances that are, and are not, PFAS based on the new definition [22].

PFAS have a wide range of different physical and chemical properties. Some PFAS may be found on solid form as a white powder or waxy substance, although some other can be found in liquid forms at room temperature depending on their chain length [26]. Physical and chemical characteristics of PFAS are influenced by their applications, compositions, and particular environmental behaviors [26][28].

Due to fluorine's high electronegativity and small atomic radius, PFAS form robust C-F bonds. The mean C – F dissociation energy for aromatic PFAS is significantly greater than that of aliphatic PFASs with a same number of carbons, and dissociation energy typically decreases as the length of the perfluoroalkyl chain rises [29]. Additionally, some PFAS have weak intermolecular interactions due to fluorine's low polarizability [26]. Longer chain PFAS, which are primarily present in soil particles and are more hydrophobic and attracted to organic materials [21] [30-31]. PFCA carry a charged functional group, which makes them more water soluble than their precursors [32]. Shorter PFCA may not be volatile, but longer PFAAs precursors are significantly more

volatile. The vapor pressure properties of PFAS change with the length of their carbon chain. Consequently, air stripping cannot get rid of PFAAS [33]. Due to their chemical and thermal stability as well as their resistance to biological deterioration, some PFAAS are referred to as "terminal" compounds. Because fluorine covers carbon, is tiny, and has a high electronegativity, PFAS have chemical and thermal stability that is dependent on the strength of C-F bonds [24]. These characteristics make PFAS resistant to the processes of oxidation, reduction, and hydrolysis [26]. Due to their distinct water and oil repellency, high surface activity, and thermostability, PFAS are useful compounds as surfactants in many industries, aqueous film forming foam (AFFF), alkaline cleaners, paints, and consumer products like non-stick cookware, carpets, food packaging, and shampoos [34-35].

Molecular fluorination appeal in agrochemicals, including aromatic PFAS, depends on its ability to precisely control their lipophilicity, stereochemical behavior, and in vivo stability. While keeping in mind the potency and range of the targeted biological activity, the adjustment of these traits produces a number of beneficial characteristics that are desired in a perfect pesticide, such as high selectivity and specificity, rapid action, and sustained residual activity [36].

2.1.1. Perfluorohexanoic acid

Since the 1970s, short chain perfluorocarboxylic acids (PFCA) have been employed in the fluorotechnology industry. Perfluorohexanoic acid (PFHxA), a six-carbon (C6) PFCA, an degradation product of short-chain fluorotelomer-based products such as side-chain fluorinated polymers and fluorosurfactants now available on the market. PFHxA are frequently detected in the environment, specifically in drinking water and foodstuffs [37]. Surface waters of the Ganges and groundwater in this region are used as sources of drinking water. Among the detected PFAS, PFHxA (0.4-4.7 ngL^{-1}) had one of the highest concentrations [38].

PFHxA has low acute toxicity based on animal bioassays; however, sub-chronic and chronic exposure studies in rodents have shown various sublethal effects. Developmental exposures in zebrafish have also revealed adverse effects. Limited epidemiological studies have been conducted on the health effects of PFHxA exposure, and they have been cross-sectional in nature [39]. Therefore, animal bioassays remain the primary source of information. Rodent studies, primarily involving oral gavage exposures

in adults, have reported no significant reproductive, developmental, or locomotor effects. However, mixed effects on body weight gain, serum chemistry, and target organ toxicity have been observed. While PFHxA appears to be less toxic than PFOS and PFOA, further assessment is needed to confidently establish its safety. Abnormal locomotor behavior has been observed in zebrafish exposed to PFHxA during development, indicating developmental toxicity. Sublethal effects and the sensitivity of juveniles to dietary exposure, behavior endpoints, and potential transgenerational effects require further investigation [39].

2.1.2. Trifloxystrobin

Trifloxystrobin (TFS) is a systemic broad-spectrum foliar fungicide widely used to control fungi in various agricultural settings such as greenhouses, nurseries, orchards, vegetable gardens, and paddy fields. It is synthesized from the natural antibiotic strobilurin and contains an oximether side chain [40].

TFS is valued for its rapid degradation in plants, soil, and water, as well as its long-lasting effects and resistance to rain, making it an important compound among strobilurins. However, the extensive use of TFS has raised significant concerns regarding public health and the potential non-target toxic effects on humans and wildlife resulting from the off-site transport of environmental residues. TFS has been frequently detected in aquatic systems, with concentrations reported at 0.73 μgL^{-1} in horticultural catchments of southeastern Australia and as high as 170 μgL^{-1} in Chinese paddy field water [40].

2.2. Environmental dynamics of PFAS

Both point and non-point sources have the potential to serve as sources of PFAS contamination into the environment [32] [41]. Industrial discharges, aqueous film forming foam usage sites, and pesticide applications are some examples of PFAS point sources of environmental contamination. Additionally, a number of designed facilities, such as landfills and wastewater treatment plants (WWTP), serve as important diffuse sources PFAS to the environment. Dry and wet air deposition, runoff from contaminated soils, leaking landfills, surface water runoff, and groundwater discharge from polluted sites are also examples of indirect sources of PFAS to the environment.

Surface water and soil have been found to be the first recipients of PFAS emissions. Industrial wastewater and atmospheric deposition to surface water are two ways that

PFAS discharge from industrial sources might later be discharged to water bodies. They can deposit into aquatic bodies, then run off into soil and terrestrial surfaces [41]. Due to their resistance to deterioration throughout the treatment process, PFAS that enter WWTPs can be discharged to surface water via effluent and sludge. Additionally, the usage of PFAS in agricultural locations, AFFF, and the transfer of WWTP biosolids to landfill sites might leak PFAS into the soil. Following their two primary sources, soil leaching and surface water seepage, PFAS can then reach groundwater [42-43]. Figure 1.1 demonstrates the emissions and exposure of PFAS during their lifecycle.

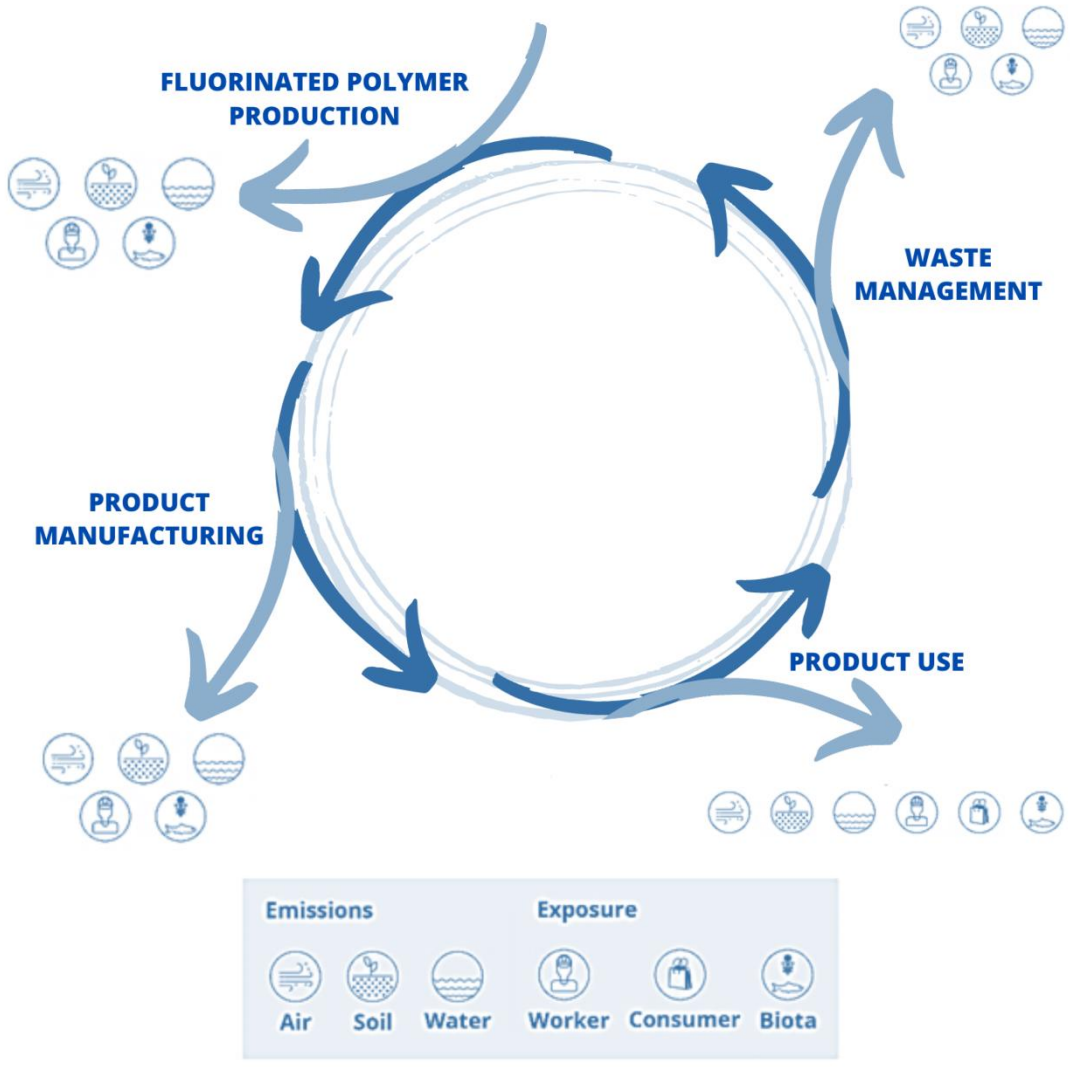

Figure 2.2: Emission of and exposure to PFAS during their lifecycle. Adapted from [44].

Accordingly, PFAS have been detected in various aquatic matrices such as surface water, wastewater, groundwater, air, soil, biota, and human blood and tissue [34] [45].

For instance, Perfluorooctanoic acid (PFOA), with concentrations ranging from 1 to >4500 ng/L, was the most prevalent PFAS component discovered in rivers receiving PFAS from fluoropolymer factories in China [46]. Surface water and sediment in the Laurentian Great Lakes contained PFAS, with varied quantities and dispersion across the lakes due to variations in PFAS sources [47].

Longer chain components were found in sediments, whereas short-chain PFAS including PFBS, PFBA, PFPeA, and PFHxA were widely present in landfill leachate in Norway [48]. Long-chain PFAS with concentrations ranging from 8.5 to 120 g/kg predominated in landfill sediments, including PFHxS, PFHpS, Perfluorooctane sulfonic acid (PFOS), PFDS, PFHpA, HPFHpA, PFOA, PFNA, PFDA, PFUnDA, PF-3,7-DMOA, PFDoA, PFTrA, and FhxDA. Long-chain PFAS concentrations in landfill leachate ranged from 5.9 to 130 g/year, whereas short-chain PFAS concentrations ranged from 68 to 6800 ng/L [48].

Surface snow and ice core samples have both included PFAS, with PFBA, PFOA, and PFNA being the most common. In contrast to surface snow samples, where shorter chains predominated, ice cores indicated higher quantities of longer-chain PFAS [49].

Additionally, PFAS have been found in numerous species, including invertebrates, fish, rats, reptiles, birds, and mammals. This evidence points to the bioaccumulation and biomagnification of these substances in the food chain [24] [50-51].

Aquatic environments have furthermore proven to be significant environmental sinks of aromatic PFAS. Fluopyram (up to 250.2 ngL^{-1}), flufenacet (up to 926 ngL^{-1}), trifluralin (up to 950 ngL^{-1}), and fluometuron (up to 1.27 gL^{-1}) are only a few of the many fluorinated pesticides that have been found in several studies on the environmental monitoring of pesticides in aquatic settings. Even though trifluralin has been prohibited in the EU since 2008, reports of its presence in various European rivers have continued for over ten years [36].

A study was conducted in Portugal, focusing on four river basins (Ave, Leça, Antuã, and Cértima) during both dry and wet seasons [52]. PFAS contamination was confirmed in all studied sites in at least one of the seasons. PFOS and PFOA were frequently detected in both sampling campaigns, reflecting their persistence and historical usage. During the dry season, PFOS and PFOA were found in 40.6% and 41.2% of samples, respectively.

In the wet season, 82.4% and 97% of samples contained PFOS and PFOA, respectively. Short-chain PFAS compounds, such as PFBS and PFBA, were also present during the wet season, with PFBA detected at the highest concentration (22.6 ng/L) in the Antuã River. The rivers with the highest PFAS contamination levels throughout the year were Cértima and Antuã, which are impacted by various industries, including ceramics, metal processing, footwear, textile, paper production, and chemicals. The average concentrations of investigated PFAS compounds across all sampling sites and campaigns were 15.9 ng/L for Cértima and 12.0 ng/L for Antuã. The dry season showed higher PFAS concentrations compared to the wet season due to dilution effects from rainfall. In the Ave River basin, the mean sum of PFASs was 9.5 ng/L, with notable differences between the dry and wet seasons (17 ng/L and 1.9 ng/L, respectively). The study identified point sources, particularly in the Ave River basin, as the primary threat to water quality [52].

2.3. Ecotoxicity of PFAS

Humans as well as animals can be exposed to PFAS through oral, inhalation, and dermic exposure. The presence of volatile PFAS in human serum and ambient levels have often been correlated in investigations on human PFAS exposure [53-54]. The moderate acute and minor chronic toxicity of PFOA and PFOS to marine and freshwater aquatic species is well documented [24]. Additionally, it has been demonstrated that PFOA, PFNA, PFOS, and PFHxS are harmful to both humans and animals [55-56]. In both animal and human bodies, PFAS cannot be metabolized and does not disintegrate through chemical processes, according to earlier studies [24].

Because PFASs have a strong affinity for serum albumin and fatty acid-binding proteins, their distribution in the biota depends on the tissue [57-60]. Additionally, the bioaccumulation potential of PFASs varies depending on the species and individual organisms as well as the physicochemical characteristics of PFASs, including the kind of chain (branched or linear), chain length, and functional group [57][61-63]. Additionally, it has been demonstrated that the PFAS structure affects the removal rate. Branched isomers, for instance, are removed more quickly than linear isomers [64]. Additionally, species, gender, and reproductive state affect the accumulation and clearance of PFAS [65-66].

Even in pristine areas, PFAS are pervasively present in the ecosystem and may even biomagnified as they move up the food chain [67-70]. As the concentration of PFOS (C8

fluorocarbon), the major PFAS in biota, rises up the food chain, demonstrating its great bioaccumulation ability. Perfluorooctanoate (PFOA, C7 fluorocarbon), in contrast, has a minimal propensity for bioaccumulation and is largely comparable among animals from various trophic levels. For instance, the maximum concentrations of PFOS and PFOA in invertebrates are comparable; however, the maximum PFOS concentration in fish, reptiles, birds, and mammals is up to three orders of magnitude higher than that of PFOA [71]. Because PFOA has a shorter perfluorocarbon chain length and a different functional group than PFOS [57], it may have a decreased potential for bioaccumulation. Due to the phase-out of PFOS in 2002, PFSA concentrations have been dropping in the biota over the past few years [71]. However, depending on the compound, trophic level, and geographic location [71], the concentrations of other PFASs, such as long-chain PFCAs, show no discernible trend and may even be rising.

Since PFAS precursors can degrade into PFCAs and PFSAs, PFAS can be thought of as persistent in the environment as a whole [72]. Because the PFASs are permanently incorporated into aquatic ecosystems, creatures downstream of the discharges may be continuously exposed to those substances. These findings hint at the long-term (chronic) exposure of aquatic animals to PFASs from other point and nonpoint sources, including wastewater discharge. Only a small number of studies have looked at the consequences for multiple generations, in contrast to the many studies looking into the acute and chronic effects of PFASs, which were reviewed by Giesy et al. [73] and more recently by Ding and Peijnenburg [74].

2.4. European and national regulations of PFAS

The risk assessment process begins with gathering relevant data and scientific information about PFAS, including their chemical properties, exposure routes, and potential toxicity. This information serves as a foundation for assessing the risks associated with various uses and sources of PFAS, such as industrial processes, consumer products, and contaminated sites. Robust risk assessment methodologies, incorporating both human health and environmental considerations, are employed to evaluate the potential adverse effects of PFAS exposure.

Through this information, regulatory authorities can identify potential exposure pathways, vulnerable populations, and ecological receptors at risk. Human health risk assessments help quantify the likelihood of health effects from PFAS exposure,

considering factors such as dose-response relationships and exposure scenarios. Environmental risk assessments evaluate the impacts of PFAS on ecosystems, including effects on wildlife, aquatic organisms, and ecological processes.

The outcomes of the risk assessment process provide valuable insights into the severity of PFAS-related risks and inform subsequent risk management decisions. Risk management measures encompass a range of actions, such as setting regulatory limits, establishing safe exposure thresholds, implementing control technologies, and promoting the adoption of safer alternatives. These measures are designed to reduce or eliminate exposure to PFAS, prevent further environmental contamination, and mitigate the potential health risks associated with these substances.

Aquatic ecosystems are particularly vulnerable to the impacts of human activities, including pollution by PFAS and other forms of environmental degradation. As a result, there has been a growing focus on developing regulations that specifically target aquatic ecosystems, with the aim of protecting these important resources [75-77].

2.4.1. European Union's Water Framework Directive

The European Union's Water Framework Directive (WFD) sets out a framework for the protection and management of Europe's freshwater resources. The directive aims to achieve "good ecological status" for all surface waters, as well as "good chemical status," with the ultimate goal of preserving and enhancing aquatic ecosystems [75-77].

In this scope, The European Commission has presented an updated list of water pollutants to be controlled, which includes the potential addition of more pesticides, certain pharmaceuticals, and some PFAS to the list of surface water pollutants. This proposal is part of the revised WFD, Environmental Quality Standards Directive (EQSD), and Groundwater Directive (GWD) aimed at protecting aquatic environments and safeguarding drinking water resources [78].

EurEau, an association representing European drinking water and wastewater service providers, welcomes these proposals and emphasizes the need to address these pollutants at their source. Specifically, they highlight the urgent need for a full ban on PFAS due to the lack of suitable removal technologies at urban wastewater treatment plants. They believe that a ban is necessary to meet the thresholds set by European legislation. The updated list of surface water pollutants also includes additional

pesticides, certain pharmaceuticals, and 24 PFAS, commonly known as "forever chemicals" found in various consumer products. European groundwater quality standards are also established for the same group of PFAS, certain pharmaceuticals, and pesticide metabolites [78].

Furthermore, the proposals pave the way for the inclusion of micro- and nanoplastics, as well as antimicrobial-resistant microorganisms, in future "watch lists" under the EQSD and GWD. The aim is to address emerging pollutants and their potential impacts on water quality. It is expected that these proposals, along with the new Urban Waste Water Treatment Directive and the recent Industrial Emissions Directive, will work together to introduce robust control measures at the source and effective Extended Producer Responsibility schemes where source control alone cannot resolve water quality issues. This holistic approach aims to ensure the protection and improvement of water quality throughout the European Union [78].

2.4.2. PFAS under Registration Evaluation Authorization and Restriction of Chemicals (REACH)

As discussed earlier, some PFAS have become contaminants of major concern, which has prompted their regulation in Europe and overseas (Canada, Australia, United States). These regulatory efforts have been mostly applied for PFOA, PFOS and their degradation products (part of the group of "long chain PFAS").

Perfluorooctanoic acid and perfluorooctane sulfonate, together with their precursors, are now included in the Stockholm Convention's list of compounds that are intended to be eliminated globally [79-80]. Certain limited applications of these substances are still permitted for a specified period. The Conference of the Parties also resolved to add perfluorohexane sulfonic acid (PFHxS) and associated compounds to the list of chemicals to be eliminated in June 2022. Additionally suggested for inclusion as POPs are long-chain perfluorocarboxylic acids (C9-C14) [80].

These foreign accords have been incorporated into European Union law. Notably, the REACH Regulation lists a number of PFAS, including PFBS, PFHxS, and PFHpS, along with their salts, as Substances of Very High Concern (SVHC). Hexafluoropropylene oxide dimer acid (HFPO-DA) and the perfluorinated carboxylic acids C9–C14 are also on this list [81]. This implies that their future uses will require

authorization. Efforts are also underway to regulate PFAS as a group rather than individual substances within the EU. For instance, the European Chemicals Agency (ECHA) has proposed a gradual ban on the production and use of all PFAS in firefighting foams with concentrations above 1 ppm within 10 years [82]. Additionally, Germany, the Netherlands, Denmark, Norway, and Sweden are collaborating on a restriction proposal that encompasses the entire group of PFAS, including fluorinated polymers, aligning with the EU's "Chemicals Strategy for Sustainability" [44]. However, the inclusion of fluoropolymers in the PFAS restriction has sparked controversy, with manufacturers arguing that they should be considered "polymers of low concern" (PLC) due to their inert, non-bioavailable, and non-toxic properties [83-84].

While European law governs chemical restrictions and prohibitions, EU member states play a crucial role in implementing and monitoring these requirements. For instance, Denmark has implemented stringent regulations, largely banning the use of PFAS in food contact materials and setting an indicator level of 20 mg F/kg in packaging materials. Additionally, national governments, such as France, have developed action plans to enhance control, reduce emissions from PFAS processing plants, and monitor environmental and population exposure to these substances [85].

2.4.2. Portugal regulation

Portugal has taken measures to regulate PFAS, that are persistent in the environment and have been associated with negative effects on human health and the environment. Below the main regulations in Portugal related to PFAS are listed:

- Decree-Law No. 152/2017: This decree-law defines the legal regime for Integrated Pollution Prevention and Control (IPPC) and establishes that facilities that use or produce PFAS must conduct air and water quality monitoring. It also requires companies that produce or use these substances to comply with best available practices to minimize their release into the environment [86].
- Ordinance No. 107/2018: This ordinance establishes standards for the control and elimination of PFAS in firefighting equipment. It prohibits the use of foams containing PFAS in new equipment starting January 1, 2019, and requires the phasing out of such equipment with the use of safer alternatives [87].

- Decree-Law No. 152-B/2017: This decree-law establishes mandatory monitoring of water quality in areas vulnerable to nitrate pollution, which may be contaminated by PFAS from agricultural activities [88].

2.5. PFAS remediation technologies

There are now several PFAS remediation solutions available for water treatment. The separation and removal processes are the two primary steps in these remediation approaches. The traditional methods of flocculation, coagulation, sedimentation, and filtration are used in the separation process, along with sorption methods like the use of activated carbon and ion exchange resins and membrane technologies like nanofiltration and reverse osmosis. Advanced oxidation and reduction, ultrasonication, and biological degradation are some of the removal approaches. The majority of PFAS remediation technologies are adapted from those already in use to treat other pollutants. However, when creating new remediation strategies for water treatment, considerable consideration should be given to the PFASs' extraordinary chemical characteristics and their behavior in water. Compared to many other pollutants, PFASs have few remedial alternatives available.

2.5.1. Separation techniques for PFAS contaminated water

Technologies for treating water use methods for separation and destruction. Although there are proven separation methods available for a variety of contaminants, it is still difficult to destroy persistent organic pollutants (POPs), especially PFAS. The pollutant's susceptibility for biodegradation and/or oxidation/reduction play a significant role in destruction. Due to their great persistence and minimal to nonexistent ability for degradation, PFAS provide a significant challenge for natural degradation.

Most drinking water treatment procedures involve conventional water treatment, which includes the steps of coagulation and flocculation, sedimentation, and filtration. However, they are inapplicable and ineffective for the elimination of PFASs. When it comes to field applications, other treatment technologies also face significant obstacles.

Activated Carbon

Activated carbon (AC) is commonly used to adsorb natural organic compounds, synthetic organic chemicals and flavor and odor compounds in drinking water treatment systems, being one of the most successful processes to effectively extract PFAS from

water, particularly for long-chain PFAS [89]. Despite being a commonly used adsorbent, AC (either granular or powdered) has significant drawbacks, such as cost, regeneration once it is used up, and decreasing adsorption efficiency because of carbon loss after each regeneration cycle [90].

Reactivation of depleted AC is a common practice for full-scale granular activated carbon (GAC) adsorbents and has lower environmental and economic impacts than replacing depleted AC with virgin AC. Several studies have evaluated the effectiveness of various reactivation processes, such as high-temperature incineration and solvent washing, in desorbing PFAS from depleted Acs [91-94]. Although Westreich *et al.* [95] compared the PFAS adsorption performance of a virgin and reactivated AC, proposing several hypotheses for the observed results, it is still unclear how reactivation can affect PFAS adsorption.

Alternative materials with high adsorption efficiency, cheap cost, and efficient regeneration or disposal are becoming more and more popular. The large porous surface area who provides a large contact surface for contaminants to be adsorbed [96], controllable pore structure, thermostability, acid/base properties, low cost, and environmentally sustainable design of the Acs make them very effective for the removal of a wide variety of organic and inorganic pollutants dissolved in aqueous or gaseous media [97-98].

Ross et al. (2018) [99] found that granular activated carbon (GAC) is effective in removing long-chain per- and polyfluoroalkyl substances (PFAAs), but it is not highly efficient for removing short-chain PFASs and their precursors. However, using GAC as an adsorbent in large-scale applications poses a disadvantage due to the additional analytical costs required for assessing PFAS breakthrough timeframes and regular monitoring. Injectable activated carbon shows promise as an *in-situ* treatment technology for groundwater.

Ion exchange resin (IXR) or polymer adsorbents

Anion exchange resins and synthesized materials have shown high effectiveness in removing a wide range of long and short-chain PFAS from water. They have adsorption capacities ranging from 100 to 2000 mg PFASs/g IXR [100], although they are less effective for the shortest-chain PFAAs. However, the regeneration process for IXRs,

mainly using toxic, flammable, volatile, and corrosive organic solvents such as methanol or sodium hydroxide, poses challenges in waste management and treatment, making it costly and unsustainable for large-scale water treatment processes.

Du et al. (2014) [101] found that porous chitosan beads, specifically molecularly imprinted polymers, have high adsorption capacities for PFOS (perfluorooctane sulfonate), attributed to micelle formation within the porous materials. They also highlighted that anion-exchange resins and porous crosslinked chitosan exhibit higher adsorption capacities for PFOS and PFOA (perfluorooctanoic acid) compared to other adsorbents [101]. Electrostatic interaction plays a crucial role in the adsorption of anionic perfluorinated compounds (PFCs) with positively charged adsorbents, suggesting that positively charged IX resins are more suitable for anionic PFC removal [101]. Zhang et al. (2019) [102] supported the idea that ion exchange resins perform better in adsorption compared to non-ion exchange resins, with anion exchange resins showing higher affinity for PFOA due to its anionic nature at environmental pH. The hydrophobicity of the resin positively correlates with the adsorption capacity for PFAS, and polyacrylic resins demonstrate faster adsorption rates and higher capacity compared to polystyrene resins [102].

High-pressure Membranes

Among the various separation processes, nanofiltration (NF) and reverse osmosis (RO) are high-pressure membrane-based processes extremely effective in removing many PFASs including PFAA precursors, regardless of their chain length and chemical structure [99] [103]. According to Ross et al. (2018) [99] the biggest disadvantage of these approaches, particularly for groundwater applications, is maintaining membrane health because of suspended particles and water geochemistry as well as the costs associated with large-scale applications.

For waters with complex matrices like ground water and wastewater, utilizing RO or NF technique as a polishing step in the treatment train rather than using such technology alone may assist minimize the amount of the consequences to membrane health. Due to their extremely high cost, NF and RO, however, are not an economically viable alternative for large-scale applications [99].

2.5.2. Removal techniques for PFAS contaminated water

The removal/degradation of PFAS compounds is challenging due to their high persistence and limited susceptibility to biodegradation or oxidation/reduction transformations. After adsorption, the exhausted adsorbent material is typically either discarded offsite or regenerated. Ross et al. (2018) [99] conducted an extensive review discussing various destruction technologies for PFAS, including incineration, microbial destruction, chemical oxidation and reduction, electrochemical oxidation.

Biological treatment

Bioremediation is a sustainable and cost-effective technology that utilizes microorganisms to break down pollutants in the natural environment. Microorganisms native to the impacted environment can efficiently degrade pollutants through metabolic pathways, leading to their partial or complete elimination. These microorganisms can utilize organic pollutants, including pharmaceuticals, either as a primary substrate or in combination with other substances. To harness the potential of these degrading microorganisms, it is important to focus on their stimulation and develop new technologies to enhance their activities [104].

Harris et al. (2022) [105] investigated soil samples taken from sites contaminated with PFAS and searched for microorganisms that could degrade PFOA/S (perfluorooctanoic acid and perfluorooctanesulfonic acid). They discovered a microorganism called *Delftia acidovorans*, which exhibited the ability to grow in a minimal medium with PFOA as its sole carbon source. When these cells were exposed to PFOA, they observed an increase in fluoride concentration, indicating the potential presence of a dehalogenase enzyme. This enzyme could be valuable in microbial remediation efforts to remove PFOA or PFAS from the environment. The researchers also identified several haloacid dehalogenases associated with the *D. acidovorans* genome. These enzymes were genetically modified and expressed in *Escherichia coli* for efficient production and purification. These engineered enzymes demonstrated the potential for defluorination, a crucial step in the biological degradation and removal of PFOA/S. Based on these findings, the researchers propose that utilizing naturally occurring microbial degradation pathways could offer a novel approach to bioremediation, effectively eliminating PFAS contamination.

Advanced oxidation (AOP) and reduction (ARP) process

Advanced oxidation processes (AOP) are powerful methods for treating organic pollutants. They involve the production of highly reactive OH· radicals that react with contaminants, breaking them down into smaller, non-toxic molecules or fully mineralizing them [106]. AOP use various techniques such as O_3, H_2O_2, catalysts, light, ultrasound, or electron beam to generate these radicals [106]. AOP for some PFAS, such fluorotelomers and PFCAs, usually follows a sequential defluorination mechanism that becomes more and more rate-limiting as the perfluoroalkyl chain gets shorter. The required AOP reaction conditions are prone to the formation of multiple by products, ranging from short chain PFAAs from precursor transformation and incomplete mineralization of long chain PFAAs to a host of secondary water quality concerns based on the ambient geochemistry. This is because of the electronegativity of the fluorine atom, the associated bond dissociation energy, and stabilization of the perfluoroalkyl chain [107].

ARPs are subject to decreased efficiency as a result of nontargeted interactions with naturally existing geochemical elements. They can be energy-intensive, require several hours of residence time for PFAS to mineralize, follow a sequential defluorination process, and be energy-intensive. Short-chain PFAAs and additional water quality issues are thus formed as related byproducts of ARP [107]. Long-chain PFAAs defluorinate more quickly than short-chain PFAAs due to lower bond dissociation energy central to the alkyl chain, according to groundbreaking research by Bentel et al. (2019) [108] that explains the ARP process as a function of bond dissociation energies along perfluoroalkyl chains. Because the associated bond dissociation energy required to achieve defluorination increases as the fluorinated alkyl chain shortens while the potential for quick scavenging reactions remains constant, this explains the lengthy residence times to achieve mineralization, especially in complex solutions.

2.6. Main goals

This work aims to develop an efficient bioremediation unit based on a synthetic bacterial consortium with defluorination capacity and explore its potential to act as a secondary water treatment step in conjunction with a ZnO and TiO_2-based nanophotocatalytic treatment to remove PFAS from aquatic matrices. So, the first approach starts with selecting the best strains with defluorination activity from the

CIIMAR culture collection and then the investigation of the biocompatibility of the pre-selected strains for the construction of the consortium. Finally comes the integration of the consortium into a downstream nanophotocatalysis bioremediation unit for PFAS removal.

Chapter 3 – Materials and Methods

3.1. Framework of adopted methodologies

This chapter focuses on the methodology used in this research, from the theoretical concepts underlying the approach to its practical application. Methodology is a critical aspect of any research study, as it allows researchers to collect and analyze data in a systematic and rigorous manner. This chapter begins with an overview of the theoretical concepts that underpin the methodology, providing a solid foundation for understanding methodology and its relevance to the research plan, followed by the practical application of the methodology, including the steps taken to collect and analyze all the data.

3.1.1. Pre-Selection of the bacterial strains for the assembly of a degrading consortium

The potential of different bacterial strains are part of CIIMAR's extensive culture collection, to outfit a potential bacterial consortium to degrade the target polyfluorinated pollutants and related sub-products was assessed. This approach purposely focused on strains with a well-defined potential to biodegrade different environmental pollutants, including fluorinated pesticides (sodium fluoroacetate and epoxiconazole) and pharmaceuticals (paroxetine), as well as different hydrocarbons (fluorobenzene and petroleum hydrocarbons) and cyanotoxins (microcystins). A full list of the bacterial strains selected for this screening are listed in Table 3.1.

Table 3.1: Species used throughout the study, the used culture media, environmental source, and tested degraded compound.

Strain	Taxonomy	Culture Media	GenBank Accession Number	Environmental source	Compound	Reference
3EE	*Hydrogenophaga eletricum*	PCA	MK129549	Estuarine sediment	Epoxiconazole	[109]
5AE	*Hydrogenophaga eletricum*	PCA	MK128663	Agricultural soil	Epoxiconazole	[109-110]
8EE	*Comamonas testosteroni*	PCA	MK131040	Estuarine sediment	Epoxiconazole	[109]
F11	*Labrys portucalensis*	PCA	DSM17916	Polluted soil	Fluorobenzene	[111]
COL1	*Comamonas testosteroni*	PCA	KX400799	Activated sludge	Monofluoroacetate	[112]
COL4	*Herbaspirillum frisingense*	PCA	KX756676	Activated sludge	Monofluoroacetate	[112]
COL5	*Delftia acidovorans*	PCA	KX400852	Activated sludge	Monofluoroacetate	[112]
COL10	*Variovorax paradoxus*	PCA	KX400967	Rhizosphere	Monofluoroacetate	[112]
COL16	*Achromobacter anxifer*	PCA	KX398363	Activated sludge	Monofluoroacetate	[112]
CPN3	*Rhodococcus erytropolis*	PCA	MN833713	Sediment - beach Cabo do Mundo	Hydrocarbons	[113]
1.7.L	*Pseudomonas sp.*	PCA	OK482776	Sediment - beach Cabo do Mundo	Hydrocarbons	[113]
19791	*Sphingosinicella microcystinivorans*	R2A	AB084247	Hypertrophic lake, Lake Suwa	Not available	[114]
DPS1	*Pseudomonas sp.*	PCA	MN128762	Estuarine sediment	Paroxetine	[115]
DPS4	*Chitinophagaceae* bacterium	PCA	MN128745	Estuarine sediment	Paroxetine	[115]
DPS5	*Acinetobacter sp.*	PCA	MN128733	Estuarine sediment	Paroxetine	[115]
DPS8	*Leadbetterella sp.*	PCA	MN128750	Estuarine sediment	Paroxetine	[115]
DPS10	*Leadbetterella sp.*	PCA	MN128751	Estuarine sediment	Paroxetine	[115]

Each strain was retrieved from cryopreserved stocks (kept at -80ºC) by streaking them in their respective culture media. Figure 3.2 shows the procedure performed for all plates.

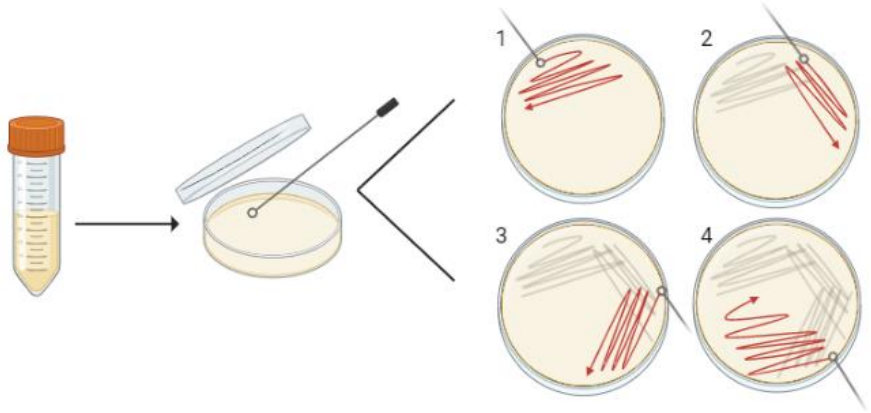

Figure 3.1: Procedure performed for the inoculation of the strains used throughout the work.

Two culture media were used, depending on the bacterial strain, including Plate Count Agar (PCA) and Reasoner's 2A (R2A). These media were selected because the strains used were previously isolated on them. PCA is non-selective and considerably rich in nutrients, tryptone, yeast extract vitamin factors, and glucose used as an energy source for the growth of most bacteria [116]. R2A medium, on the other hand, is a low-nutrient medium designed to support the growth of bacteria that are metabolically slow or stressed [117].

3.1.2. Assessment of the catabolic viability of the pre-selected bacterial strains

The determination of the viability of each pre-selected bacterial strain was based on their capacity to replicate their original catabolic efficiencies, for the case of defluorinating strains, or their capacity to showcase defluorination phenotypes, for the case of the pre-selected cyanotoxin and hydrocarbon-degrading bacteria. This was investigated by inoculating each strain, axenically, in their original isolation and/or enrichment conditions with their preferred fluorinated substrate. For the bacterial strains degrading non-fluorinated compounds (strains 1.7L, CPN3 and 19791), their viability was assessed based on their capacity to degrade fluorobenzene and/or fluoroacetate.

Each viability assay was established in 100 mL serum vials containing 30 mL of MSM (the composition of this medium is provided in Annex A), inoculated with each

strain individually at an OD (600 nm) of 0.5 ± 0.1 and supplemented with fluorobenzene (50 mgL^{-1}), fluoroacetate (50 mgL^{-1}), paroxetine (1 mgL^{-1}) or epoxiconazole (5 mgL^{-1}). All assays were run in duplicate and were incubated at 28 ºC under orbital agitation (130 rpm) and in the absence of light for 21 days. Biodegradation of the supplemented fluorinated substrates was monitored by evaluating bacterial growth (by spectrophotometry) and fluoride ion release (by potentiometry) on a weekly basis. Figure 3.2 displays a schematic representation of the abovementioned methodology.

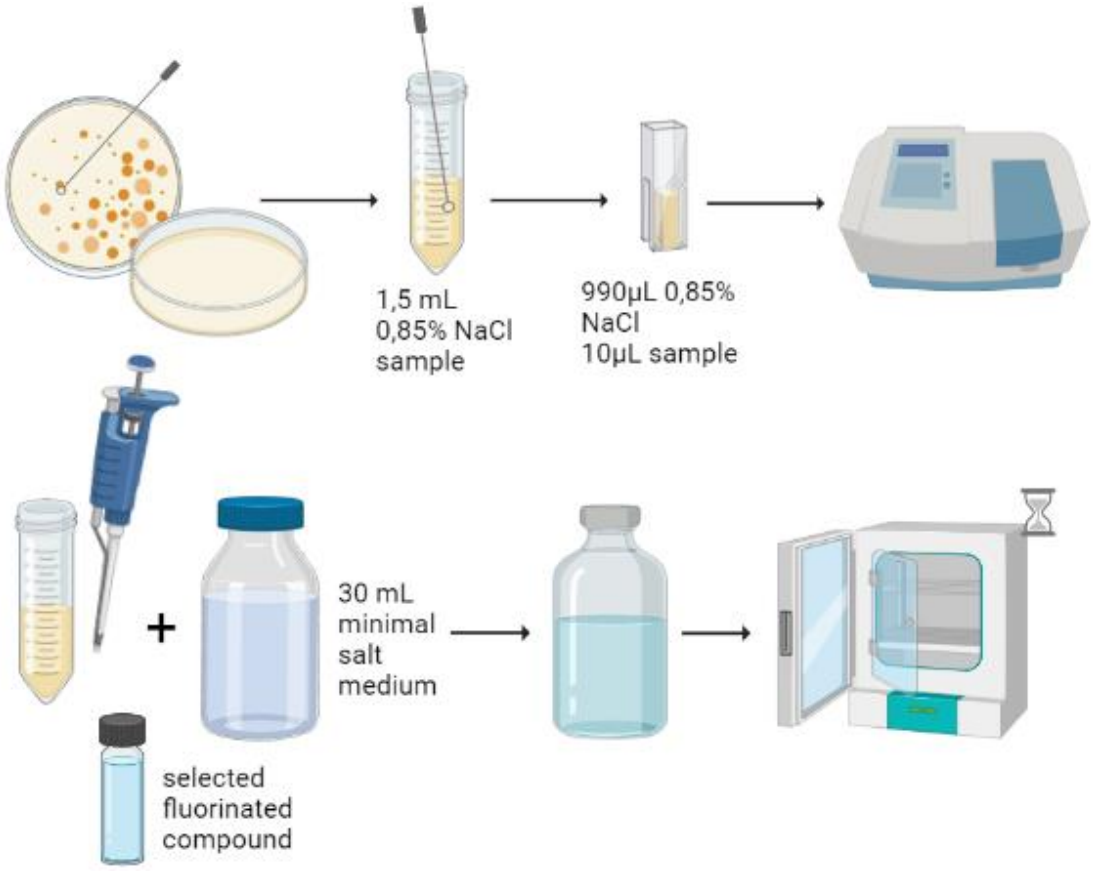

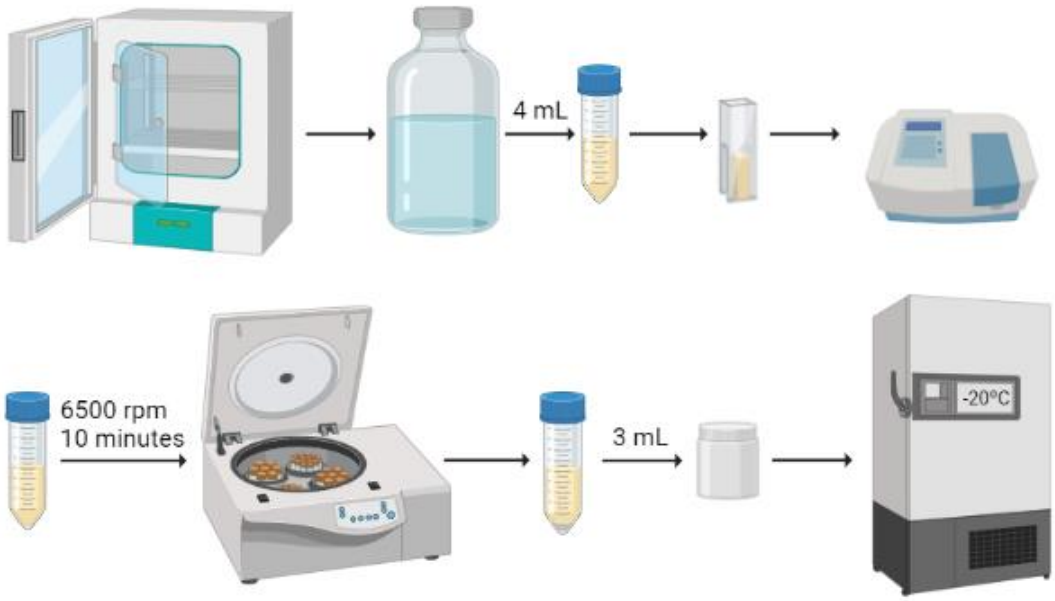

Figure 3.2: Procedure for the realization of assays of viability.

3.1.3. Biocompatibility assays

Biocompatibility assays between the best performing bacterial strains were performed to infer on the suitability of their co-cultivation in a consortium. For this, an adaptation of the disk diffusion assay was implemented. Briefly, each selected strain was pre-grown in Nutrient Broth (NB) for 72-96 h at 28 ºC under orbital agitation (130 rpm). Then, the turbidity of the liquid cultures of each bacterial strain was adjusted to an OD (600 nm) in the range of 0.08-0.10 and were then used to inoculate PCA plates by evenly streaking the plates with cotton swabs. In parallel to this, 0.2 mL aliquots of each liquid culture were centrifuged (3500 rpm for 1 min) and the resulting supernatants were reserved until further used. Blank paper discs were then placed on the surface of the inoculated agar plates with sterile forceps and loaded with 15 µL of each supernatant. In each plate, sterile NB was also loaded on a blank disc to serve as negative control. Inoculated plates were incubated for 48h at 28 ºC, after which the presence of inhibition halos was inspected. Figure 3.3 displays a schematic representation of the abovementioned methodology.

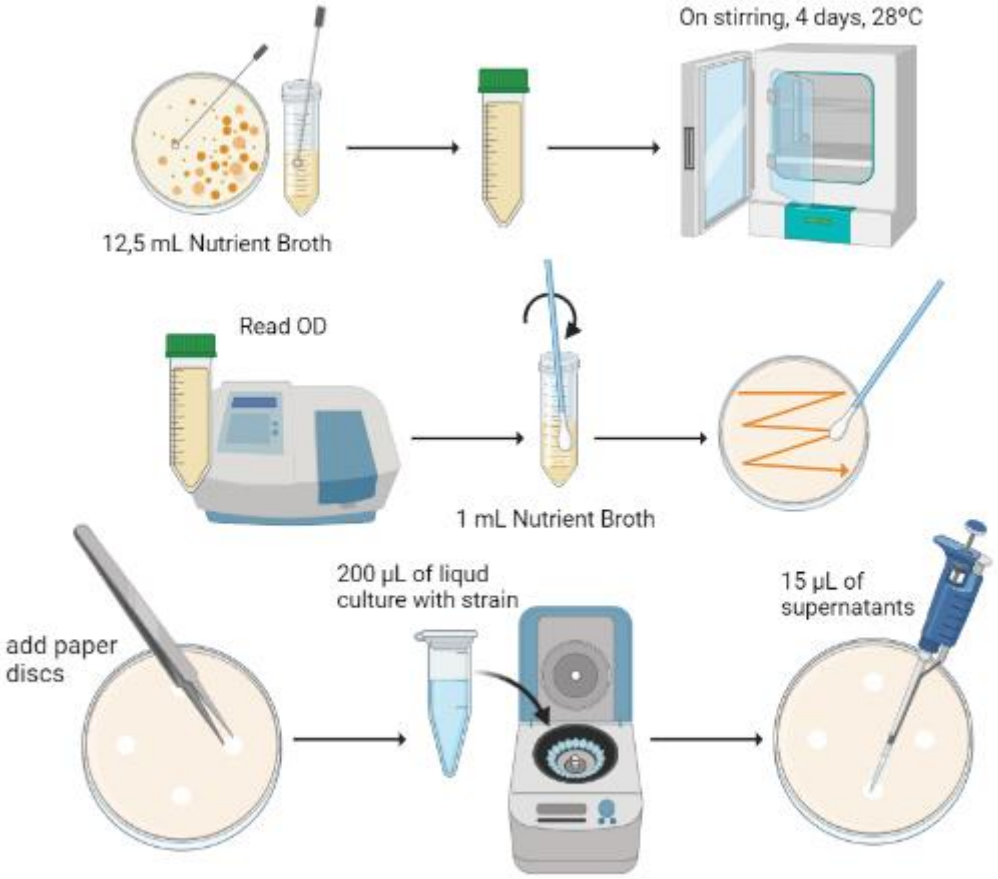

Figure 3.3: Procedure for the realization of biocompatibility assay.

3.1.4. Assembly of a degrading bacterial consortium and evaluation of its efficiency

After selecting the strains with the highest efficiency in defluorinating the chosen compounds, a synthetic degradation consortium was set up. The strains were prepared separately, where a portion of each strain was suspended in 1.5 mL of 0.85% NaCl solution and the OD adjusted to 0.3. Equal portions of inoculum of each strain were taken to form the consortium. Figure 3.4 is a schematic representation of the methodology.

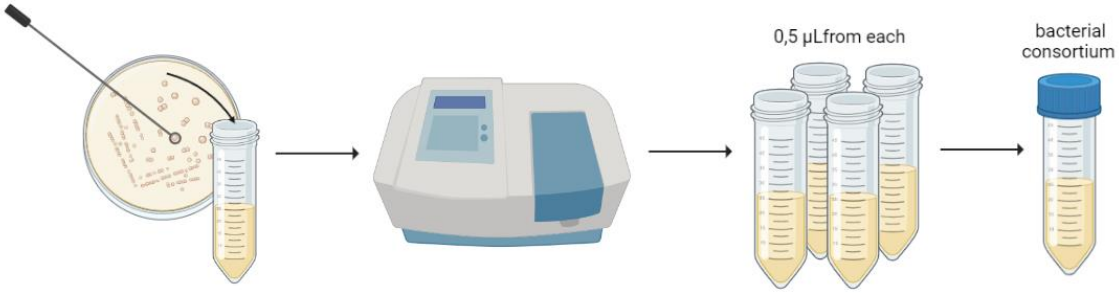

Figure 3.4: Synthetic bacterial consortium building procedure.

The capacity of the synthetic consortium to defluorinate 1 mgL^{-1} of perfluorohexanoic acid or trifloxystrobin was investigated by inoculating the consortium in 100 mL Erlenmeyer flasks containing 30 mL of MM, 1 mgL^{-1} of the mentioned compounds, added individually, 500 mgL^{-1} of sodium acetate . The initial OD of the cultures was 0.5. Every week, over a period of 21 days, samples were taken for OD and fluoride release measurement.

3.1.5. Nanophotocatalytic assays

All nanophotocatalytic assays were performed in the scope of an ongoing collaboration with researchers from the Electroactive Smart Materials from the Center of Physics of the University of Minho.

The photocatalytic efficiency of the nanoparticles was tested in a solution of deionized water with trifloxystrobin or perfluorohexanoic acid at the concentrations of 10 mgL^{-1} and 1 mgL^{-1}. The tests were performed using two types of nanoparticles, namely titanium dioxide (TiO_2) and zinc oxide (ZnO). Each nanoparticle was added as a colloid to deionized water at a concentration of 1 gL^{-1}. These were placed under stirring for 30 minutes in the dark to reach adsorption-desorption equilibrium.

Subsequently, each goblet was placed inside a photoreactor to be irradiated vertically at a distance of 14 cm by 8 lamps (Philips 8W) with a maximum wavelength of 365nm. A 5 mL sample was taken 30 minutes before the start of the assay (-30 minutes), at the start of the assay (0 minutes) and 6 hours later.

The percentage of defluorination of the compound by these nanoparticles was determined by potentiometry.

3.1.6. Biodegradation of trifloxystrobin or perfluorohexanoic acid spiked water treated by nanophotocatalysis

Biodegradation of the water samples spiked individually with 10 mgL^{-1} of trifloxystrobin and resulting from the nanophotocatalytic pre-treatment described previously, was tested using the synthetic consortium. In this assay, the pre-treated effluent was diluted tenfold, into a final volume of 30 mL of MM (27 mL of MM + 3 mL of pre-treated water), to investigate the capacity of the consortium to degrade a similar theoretical concentration of trifloxystrobin (ca 1 mgL^{-1}) as in the standalone assays. After this dilution, cultures were inoculated with the consortium (OD of 0.5) and supplemented

once with sodium acetate (500 mgL^{-1}) at the beginning of the assay. The assay was incubated for 21 days at 28°C under orbital shaking (130 rpm) and samples were taken at the beginning of the assay, 7, 14 and 21 days later. These samples allowed the OD to be read and the defluorination to be determined by fluoride potentiometry. The assays were performed in triplicate.

In parallel to this, two additional experiments were conducted to verify if the consortium would be able to grow in the water sample resulting from the nanophotocatalytic pretreatment and to investigate the abiotic degradation of this water sample. The abiotic assay consisted of adding 30 mL of the water sample (used in the photocatalytic testes with 10 mgL^{-1} of trifloxystrobin) into a 100 mL Erlenmeyer flask and incubating for 21 days at a temperature of 28 °C under orbital agitation (130 rpm). The ability of the synthetic consortium to directly defluorinate the nanophotocatalytic-treated water sample spiked with 10 mg L^{-1} of trifloxystrobin was investigated by inoculating the synthetic consortium (OD =0.5) in 30 mL of undiluted water. For both sets of cultures, OD values were measured on a weekly basis and samples were taken from these time periods for later determination of defluorination using a fluoride selective electrode. These assays were performed in duplicate.

3.2. Analytical methods

Throughout this study, two analytical methods, potentiometry and optical density were used to study the degradation efficiency.

OD read refers to the measurement of optical density, which is a technique used to determine the microbial growth.

The methodology of potentiometry assays involves measuring the potential difference between a fluoride ion selective electrode (ISE) and a reference electrode in a solution containing the analyte. The potential difference established obeys Nernst's law and is related to the logarithm of the fluoride concentration, in the range of fluoride concentrations from 0.001 to 1 mM [118]. In the containers containing the samples from the previously performed analysis, 10% of the sample volume is added in TISAB III (3 mL), allowing for the removal of interfering compounds once fluoride measurement is influenced by ionic strength, pH, and polyvalent cationic species. The fluoride ISE is then

immersed in the sample and the potential difference between the fluoride ISE and the reference electrode is measured and recorded. The concentration of fluoride in the sample is determined using a calibration curve, which relates the potential difference to known fluoride concentrations.

Chapter 4 – Results and Discussion

This chapter presents the results of the research and a discussion of them. These results provide valuable information about the research question and present the effectiveness of the methodology used. In this section, I present the results in a clear and concise manner, highlighting their significance and implications for the field of study.

4.1. Selection of prospective bacterial strains for the construction of a degrading consortium

Sodium fluoroacetate

The first compound tested in this assay was sodium fluoroacetate with a concentration of 50 mgL^{-1}. Sodium fluoroacetate is a highly toxic pesticide and rodenticide that is used in a few countries to control populations of invasive species such as rodents, rabbits, and coyotes [119]. Chemically, sodium fluoroacetate is composed of a fluorine atom attached to an acetate group. This fluorine substitution is believed to enhance the toxicity and stability of the compound. The results obtained for the degradation of this compound by the several bacterial strains tested are presented in Figure 4.1.

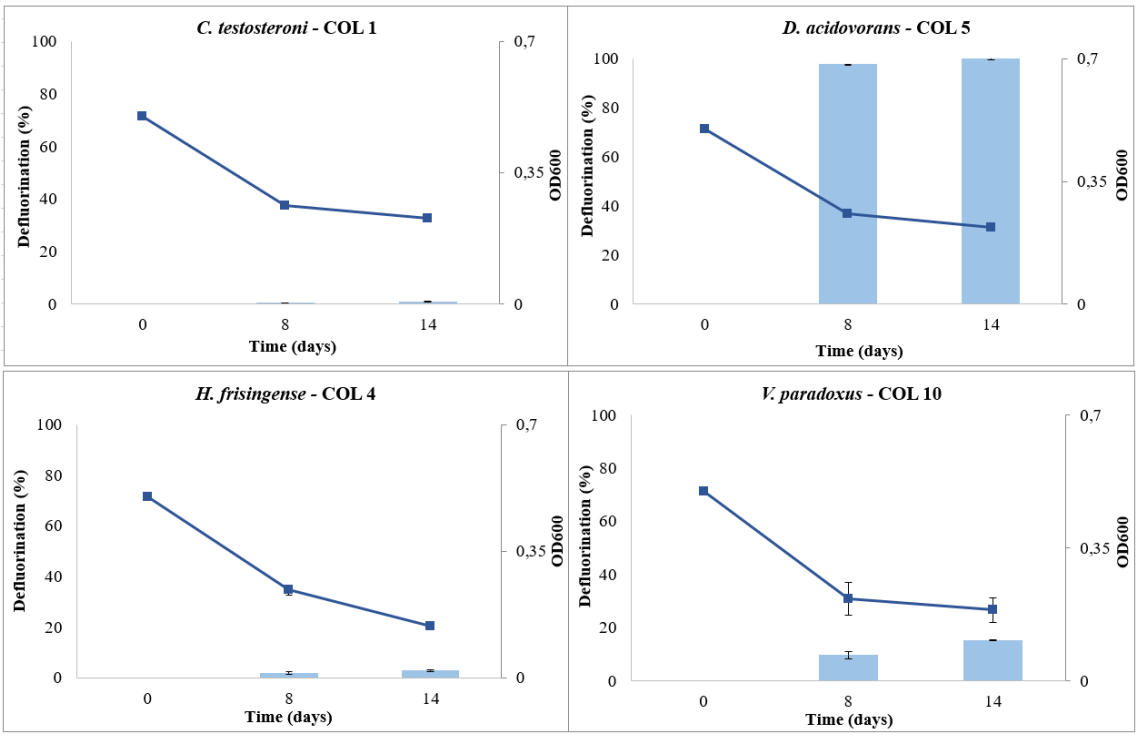

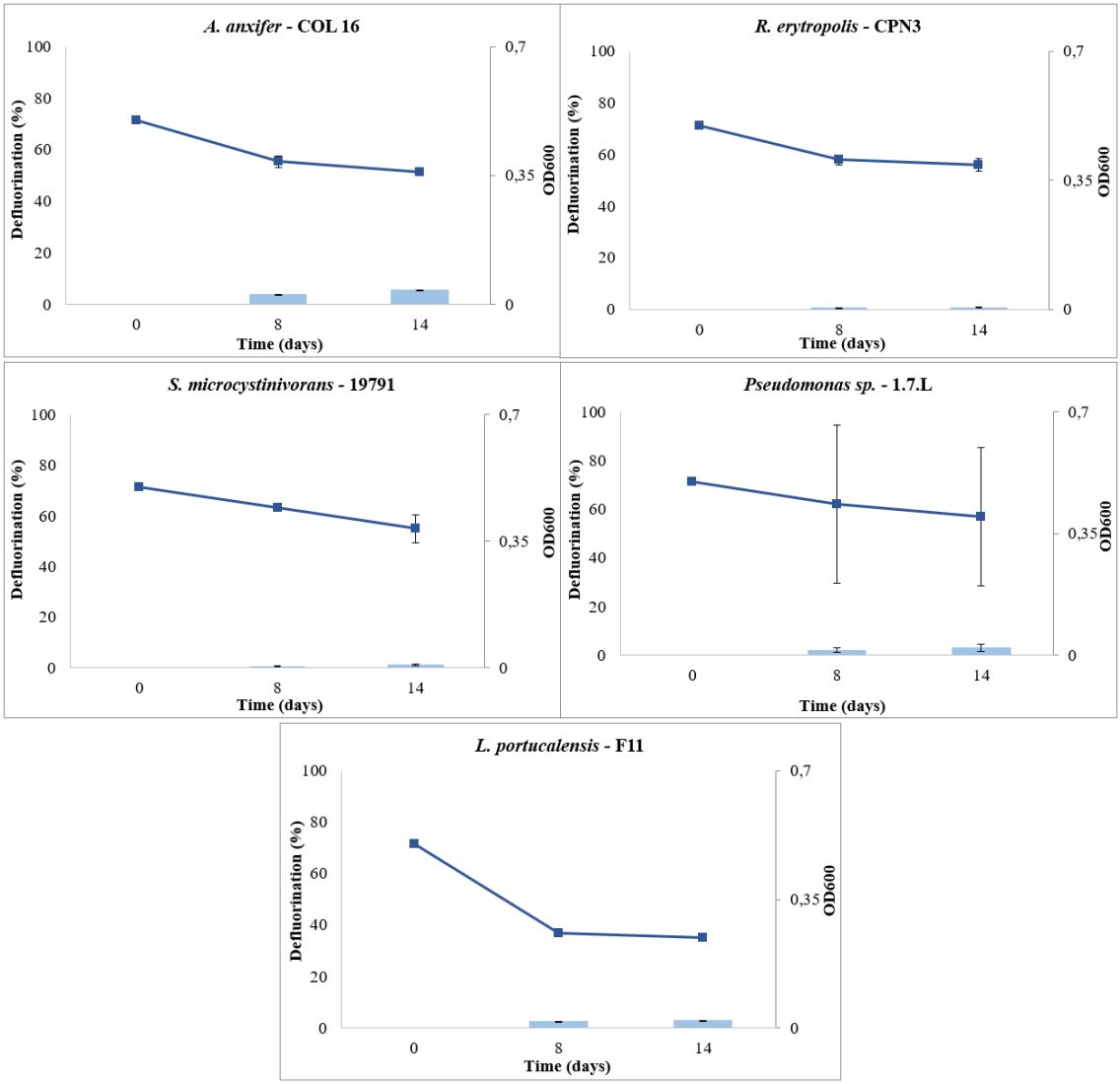

Figure 4.1: Results of sodium fluoroacetate biodegradation by the several bacterial strains tested in this study. Results are the average of duplicate samples and standard deviation is represented. The % of defluorination is represented by the bars and OD measurement is represented by the datapoints.

Analyzing Figure 4.1, it is possible to highlight strain COL 5. It showed a defluorination efficiency of 100% for the sodium fluoroacetate compound after 8 days, but no microbial growth was observed in time points measured. This degradation, resulting from microbial activity, may have occurred before the completion of 8 days, justifying the decrease in OD. This strain was chosen to perform the biocompatibility tests.

Although strain COL 10 showed percentages of 15% degradation after 8 days, this strain was not selected due to the high efficiency exhibited by strain COL 5.

The remaining strains, COL 1, COL 4, COL 16, CPN3, 19791, F11 and 1.7.L, were not able to defluorinate sodium fluoroacetate, showing defluorination percentages less than 5%.

Fluorobenzene

Fluorobenzene is a colorless liquid with a strong, sweet odor and is used primarily as a solvent and as a starting material in the synthesis of other fluorine-containing compounds. Chemically, fluorobenzene is composed of a fluorine atom attached to a benzene ring. This fluorine substitution is believed to enhance the reactivity and stability of the molecule [120]. This compound was tested in a concentration of 50 mgL^{-1}. Figure 4.2 presents the results obtained for the biodegradation of fluorobenzene by the tested strains.

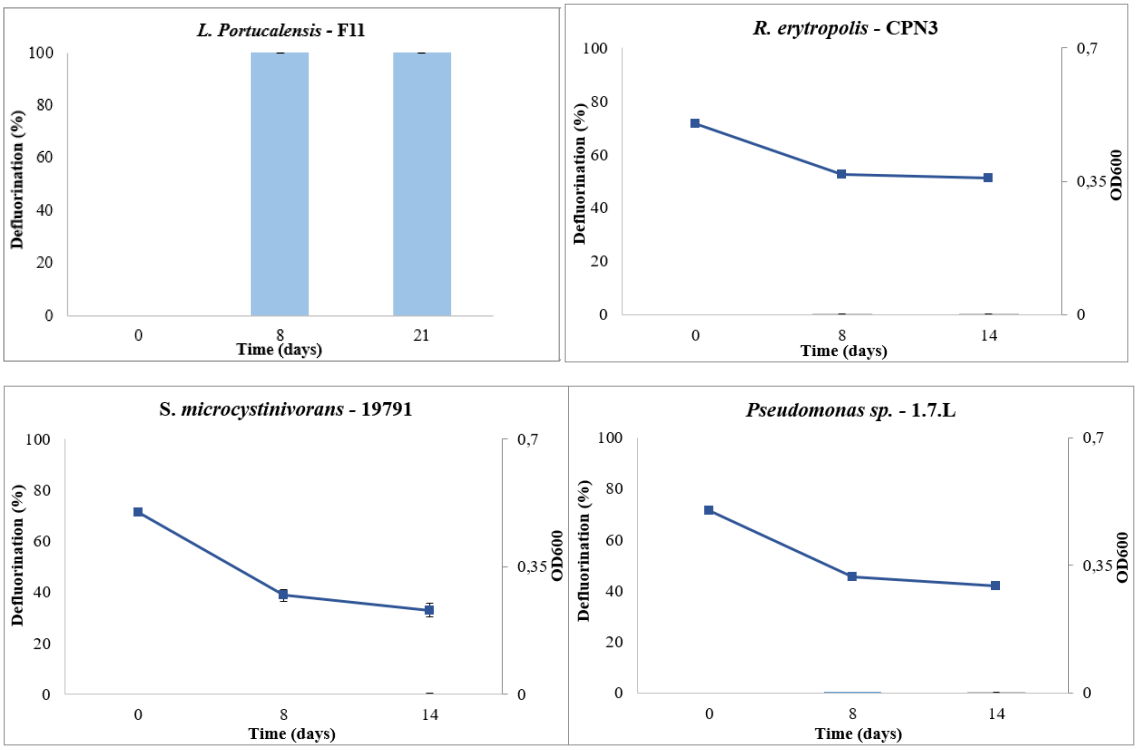

Figure 4.2: Results of fluorobenzene biodegradation by the several bacterial strains tested in this study. Results are the average of duplicate samples and standard deviation is represented. The % of defluorination is represented by the bars and OD measurement is represented by the datapoints.

By interpreting the results obtained in Figure 4.2, it is possible to highlight strain F11 in the degradation of the fluorobenzene compound. It showed 100% defluorination efficiency after 8 days, which means that this strain was able to degrade the carbon-fluorine bonds present in this ring. F11 was thus selected to integrate the constructed consortium.

The remaining strains under study (COL5, CPN3, 19791 and 1.7.L) did not show promising results, as all of them showed near 0% defluorination and a reduction in microbial growth after 8 days.

Regrettably, a failure occurred when recording ODs data for strains COL5 and F11, leading to a lack of information regarding these strains in the analysis performed.

Paroxetine

Paroxetine is a selective serotonin reuptake inhibitor used primarily as an antidepressant and anxiolytic medication. Chemically, paroxetine is a member of the fluoxetine class of compounds and is composed of a fluorine atom attached to a phenyl ring. This substitution of fluorine is thought to increase the potency and selectivity of the drug [121]. The concentration that was tested was 5 mgL^{-1}. The results obtained for the biodegradation of this compound by the several tested strains are presented in Figure 4.3.

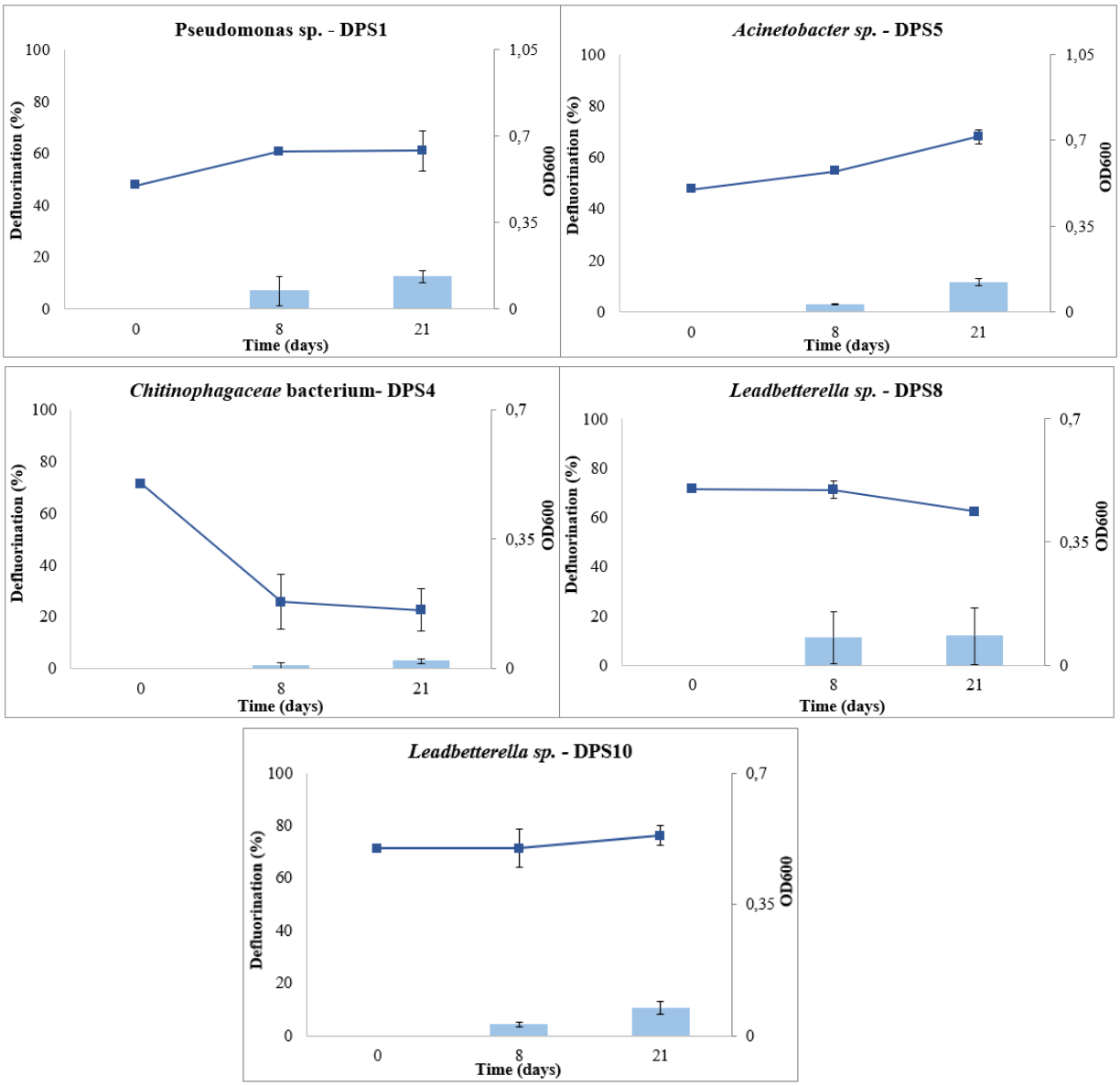

Figure 4.3: Results of paroxetine biodegradation by the several bacterial strains tested in this study. Results are the average of duplicate samples and standard deviation is represented. The % of defluorination is represented by the bars and OD measurement is represented by the datapoints.

Analyzing Figure 4.3, it is possible to conclude that none of the strains used in this assay was able to degrade the compound paroxetine completely. However, among the strains under study, DPS8 showed a defluorination of about 18.5% of the compound.

Analyzing the strains DPS1, DPS5 and DPS10, all of them present an increase in their microbial growth and some defluorination was also observed. However, despite these characteristics, they were not selected for the consortium, since from this group, DPS8 was the one that presented the highest degradation. Strain DPS4 was the one that presented the lowest defluorination percentage.

Although strain DPS8 did not show a defluorination efficiency as higher as the previously selected strains, it was still selected to integrate the constructed consortium as it exhibited the best performance in terms of defluorination of paroxetine.

Epoxiconazole

Epoxiconazole is a systemic fungicide used in agriculture to control a wide range of fungal diseases on crops such as wheat, barley, and rice. It works by inhibiting the synthesis of ergosterol, an essential component of fungal cell membranes, leading to cell death. Chemically, epoxiconazole is composed of a fluorine atom attached to a triazole ring and an epoxide group. This fluorine substitution is believed to enhance the potency and stability of the molecule [122]. In this assay, the concentration used of this compound was 1 mgL^{-1}. Figure 4.4 shows the results obtained for the biodegradation of epoxiconazole by the bacterial strains tested.

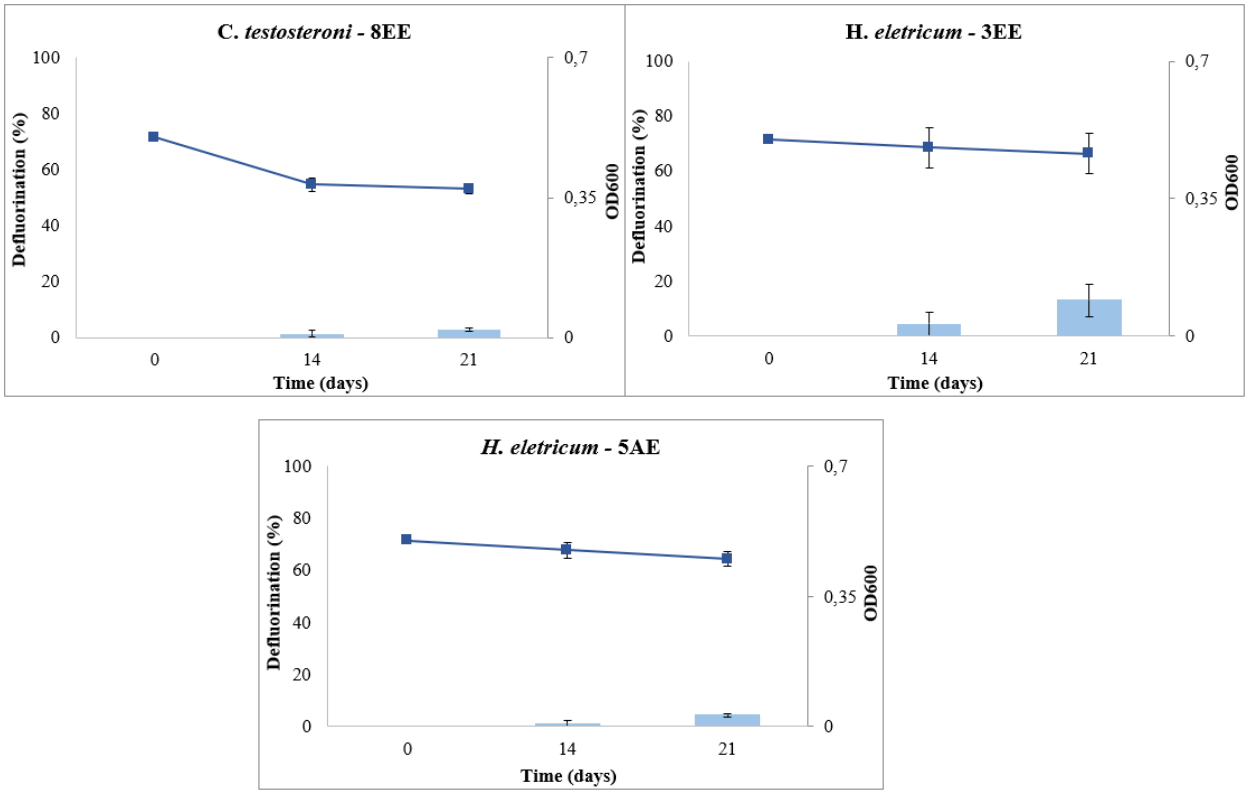

Figure 4.4: Results of epoxiconazole biodegradation by the several bacterial strains tested in this study. Results are the average of duplicate samples and standard deviation is represented. The % of defluorination is represented by the bars and OD measurement is represented by the datapoints.

Analyzing Figure 4.4, it is possible to conclude that, for this compound, none of the strains used was able to completely defluorinate epoxiconazole. However, strain 3EE presented the highest percentage of defluorination compared to the others (17% after 21

days). Therefore, this strain was chosen for the construction of the consortium and to test the compatibility with all the strains selected so far.

Analyzing the remaining strains tested, they did not show relevant degradation percentages.

4.2. Analysis of species compatibilities

The methodology initially involved the selection of bacterial strains with the potential to defluorinate fluorinated molecules. Subsequently, compatibility tests were conducted to verify whether the chosen strains could hinder each other's growth. The objective was to construct a consortium with compatible species. However, despite rigorous application of the procedures described in the Materials and methods section, all attempts produced inconclusive results, since between the various assays, contaminations appeared on the used disks, negative control, or the used medium.

The occurrence of contamination in each compatibility test had a significant impact on the outcomes. This contamination alters the results and render the compatibility assessment invalid. The presence of contaminating species interferes with the growth and interactions of the target strains, compromising the reliability of subsequent experiments and hindering the development of the intended consortium. Several factors could have contributed to the contamination issue. The sterility of the experimental environment, including equipment, media, and handling procedures, is crucial to prevent the introduction of unintended microorganisms. Failure to maintain strict aseptic conditions can lead to the inadvertent presence of contaminating species, rendering the compatibility assessment unreliable.

Despite the challenges encountered in assessing species compatibility and the presence of contamination, a decision was made to proceed with the construction of the consortium using all the strains available. While the contaminated results from the compatibility tests raised concerns regarding the potential effects on the consortium's performance, it was deemed necessary to explore the collective capabilities of the selected strains in the context of fluoride degradation. By including all the strains in the consortium, it was intended to take advantage of their individual strengths and synergistic interactions, even though their compatibility could not be conclusively established due to

contamination. This approach acknowledges the complexity of microbial interactions and the possibility of emergent properties arising from the coexistence of multiple strains.

4.3. Technology Deployment

4.3.1. Nanophotocatalysis treatment

Perfluorohexanoic acid and trifloxystrobin were used in this assay to verify the degradation ability of TiO_2 and ZnO nanoparticles.

Table 4.1 presents the results of the nanoparticles treatment for the degradation of the compounds Trifloxystrobin and Perfluorohexanoic acid with 1 mgL^{-1} of concentration. The study aimed to assess the effectiveness of TiO_2 and ZnO nanoparticles in the nanophotocatalytic degradation of these compounds. This table provides a comparative analysis of the defluorination percentages achieved by each nanoparticle of concentration of 1 gL^{-1} and the corresponding treatment duration.

Table 4.1: Data obtained from fluoride potentiometry for the analysis of the degradation capability of nanophotocatalysis technology.

	ZnO		**TiO_2**	
	Perfluorohexanoic acid	**Trifloxystrobin**	**Perfluorohexanoic acid**	**Trifloxystrobin**
0h	0	0	0	0
6 h	0	27.41%	1.79%	0

In the case of trifloxystrobin, treatment of a solution containing 1 mgL^{-1} of this compound with ZnO nanoparticles led to a defluorination of 27% within a 6-hour timeframe. This indicates that ZnO nanoparticles possess the necessary photocatalytic properties to initiate the degradation process of trifloxystrobin. The photocatalytic activity of ZnO nanoparticles can be attributed to their unique crystal structure and bandgap properties, which enable them to generate reactive oxygen species (ROS) upon exposure to ultraviolet light (UV) [123]. These ROS species play a crucial role in breaking down organic compounds through oxidative processes. On the other hand, the results showed that ZnO nanoparticles were not capable of degrading perfluorohexanoic acid at a concentration of 1 mgL^{-1}. This suggests that perfluorohexanoic acid is more stable and less reactive than trifloxystrobin. Different compounds can exhibit varying degrees of susceptibility to photocatalytic degradation, depending on their molecular structure,

stability, and reactivity towards ROS. In the case of perfluorohexanoic acid, its chemical composition may hinder its interaction with the ZnO nanoparticles, resulting in the observed lack of degradation.

The TiO_2 nanoparticles showed limited to no degradation for the tested compounds. TiO2 has several limitations in its practical applications due to the high probability of recombination of photogenerated electron holes coexisting in TiO_2 particles [124]. The high probability of recombination of photogenerated electron holes in TiO_2 particles means that when TiO_2 is exposed to light, it generates pairs of electrons and electron holes. These electron-hole pairs are crucial for the photocatalytic activity of TiO_2, as they participate in chemical reactions that lead to the degradation of pollutants or the production of reactive oxygen species. However, in practical applications, there is a significant likelihood that these photogenerated electron-hole pairs recombine with each other before they can participate in desired chemical reactions. This recombination process occurs when electrons and holes encounter each other and cancel each other out, resulting in a loss of their individual reactivity. The recombination of photogenerated electron holes reduces the efficiency of TiO_2-based processes, such as photocatalysis, for pollutant degradation. It means that a portion of the electron-hole pairs, which could potentially contribute to the desired chemical reactions, are lost due to recombination, leading to a lower overall reaction rate.

4.3.2. Bioremediation treatment

Figure 4.5 shows the results for the biodegradation of perfluorohexanoic acid and trifloxystrobin, by the consortium constructed with the strains that showed the best results in the degradation of fluoroacetate, fluorobenzene, paroxetine and epoxiconazole.

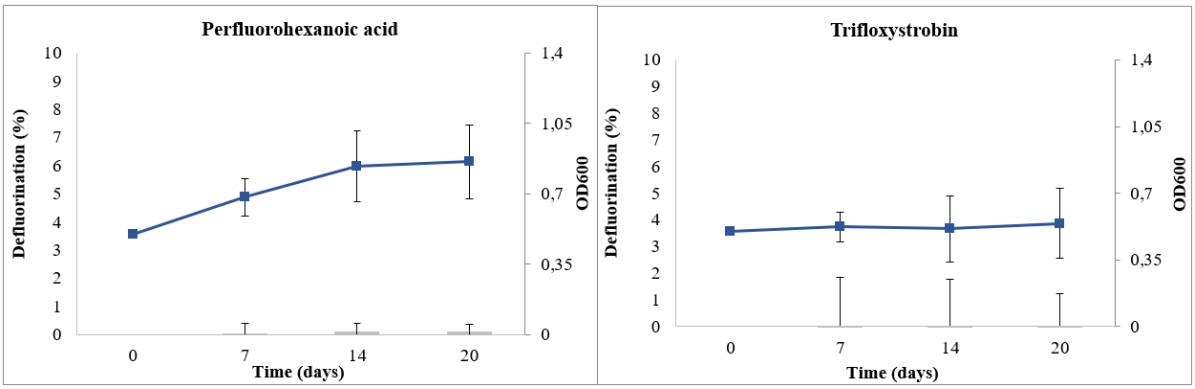

Figure 4.5: Efficiency of the constructed consortium to degrade the compounds perfluorohexanoic acid and trifloxystrobin. The % of defluorination is represented by the bars and OD measurement is represented by the line.

The results obtained from the assay using the consortium composed of strains 3EE, DPS 8, F11, and COL 5 for the degradation of perfluorohexanoic acid and trifloxystrobin were unexpected, as limited defluorination efficiencies were observed for either compound.

There are several potential explanations for the lack of defluorination by the consortium. Firstly, it is possible that the selected strains do not possess the necessary enzymes or metabolic pathways to degrade perfluorohexanoic acid and trifloxystrobin. These compounds may have specific chemical structures that require specialized enzymes for efficient degradation, which the strains in the consortium may lack. It is worth noting that the degradation of perfluorohexanoic acid and trifloxystrobin is expected to be a complex process that may involve multiple enzymatic steps and metabolic reactions. The absence or limited expression of specific catabolic enzymes required for the degradation of these compounds could have contributed to the observed results.

In addition, the concentrations of the tested compounds and the exposure time may have influenced the degradation efficiency of the consortium. It is possible that the concentrations used in the trial were too high, inhibiting microbial activity and preventing effective defluorination. According to the literature [40], trifloxystrobin can be found at concentrations of 0.73 μgL^{-1} in aquatic matrices which is a much lower concentration than the one tested. PFHxA can be present at concentrations up to 0.4-4.7 ngL^{-1} [38], which is also much lower than the one tested in this study. The concentrations used in the study were chosen given the limitation regarding the quantification of fluoride. Similarly, the duration of the trial may not have been sufficient for the consortium to fully degrade the compounds, requiring longer exposure times for further adaptation or optimization of growth conditions.

Furthermore, it is important to consider the compatibility and synergistic interactions among the selected strains in the consortium. The lack of defluorination observed could indicate that the strains were not compatible or did not exhibit synergistic effects necessary for efficient degradation of perfluorohexanoic acid and trifloxystrobin. Incompatibilities or competition for resources within the consortium may have hindered the overall degradation process.

4.3.3. Implementation of hybrid technology

In environmental remediation, the combination of different technologies can increase the efficiency of pollutants degradation. In this study, a hybrid approach was employed, in which ZnO and TiO_2 nanoparticles were used for the nanophotocatalytic treatment of perfluorohexanoic acid and trifloxystrobin, and the bacterial consortium constructed previously was employed to treat the effluent resultant from the nanophotocatalytic treatment. This hybrid approach was used to increase the chances of a successful biodegradation of the studied PFAS.

Given the previous setbacks encountered in using TiO_2 nanoparticles for the degradation of perfluorohexanoic acid and trifloxystrobin, as well as the unsuccessful degradation of perfluorohexanoic acid using ZnO nanoparticles, experiments combining nanophotocatalysis with bioremediation were not carried out for these three nanoparticles/PFAS combinations. Therefore, the decision was made to focus only on water samples containing trifloxystrobin subjected to photocatalytic treatment with ZnO nanoparticles, as the fluorides released in this treatment indicated some alteration in the initial structure of the molecule.

Figure 4.6 shows the results of the biodegradation of the tenfold-diluted effluent containing trifloxystrobin, after the photocatalytic treatment with ZnO nanoparticles.

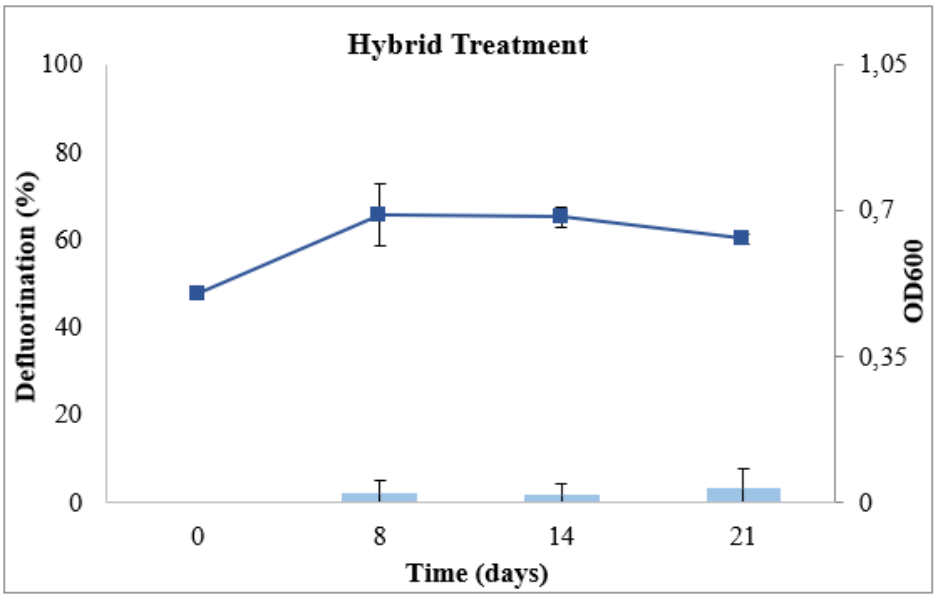

Figure 4.6: Biodegradation of the tenfold-diluted effluent containing trifloxystrobin (theoretical concentration of 1 mgL^{-1}), after the photocatalytic treatment with ZnO nanoparticles. The % of defluorination is represented by the bars and OD measurement is represented by the datapoints.

In environmental remediation, the combination of different technologies can increase the efficiency of pollutant degradation. In this study, a hybrid approach was employed, in which ZnO nanoparticles were used for the nanophotocatalytic treatment of trifloxystrobin and a synthetic consortium of bacterial strains was added to enhance the biodegradation process.

Interestingly, although the nanophotocatalytic treatment demonstrated a defluorination efficiency of up to 27%, the addition of the consortium resulted in a higher but rather limited percentage of degradation. Defluorination after 21 days, resulting from the pairing of the two technologies, resulted in a percentage of about 30%. Although this is not an extensive defluorination, it is a promising result given that the most relevant by-product of this compound retains the three fluorines present in its structure.

The introduction of the consortium as a secondary technology may have the potential to improve the overall degradation process. While nanophotocatalysis alone showed limited degradation capacity, the consortium could potentially target and degrade the intermediate by-products produced by the catalytic reaction. This sequential treatment approach could lead to a more complete and efficient degradation of trifloxystrobin, which did not occur.

The experiment to investigate the abiotic degradation of trifloxystrobin, showed that this did not occur and the experiment to analyze the ability of the synthetic consortium to adapt to the water sample containing trifloxystrobin and treated by nanophotocatalysis showed that the consortium, under these conditions, does not survive.

Chapter 5 – Conclusion and Suggestions for Future Work

The objectives of this study were to develop an efficient bioremediation technology for two PFAS, perfluorohexanoic acid and trifloxystrobin, based on a synthetic bacterial consortium with defluorination capacity, and to explore this technique as a secondary treatment in conjunction with a prior nanophotocatalysis treatment using ZnO and TiO_2 nanoparticles to remove PFAS from aquatic ecosystems.

The first approach involved selecting strains with better defluorination activity and assessing their biocompatibility. Four strains were chosen: *Delftia acidovorans* COL5 that showed the ability to degrade sodium fluoroacetate at a concentration of 50 mgL^{-1}; *Labrys portucalensis* strain F11 that demonstrated degradation of fluorobenzene at a concentration of 50 mgL^{-1}; Leadbetterella sp. DPS8, which exhibited approximately 20% defluorination of paroxetine at a concentration of 5 mgL^{-1}; and *Hydrogenophaga eletricum* strain 3EE that achieved around 20% degradation of the pesticide epoxiconazole at a concentration of 1 mgL^{-1}. Unfortunately, conclusive results could not be obtained from the biocompatibility assays due to contamination issues.

The subsequent approach involved analyzing photocatalytic and biodegradation treatments individually and in combination. Nanophotocatalysis showed interesting results for trifloxystrobin, as the ZnO nanoparticle treatment at a concentration of 1 gL^{-1} achieved a defluorination efficiency of 27% of trifloxystrobin. However, the same efficacy was not observed for perfluorohexanoic acid, and the TiO_2 nanoparticle did not exhibit defluorination for either of the studied compounds. The synthetic consortium individually was also unable to degrade the target PFASs, which can be attributed to the stability of these compounds and uncertainty regarding compatibility between the species. When the two technologies were combined, the synthetic consortium contributed, albeit to a limited extent, to the defluorination of a water sample resulting from photocatalytic treatment with ZnO nanoparticles containing the compound trifloxystrobin by about 30%.

In conclusion, the results demonstrate the challenges encountered in achieving efficient degradation of perfluorohexanoic acid and trifloxystrobin using the developed bioremediation technology. Although nanophotocatalysis with ZnO nanoparticles showed some potential to defluorinate trifloxystrobin, the synthetic consortium does not appear to have sufficient robustness to degrade these compounds. However, the union of

the two technologies allowed the defluorination efficiency of this compound to be around 30%. The complex nature of the compounds and uncertainties regarding compatibility between species likely contributed to these outcomes. Future research should focus on further exploring the compatibility and synergistic effects of different remediation techniques, improving the biocompatibility assessment methodology, and optimizing conditions for hybrid treatments. As well as testing other lower concentrations of the PFAS targeted in this study

Bibliographic References

1. Wong, M. H. (2012). Environmental Contamination. CRC Press eBooks. https://doi.org/10.1201/b12531

2. Ukaogo, P. O., Ewuzie, U., & Onwuka, C. V. (2020). Environmental pollution: causes, effects, and the remedies. In Elsevier eBooks (pp. 419–429). https://doi.org/10.1016/b978-0-12-819001-2.00021-8

3. Appannagari, R. R. R. (2017). Environmental Pollution Causes and Consequences: A study. ResearchGate, 3(8), 151-161.

4. Houtman, C. J. (2010). Emerging contaminants in surface waters and their relevance for the production of drinking water in Europe. Journal of Integrative Environmental Sciences, 7(4), 271–295. https://doi.org/10.1080/1943815x.2010.511648

5. Marine Pollution. (2022, May 20). National Geographic. Retrieved November 15, 2023, from https://education.nationalgeographic.org/resource/marine-pollution/

6. UNEP (2016). UNEP Frontiers 2016 Report: Emerging Issues of Environmental Concern. United Nations Environment Programme, Nairobi.

7. FAO, IFAD, UNICEF, WFP and WHO. 2020. The State of Food Security and Nutrition in the World 2020. Transforming food systems for affordable healthy diets. Rome, FAO. https://doi.org/10.4060/ca9692en

8. World Health Organization: WHO. (2022). Drinking-water. WHO. Retrieved February 16, 2023, from https://www.who.int/news-room/fact-sheets/detail/drinking-water

9. Suresh, K. R., & Nagesh, M. (2015). Experimental Studies on Effect of Water and Soil quality on Crop Yield. Aquatic Procedia, 4, 1235–1242. https://doi.org/10.1016/j.aqpro.2015.02.161

10. Circular Economy: Global Perspective. (2020). In Springer eBooks. https://doi.org/10.1007/978-981-15-1052-6

11. The Issue | US EPA. (2022, August 11). US EPA. Retrieved June 19, 2023, from https://www.epa.gov/nutrientpollution/issue

12. Emídio, V. J. G. (2012). A problemática do fósforo nas águas para consumo humano e águas residuais e soluções para o seu tratamento, Faculdade de Ciências e Tecnologia da Universidade do Algarve. 118pp.

13. ASAE [Autoridade de Segurança Alimentar e Económica]. (2007, April). Nitratos. ASAE. Retrieved June 19, 2023, from https://www.asae.gov.pt/seguranca-alimentar/riscos-quimicos/nitratos.aspx

14. Morin-Crini, N., Sharma, V. K., Zheng, M., Balaram, V., Ribeiro, A. C., Lu, Z., Stock, F., Carmona, E., Teixeira, M. R., Picos-Corrales, L. A., Moreno-Piraján, J. C., Giraldo, L., Li, C., Pandey, A., Hocquet, D., Torri, G., & Crini, G. (2022). Worldwide cases of water pollution by emerging contaminants: a review. Environmental Chemistry Letters, 20(4), 2311–2338. https://doi.org/10.1007/s10311-022-01447-4

15. Department of Environment and Science. (2022, July 8). Oil spill response. Environment | Department of Environment and Science, Queensland. Retrieved June 19, 2023, from https://environment.des.qld.gov.au/management/water/pollution/oil-spill-response

16. Kumar, J., Krithiga, T., Sathish, S., Renita, A. A., Prabu, D. L., Lokesh, S., Geetha, R., Namasivayam, S. K. R., & Sillanpaa, M. (2022). Persistent organic pollutants in water resources: Fate, occurrence, characterization and risk analysis. Science of the Total Environment, 831, 154808. https://doi.org/10.1016/j.scitotenv.2022.154808

17. Alharbi, O. M., Basheer, A. A., Khattab, R. A., & Ali, I. (2018). Health and environmental effects of persistent organic pollutants. Journal of Molecular Liquids, 263, 442–453. https://doi.org/10.1016/j.molliq.2018.05.029

18. Fry, K., & Power, M. C. (2017). Persistent organic pollutants and mortality in the United States, NHANES 1999–2011. Environmental Health, 16(1). https://doi.org/10.1186/s12940-017-0313-6

19. Nutrition, C. F. F. S. a. A. (2023). Per- and Polyfluoroalkyl Substances (PFAS). U.S. Food And Drug Administration. https://www.fda.gov/food/environmental-contaminants-food/and-polyfluoroalkyl-substances-pfas

20. Brooke, D., Footitt, A., & Nwaogu, T. (2004). Environmental Risk Evaluation Report: Perfluorooctanesulphonate (PFOS). In EPA. EPA (Environmental Protection Agency).

21. Houde, M., De Silva, A. O., Muir, D. C. G., & Letcher, R. J. (2011). Monitoring of Perfluorinated Compounds in Aquatic Biota: An Updated Review. Environmental Science & Technology, 45(19), 7962–7973. https://doi.org/10.1021/es104326w

22. A New OECD Definition for Per- and Polyfluoroalkyl Substances. Zhanyun Wang, Andreas M. Buser, Ian T. Cousins, Silvia Demattio, Wiebke Drost, Olof Johansson, Koichi Ohno, Grace Patlewicz, Ann M. Richard, Glen W. Walker, Graham S. White, Eeava Leinala. 23, s.l. : Environmental Science & Technology , 2021, Vol. 55. ISSN 15575-15578

23. Organization for Economic Co-operation and Development [OECD]. (2018). Toward a new comprehensive global database of per- and polyfluoroalkyl substances (PFASs): Summary report on updating the OECD 2007 list of per- and polyfluoroalkyl substances (PFASs). In OECD. Organization for Economic Co-operation and Development.

24. Tavasoli, E. (2020). Distribution and Fate of Per- and Polyfluorinated Alkyl Substances (PFAS) in Wastewater Treatment Plants Discharging to Great Bay, University of New Hampshire. 157pp

25. Guanghui, D., & Willie, P. (2009). Physicochemical Properties and Aquatic Toxicity of Poly- and Perfluorinated Compounds. Environmental Science and Technology, 43(6), 598–678.

26. Interstate Technology and Regulatory Council [(ITRC)]. (2017, July). Fact Sheets – PFAS — Per- and Polyfluoroalkyl Substances. ITRC. Retrieved May 30, 2023, from https://pfas-1.itrcweb.org/fact-sheets/

27. OECD(2013), OECD/UNEP Global PFC Group, Synthesis paper on per- and polyfluorinated chemicals (PFCs), Environment, Health and Safety, Environment Directorate, OECD

28. Bhhatarai, B., & Gramatica, P. (2010). Prediction of Aqueous Solubility, Vapor Pressure and Critical Micelle Concentration for Aquatic Partitioning of Perfluorinated Chemicals. Environmental Science & Technology, 45(19), 8120–8128. https://doi.org/10.1021/es101181g

29. Su, A., & Rajan, K. (2021). A database framework for rapid screening of structure-function relationships in PFAS chemistry. Scientific Data, 8(1). https://doi.org/10.1038/s41597-021-00798-x

30. O'Hagan, D. (2008). Understanding organofluorine chemistry. An introduction to the C–F bond. Chemical Society Reviews, 37(2), 308–319. https://doi.org/10.1039/b711844a

31. Codling, G., Hosseini, S., Corcoran, M. B., Bonina, S., Lin, T., Li, A., Ahmed, M. M., Rockne, K. J., Ji, K., Peng, H., & Giesy, J. P. (2018). Current and historical concentrations of poly and perfluorinated compounds in sediments of the northern Great Lakes – Superior, Huron, and Michigan. Environmental Pollution, 236, 373–381. https://doi.org/10.1016/j.envpol.2018.01.065

32. Ahrens, L. A. (2011). Polyfluoroalkyl compounds in the aquatic environment: a review of their occurrence and fate. Journal of Environmental Monitoring, 13(1), 20–31. https://doi.org/10.1039/c0em00373e

33. Prevedouros, K., Cousins, I. T., Buck, R. C., & Korzeniowski, S. H. (2005). Sources, Fate and Transport of Perfluorocarboxylates. Environmental Science & Technology, 40(1), 32–44. https://doi.org/10.1021/es0512475

34. Rahman, M. M., Peldszus, S., & Anderson, W. F. (2014). Behaviour and fate of perfluoroalkyl and polyfluoroalkyl substances (PFASs) in drinking water treatment: A review. Water Research, 50, 318–340. https://doi.org/10.1016/j.watres.2013.10.045

35. Shoemaker, J. & Dan Tettenhorst. (2018). Method 537.1: Determination of Selected Per- and Polyfluorinated Alkyl Substances in Drinking Water by Solid Phase Extraction and Liquid Chromatography/Tandem Mass Spectrometry (LC/MS/MS). U.S. Environmental Protection Agency, Office of Research and Development, National Center for Environmental Assessment, Washington, DC

36. Alexandrino, D. A., Almeida, C. M. R., Mucha, A. P., & Ferriani, M. D. G. C. (2022). Revisiting pesticide pollution: The case of fluorinated pesticides. Environmental Pollution, 292, 118315. https://doi.org/10.1016/j.envpol.2021.118315

37. Anderson, J., Luz, A. L., Goodrum, P. E., & Durda, J. L. (2019). Perfluorohexanoic acid toxicity, part II: Application of human health toxicity value for risk characterization. Regulatory Toxicology and Pharmacology, 103, 10–20. https://doi.org/10.1016/j.yrtph.2019.01.020

38. Sharma, B., Bharat, G. K., Tayal, S., Larssen, T., Bečanová, J., Karásková, P., Whitehead, P., Bishop, K., Butterfield, D., & Nizzetto, L. (2016). Perfluoroalkyl substances (PFAS) in river and ground/drinking water of the Ganges River basin:

Emissions and implications for human exposure. Environmental Pollution, 208, 704–713. https://doi.org/10.1016/j.envpol.2015.10.050

39. Rericha, Y., Truong, L., Leong, C., Cao, D., Field, J. A., & Tanguay, R. L. (2022). Dietary Perfluorohexanoic Acid (PFHxA) Exposures in Juvenile Zebrafish Produce Subtle Behavioral Effects across Generations. Toxics, 10(7), 372. https://doi.org/10.3390/toxics10070372

40. Wang, H., Qiu, T., Lu, J., Liu, H., Hu, L., Liu, L., & Chen, J. (2021). Potential aquatic environmental risks of trifloxystrobin: Enhancement of virus susceptibility in zebrafish through initiation of autophagy. Zoological Research, 42(3), 339–349. https://doi.org/10.24272/j.issn.2095-8137.2021.056

41. Ahrens, L. A., & Bundschuh, M. (2014). Fate and effects of poly- and perfluoroalkyl substances in the aquatic environment: A review. Environmental Toxicology and Chemistry, 33(9), 1921–1929. https://doi.org/10.1002/etc.2663

42. Liu, Z., Lu, Y., Wang, P., Wang, T., Liu, S., Johnson, A. D., Sweetman, A. J., & Baninla, Y. (2017). Pollution pathways and release estimation of perfluorooctane sulfonate (PFOS) and perfluorooctanoic acid (PFOA) in central and eastern China. Science of the Total Environment, 580, 1247–1256. https://doi.org/10.1016/j.scitotenv.2016.12.085

43. Xiao, F., Halbach, T. R., Simcik, M. F., & Gulliver, J. S. (2012). Input characterization of perfluoroalkyl substances in wastewater treatment plants: Source discrimination by exploratory data analysis. Water Research, 46(9), 3101–3109. https://doi.org/10.1016/j.watres.2012.03.027

44. European Union [EU]. (2020, February 19). Communication From the Commission to the European Parliament, The Council, The European Economic And Social Committee And The Committee Of The Regions. EUR-Lex. Retrieved April 5, 2023, from https://eur-lex.europa.eu/legal-content/EN/TXT/?uri=CELEX%3A52020DC0066

45. Post, G. B., Cohn, P., & Cooper, K. D. (2012). Perfluorooctanoic acid (PFOA), an emerging drinking water contaminant: A critical review of recent literature. Environmental Research, 116, 93–117. https://doi.org/10.1016/j.envres.2012.03.007

46. Wang, P., Lu, Y., Wang, T., Fu, Y., Zhu, Z., Liu, S., Xie, S., Xiao, Y., & Giesy, J. P. (2014). Occurrence and transport of 17 perfluoroalkyl acids in 12 coastal rivers in south

Bohai coastal region of China with concentrated fluoropolymer facilities. Environmental Pollution, 190, 115–122. https://doi.org/10.1016/j.envpol.2014.03.030

47. Yeung, L. W. Y., & Mabury, S. A. (2016). Are humans exposed to increasing amounts of unidentified organofluorine? Environmental Chemistry, 13(1), 102. https://doi.org/10.1071/en15041

48. Knutsen, H., Mæhlum, T., Haarstad, K., Slinde, G. A., & Arp, H. P. H. (2019). Leachate emissions of short- and long-chain per- and polyfluoralkyl substances (PFASs) from various Norwegian landfills. Environmental Science: Processes & Impacts, 21(11), 1970–1979. https://doi.org/10.1039/c9em00170k

49. Kwok, K. Y., Yamazaki, E., Yamashita, N., Taniyasu, S., Murphy, M., Horii, Y., Petrick, G., Kallerborn, R., Kannan, K., Murano, K., & Lam, P. K. (2013). Transport of Perfluoroalkyl substances (PFAS) from an arctic glacier to downstream locations: Implications for sources. Science of the Total Environment, 447, 46–55. https://doi.org/10.1016/j.scitotenv.2012.10.091

50. Yang, L., Tian, S., Zhu, L., Liu, Z., & Zhang, Y. (2012). Bioaccumulation and distribution of perfloroalkyl acids in seafood products from Bohai Bay, China. Environmental Toxicology and Chemistry, 31(9), 1972–1979. https://doi.org/10.1002/etc.1917

51. Simonnet-Laprade, C., Budzinski, H., Maciejewski, K., Menach, K. L., Santos, R. F., Alliot, F., Goutte, A., & Labadie, P. (2019). Biomagnification of perfluoroalkyl acids (PFAAs) in the food web of an urban river: assessment of the trophic transfer of targeted and unknown precursors and implications. Environmental Science: Processes & Impacts, 21(11), 1864–1874. https://doi.org/10.1039/c9em00322c

52. Barbosa, M. O., Ratola, N., Homem, V., Pereira, M. F. R., Silva, A. M., Ribeiro, A. C., Llorca, M., & Farré, M. (2023). Per- and Poly-Fluoroalkyl Substances in Portuguese Rivers: Spatial-Temporal Monitoring. Molecules, 28(3), 1209. https://doi.org/10.3390/molecules28031209

53. Hoffman, K., Webster, T. F., Bartell, S. M., Weisskopf, M. G., Fletcher, T., & Vieira, V. M. (2011). Private drinking water wells as a source of exposure to perfluorooctanoic acid (PFOA) in communities surrounding a fluoropolymer production

facility. *Environmental health perspectives*, *119*(1), 92–97. https://doi.org/10.1289/ehp.1002503

54. Agency For Toxic Substances And Disease Registry (2020). Toxicological Profile for Perfluoroalkyls. Retrieved April 16, 2023, from Https://Www.Atsdr.Cdc.Gov/Toxprofiles/Tp200.Pdf

55. Braun, J. M., Chen, A., Romano, M. E., Calafat, A. M., Webster, G. M., Yolton, K., & Lanphear, B. P. (2016). Prenatal perfluoroalkyl substance exposure and child adiposity at 8 years of age: The HOME study. *Obesity (Silver Spring, Md.)*, *24*(1), 231–237. https://doi.org/10.1002/oby.21258

56. National Service Center for Environmental Publications [NSCEP]. (2014). Emerging Contaminants Perfluorooctane Sulfonate (PFOS) and Perfluorooctanoic Acid (PFOA). EPA. Retrieved June 20, 2023, from https://nepis.epa.gov/Exe/ZyNET.exe/P100LTG6.TXT?ZyActionD=ZyDocument&Client=EPA&Index=2011+Thru+2015&Docs=&Query=&Time=&EndTime=&SearchMethod=1&TocRestrict=n&Toc=&TocEntry=&QField=&QFieldYear=&QFieldMonth=&QFieldDay=&IntQFieldOp=0&ExtQFieldOp=0&XmlQuery=&File=D%3A%5Czyfiles%5CIndex%20Data%5C11thru15%5CTxt%5C00000014%5CP100LTG6.txt&User=ANONYMOUS&Password=anonymous&SortMethod=h%7C-&MaximumDocuments=1&FuzzyDegree=0&ImageQuality=r75g8/r75g8/x150y150g16/i425&Display=hpfr&DefSeekPage=x&SearchBack=ZyActionL&Back=ZyActionS&BackDesc=Results%20page&MaximumPages=1&ZyEntry=1&SeekPage=x&ZyPURL

57. Martin, J. W., Mabury, S. A., Solomon, K. R., & Muir, D. C. (2003). Bioconcentration and tissue distribution of perfluorinated acids in rainbow trout (Oncorhynchus mykiss). *Environmental toxicology and chemistry*, *22*(1), 196–204.

58. Luebker, D. J., Hansen, K. J., Bass, N. M., Butenhoff, J. L., & Seacat, A. M. (2002). Interactions of fluorochemicals with rat liver fatty acid-binding protein. *Toxicology*, *176*(3), 175–185. https://doi.org/10.1016/s0300-483x(02)00081-1

59. Ahrens, L., Siebert, U., & Ebinghaus, R. (2009). Total body burden and tissue distribution of polyfluorinated compounds in harbor seals (Phoca vitulina) from the German Bight. *Marine pollution bulletin*, *58*(4), 520–525. https://doi.org/10.1016/j.marpolbul.2008.11.030

60. Shi, Y., Wang, J., Pan, Y., & Cai, Y. (2012). Tissue distribution of perfluorinated compounds in farmed freshwater fish and human exposure by consumption. *Environmental toxicology and chemistry*, *31*(4), 717–723. https://doi.org/10.1002/etc.1758

61. Inoue, Y., Hashizume, N., Yakata, N., Murakami, H., Suzuki, Y., Kikushima, E., & Otsuka, M. (2012). Unique physicochemical properties of perfluorinated compounds and their bioconcentration in common carp Cyprinus carpio L. *Archives of environmental contamination and toxicology*, *62*(4), 672–680. https://doi.org/10.1007/s00244-011-9730-7

62. Kwadijk, C. J., Korytár, P., & Koelmans, A. A. (2010). Distribution of perfluorinated compounds in aquatic systems in the Netherlands. *Environmental science & technology*, *44*(10), 3746–3751. https://doi.org/10.1021/es100485e

63. Labadie, P., & Chevreuil, M. (2011). Partitioning behaviour of perfluorinated alkyl contaminants between water, sediment and fish in the Orge River (nearby Paris, France). *Environmental pollution (Barking, Essex : 1987)*, *159*(2), 391–397. https://doi.org/10.1016/j.envpol.2010.10.039

64. Benskin, J. P., Holt, A., & Martin, J. W. (2009). Isomer-specific biotransformation rates of a perfluorooctane sulfonate (PFOS)-precursor by cytochrome P450 isozymes and human liver microsomes. *Environmental science & technology*, *43*(22), 8566–8572. https://doi.org/10.1021/es901915f

65. Sharpe, R. L., Benskin, J. P., Laarman, A. H., Macleod, S. L., Martin, J. W., Wong, C. S., & Goss, G. G. (2010). Perfluorooctane sulfonate toxicity, isomer-specific accumulation, and maternal transfer in zebrafish (Danio rerio) and rainbow trout (Oncorhynchus mykiss). *Environmental toxicology and chemistry*, *29*(9), 1957–1966. https://doi.org/10.1002/etc.257

66. Lee, J. J., & Schultz, I. R. (2010). Sex differences in the uptake and disposition of perfluorooctanoic acid in fathead minnows after oral dosing. *Environmental science & technology*, *44*(1), 491–496. https://doi.org/10.1021/es901838y

67. Giesy, J. P., & Kannan, K. (2001). Global distribution of perfluorooctane sulfonate in wildlife. *Environmental science & technology*, *35*(7), 1339–1342. https://doi.org/10.1021/es001834k

68. Houde, M., Martin, J. W., Letcher, R. J., Solomon, K. R., & Muir, D. C. (2006). Biological monitoring of polyfluoroalkyl substances: A review. *Environmental science & technology*, *40*(11), 3463–3473. https://doi.org/10.1021/es052580b

69. Gebbink, W. A., Letcher, R. J., Hebert, C. E., & Weseloh, D. V. C. (2011). Twenty years of temporal change in perfluoroalkyl sulfonate and carboxylate contaminants in herring gull eggs from the Laurentian Great Lakes. Journal of Environmental Monitoring, 13(12), 3365. https://doi.org/10.1039/c1em10663e

70. Loi, E. I., Yeung, L. W., Taniyasu, S., Lam, P. K., Kannan, K., & Yamashita, N. (2011). Trophic magnification of poly- and perfluorinated compounds in a subtropical food web. *Environmental science & technology*, *45*(13), 5506–5513. https://doi.org/10.1021/es200432n

71. Ahrens, L., & Bundschuh, M. (2014). Fate and effects of poly- and perfluoroalkyl substances in the aquatic environment: a review. *Environmental toxicology and chemistry*, *33*(9), 1921–1929. https://doi.org/10.1002/etc.2663

72. Butt, C. M., Muir, D. C., & Mabury, S. A. (2014). Biotransformation pathways of fluorotelomer-based polyfluoroalkyl substances: a review. *Environmental toxicology and chemistry*, *33*(2), 243–267. https://doi.org/10.1002/etc.2407

73. Giesy, J. P., Naile, J. E., Khim, J. S., Jones, P. D., & Newsted, J. L. (2010). Aquatic toxicology of perfluorinated chemicals. *Reviews of environmental contamination and toxicology*, *202*, 1–52. https://doi.org/10.1007/978-1-4419-1157-5_1

74. Guanghui Ding & Willie J. G. M. Peijnenburg (2013): Physicochemical Properties and Aquatic Toxicity of Poly- and Perfluorinated Compounds, Critical Reviews in Environmental Science and Technology, 43:6, 598-678

75. European Comission. (2022, October). Water Framework Directive. Environment. Retrieved February 16, 2023, from https://environment.ec.europa.eu/topics/water/water-framework-directive_en

76. Summary of the Clean Water Act | US EPA. (2023, June 22). US EPA. Retrieved February 16, 2023, from https://www.epa.gov/laws-regulations/summary-clean-water-act

77. Gómez-Baggethun, E., De Groot, R., Lomas, P. L., & Montes, C. (2010). The history of ecosystem services in economic theory and practice: From early notions to markets and payment schemes. Ecological Economics, 69(6), 1209–1218. https://doi.org/10.1016/j.ecolecon.2009.11.007

78. Greene, C. (2022, October 27). EQS: Full ban of PFAS needed to meet environmental thresholds. Retrieved June 26, 2023, from https://www.eureau.org/news/729-eqs-full-ban-of-pfas-needed-to-meet-environmental-thresholds

79. Interstate Technology and Regulatory Council [ITRC]. (2022, June). 8 Basis of Regulations – PFAS — Per- and Polyfluoroalkyl Substances. Interstate Technology and Regulatory Council. Retrieved December 26, 2022, from https://pfas-1.itrcweb.org/8-basis-of-regulations/

80. Stockholm Convention on Persistent Organic. (2022). Proposal To List Long-Chain Perfuorocarboxylic Acids, Their Salts and Related Compounds in Annexes A, B and/or C to The Stockholm Convention On Persistent Organic Pollutants. Retrieved June 26, 2023, from Https://Chm.Pops.Int/.

81. European Chemicals Agency [ECHA]. (2011). Lista de substâncias que suscitam elevada preocupação candidatas a autorização - ECHA. ECHA. Retrieved June 1, 2023, from https://echa.europa.eu/pt/candidate-list-table

82. European Chemicals Agency [(ECHA)]. (2022). ANNEX XV RESTRICTION REPORT: Per- and polyfluoroalkyl substances (PFAS) in firefighting foams. In European Chemicals Agency (ECHA).

83. Korzeniowski, S. H., Buck, R. C., Newkold, R. M., Kassmi, A. E., Laganis, E., Matsuoka, Y., Dinelli, B., Beauchet, S., Adamsky, F., Weilandt, K., Soni, V. K., Kapoor, D., Gunasekar, P., Malvasi, M., Brinati, G., & Musio, S. (2023). A critical review of the application of polymer of low concern regulatory criteria to fluoropolymers II: Fluoroplastics and fluoroelastomers. *Integrated environmental assessment and management*, *19*(2), 326–354. https://doi.org/10.1002/ieam.4646

84. Henry, B. J., Carlin, J. P., Hammerschmidt, J. A., Buck, R. C., Buxton, L. W., Fiedler, H., Seed, J., & Hernandez, O. (2018). A critical review of the application of polymer of low concern and regulatory criteria to fluoropolymers. *Integrated environmental assessment and management*, *14*(3), 316–334. https://doi.org/10.1002/ieam.4035

85. Hélène, N. (2023). Plan d'action ministériel sur les PFAS. Ministères Écologie Énergie Territoires. https://www.ecologie.gouv.fr/plan-daction-ministeriel-sur-pfas

86. Diário Da República. (2017). Decreto-Lei n.º 152/2017, de 7 de dezembro. Diário da República, Série I, n.º 234, de 7 de dezembro de 2017

87. Menezes, Gui Manuel Machado. (2018). Portaria n.º 57/2018 de 30 de maio de 2018. S.L.: Secretaria Regional do Mar, Ciência e Tecnologia

88. Diário Da República. (2017). Decreto-Lei n.º 152B/2017, de 7 de dezembro. Diário da República, Série I, n.º 234, de 7 de dezembro de 2017

89. Appleman, T. D., Higgins, C. P., Quiñones, O., Vanderford, B. J., Kolstad, C., Zeigler-Holady, J. C., & Dickenson, E. R. (2014). Treatment of poly- and perfluoroalkyl substances in U.S. full-scale water treatment systems. *Water research*, *51*, 246–255. https://doi.org/10.1016/j.watres.2013.10.067

90. Interstate Technology and Regulatory Council [ITRC]. (2018). Treatment Technologies and Methods for Per- and Polyfluoroalkyl Substances (PFAS). In ITRC.

91. Deng, S., Nie, Y., Du, Z., Huang, Q., Meng, P., Wang, B., Huang, J., & Yu, G. (2015). Enhanced adsorption of perfluorooctane sulfonate and perfluorooctanoate by bamboo-derived granular activated carbon. *Journal of hazardous materials*, *282*, 150–157. https://doi.org/10.1016/j.jhazmat.2014.03.045

92. Senevirathna, S. T., Tanaka, S., Fujii, S., Kunacheva, C., Harada, H., Shivakoti, B. R., & Okamoto, R. (2010). A comparative study of adsorption of perfluorooctane sulfonate (PFOS) onto granular activated carbon, ion-exchange polymers and non-ion-exchange polymers. *Chemosphere*, *80*(6), 647–651. https://doi.org/10.1016/j.chemosphere.2010.04.053

93. Chen, W., Zhang, X., Mamadiev, M., & Wang, Z. (2017). Sorption of perfluorooctane sulfonate and perfluorooctanoate on polyacrylonitrile fiber-derived activated carbon fibers: in comparison with activated carbon. RSC Advances, 7(2), 927–938. https://doi.org/10.1039/c6ra25230c

94. Chularueangaksorn, P., Tanaka, S., Fujii, S., & Kunacheva, C. (2013). Batch and column adsorption of perfluorooctane sulfonate on anion exchange resins and granular

activated carbon. Journal of Applied Polymer Science, 131(3), n/a. https://doi.org/10.1002/app.39782

95. Westreich, P., Mimna, R., Brewer, J., & Forrester, F. (2018). The removal of short-chain and long-chain perfluoroalkyl acids and sulfonates via granular activated carbons: A comparative column study. Remediation Journal, 29(1), 19–26. https://doi.org/10.1002/rem.21579

96. Lenntech. (2018). PFAS removal by activated carbon adsorption. Retrieved December 13, 2022, from https://www.lenntech.com/processes/pfas-removal-by-activated-carbon-adsorption.htm

97. Huang, W., Zhang, H., Huang, Y., Wang, W., & Wei, S. (2011). Hierarchical porous carbon obtained from animal bone and evaluation in electric double-layer capacitors. Carbon, 49(3), 838–843. https://doi.org/10.1016/j.carbon.2010.10.025

98. Largitte, L., & Pasquier, R. (2016). A review of the kinetics adsorption models and their application to the adsorption of lead by an activated carbon. Chemical Engineering Research & Design, 109, 495–504. https://doi.org/10.1016/j.cherd.2016.02.006

99. Ross, I., McDonough, J. K., Miles, J., Storch, P., Kochunarayanan, P. T., Kalve, E., Hurst, J., Dasgupta, S. S., & Burdick, J. (2018). A review of emerging technologies for remediation of PFASs. Remediation Journal, 28(2), 101–126. https://doi.org/10.1002/rem.21553

100. Vo, H. N. P., Ngo, H. H., Guo, W., Nguyen, T. H. O., Li, J., Li, G., Deng, L., Chen, Z., & Nguyen, T. H. O. (2020). Poly-and perfluoroalkyl substances in water and wastewater: A comprehensive review from sources to remediation. Journal of Water Process Engineering, 36, 101393. https://doi.org/10.1016/j.jwpe.2020.101393

101. Du, Z., Deng, S., Bei, Y., Huang, Q., Wang, B., Huang, J., & Yu, G. (2014). Adsorption behavior and mechanism of perfluorinated compounds on various adsorbents--a review. *Journal of hazardous materials*, *274*, 443–454. https://doi.org/10.1016/j.jhazmat.2014.04.038

102. Zhang, D. Q., Zhang, W. L., & Liang, Y. N. (2019). Adsorption of perfluoroalkyl and polyfluoroalkyl substances (PFASs) from aqueous solution - A review. *The Science of the total environment*, *694*, 133606. https://doi.org/10.1016/j.scitotenv.2019.133606

103. Lee, T. H., Speth, T. F., & Nadagouda, M. N. (2022). High-pressure membrane filtration processes for separation of Per- and polyfluoroalkyl substances (PFAS). Chemical Engineering Journal, 431, 134023. https://doi.org/10.1016/j.cej.2021.134023

104. Fernandes, J. O., Duarte, P., Almeida, C. M. R., Ferriani, M. D. G. C., & Mucha, A. P. (2020). Potential of bacterial consortia obtained from different environments for bioremediation of paroxetine and bezafibrate. Journal of Environmental Chemical Engineering, 8(4), 103881. https://doi.org/10.1016/j.jece.2020.103881

105. Harris, J., Coon, C. M., Doherty, M., McHugh, E. A., Warner, M., Walters, C. L., Orahood, O. M., Loesch, A. E., Hatfield, D. C., Sitko, J. C., Almand, E. A., & Steel, J. J. (2022). Engineering and characterization of dehalogenase enzymes from Delftia acidovorans in bioremediation of perfluorinated compounds. Synthetic and Systems Biotechnology, 7(2), 671–676. https://doi.org/10.1016/j.synbio.2022.02.005

106. Babu, S. G., Ashokkumar, M., & Neppolian, B. (2016). The Role of Ultrasound on Advanced Oxidation Processes. *Topics in current chemistry (Cham)*, *374*(5), 75. https://doi.org/10.1007/s41061-016-0072-9

107. Horst, J. A., McDonough, J. K., Ross, I., & Houtz, E. F. (2020). Understanding and Managing the Potential By-Products of PFAS Destruction. Ground Water Monitoring and Remediation, 40(2), 17–27. https://doi.org/10.1111/gwmr.12372

108. Bentel, M. J., Yu, Y., Xu, L., Li, Z., Wong, B. M., Men, Y., & Liu, J. (2019). Defluorination of Per- and Polyfluoroalkyl Substances (PFASs) with Hydrated Electrons: Structural Dependence and Implications to PFAS Remediation and Management. *Environmental science & technology*, *53*(7), 3718–3728. https://doi.org/10.1021/acs.est.8b06648

109. Alexandrino, D. A. M., Mucha, A. P., Almeida, C. M. R., & Carvalho, M. F. (2020). Microbial degradation of two highly persistent fluorinated fungicides - epoxiconazole and fludioxonil. *Journal of hazardous materials*, *394*, 122545. https://doi.org/10.1016/j.jhazmat.2020.122545

110. Alexandrino, D. A. M., Mucha, A. P., Tomasino, M. P., Almeida, C. M. R., & Carvalho, M. F. (2021). Combining Culture-Dependent and Independent Approaches for the Optimization of Epoxiconazole and Fludioxonil-Degrading Bacterial

Consortia. *Microorganisms*, *9*(10), 2109. https://doi.org/10.3390/microorganisms9102109

111. Carvalho, M. F., De Marco, P., Duque, A. F., Pacheco, C. C., Janssen, D. B., & Castro, P. M. (2008). Labrys portucalensis sp. nov., a fluorobenzene-degrading bacterium isolated from an industrially contaminated sediment in northern Portugal. *International journal of systematic and evolutionary microbiology*, *58*(Pt 3), 692–698. https://doi.org/10.1099/ijs.0.65472-0

112. Alexandrino, D. A., Ribeiro, I., Pinto, L. A., Cambra, R., Oliveira, R. F., Pereira, F., & Ferriani, M. D. G. C. (2018). Biodegradation of mono-, di- and trifluoroacetate by microbial cultures with different origins. New Biotechnology, 43, 23–29. https://doi.org/10.1016/j.nbt.2017.08.005

113. Perdigão, R., Almeida, C. M. R., Magalhães, C., Ramos, S., Carolas, A. L., Ferreira, B. S., Carvalho, M. F., & Mucha, A. P. (2021). Bioremediation of Petroleum Hydrocarbons in Seawater: Prospects of Using Lyophilized Native Hydrocarbon-Degrading Bacteria. *Microorganisms*, *9*(11), 2285. https://doi.org/10.3390/microorganisms9112285

114. Maruyama, T., Park, H. D., Ozawa, K., Tanaka, Y., Sumino, T., Hamana, K., Hiraishi, A., & Kato, K. (2006). Sphingosinicella microcystinivorans gen. nov., sp. nov., a microcystin-degrading bacterium. *International journal of systematic and evolutionary microbiology*, *56*(Pt 1), 85–89. https://doi.org/10.1099/ijs.0.63789-0

115. Fernandes, J. O., Duarte, P., Almeida, C. M. R., Ferriani, M. D. G. C., & Mucha, A. P. (2020b). Potential of bacterial consortia obtained from different environments for bioremediation of paroxetine and bezafibrate. Ournal of Environmental Chemical Engineering, 8(4), 103881. https://doi.org/10.1016/j.jece.2020.103881

116. Medical Microbiology. (2022). PCA Agar. Microbiologie Clinique. Retrieved March 30, 2023, from https://microbiologie-clinique.com/pca-agar-plate-count.html

117. R2A Agar | Neogen. (2022). Microbiologia. Retrieved March 30, 2023, from https://www.neogen.com/pt/categories/microbiology/r2a-agar/

118. Almeida, C. M. M. (2011). Ocorrência de fluoretos em sumos, néctares e refrigerantes comercializados em Portugal continental. https://repositorio.ul.pt/handle/10451/11219

119. Environmental Protection Agency [EPA]. (1995, June). Sodium Fluoroacetate. R.E.D. FACTS. Retrieved April 28, 2023, from https://www3.epa.gov/pesticides/chem_search/reg_actions/reregistration/fs_PC-075003_1-Jun-95.pdf

120. PubChem. (2023). Fluorobenzene. PubChem. Retrieved April 29, 2023, from https://pubchem.ncbi.nlm.nih.gov/compound/Fluorobenzene

121. PubChem. (2023). Paroxetine. PubChem. Retrieved April 29, 2023, from https://pubchem.ncbi.nlm.nih.gov/compound/Paroxetine

122. PubChem. (2023a). Epoxiconazole. PubChem. Retrieved April 29, 2023, from https://pubchem.ncbi.nlm.nih.gov/compound/Epoxiconazole

123. Mirzaei, A., Yerushalmi, L., Chen, Z., Haghighat, F., & Guo, J. (2018). Enhanced photocatalytic degradation of sulfamethoxazole by zinc oxide photocatalyst in the presence of fluoride ions: Optimization of parameters and toxicological evaluation. *Water research*, *132*, 241–251. https://doi.org/10.1016/j.watres.2018.01.016

124. Suhan, M. B. K., Shuchi, S. B., Al-Mamun, M. R., Roy, H., & Islam, M. S. (2023). Enhanced UV light-driven photocatalytic degradation of methyl orange using MoO3/WO3-fluorinated TiO2 nanocomposites. Environmental Nanotechnology, Monitoring and Management, 19, 100768. https://doi.org/10.1016/j.enmm.2022.100768

Appendices

The following appendices serve to provide and supplement additional information and arguments to support the research presented in the main body of the document.

A. Liquid and solid culture media preparation

Each medium was carefully measured and sterilized using autoclaving techniques to ensure its purity and sterility. The agar plates were prepared by pouring the media into sterile Petri dishes and allowing them to cool and solidify before use. The procedure followed for the realization of 1 liter of each medium is described in the Table A.1.

Table A.1: Nutrient composition of the culture media used to grow the preselected strains.

Medium		
PCA	**R2A**	**MSM**
Suspend 23.5 g of powder consisting of 1 g glucose, 5 g tryptone, 2.5 g yeast extract and 15 g agar.	Suspend 18.1 g of powder consisting of 0.5 g proteose peptone, yeast extract, acid digest of casein, glucose, and soluble starch, 0.3 sodium pyruvate and dipotassium phosphate, 0.024 g magnesium sulfate and 15 g agar.	2.7 g of Na_2HPO_4, 1.4 g of KH_2PO_4, 0.5 g of $(NH_4)_2SO_4$ and 0.2 g of $MgSO_4 \cdots 7H_2O$ and added in a schott flask and 10 mL of a trace element solution* was added

The trace element solution contains the following compounds: 12 g Disodium ethylenediaminetetraacetate dihydrate ($Na_2EDTA\text{-}2H_2O$), 2 g Sodium hydroxide (NaOH), 0.4 g Manganese (II) Sulfate Tetrahydrate ($MnSO_4\text{-}4H_2O$), 0.4 g Zinc sulfate heptahydrate ($ZnSO_4\text{-}7H_2O$), 0.5 mL concentrated Sulfuric acid (H_2SO_4), 10 g Sodium sulfate (Na_2SO_4), 0.1 g Sodium molybdate dihydrate ($Na_2MoO_4\text{-}2H_2O$), 2 g Iron (II) sulfate heptahydrate ($FeSO_4\text{-}7H_2O$), 0.1 g Copper (II) sulfate pentahydrate ($CuSO_4\text{-}5H_2O$), 1 g Calcium chloride ($CaCl_2$).

B. Assessment of the catabolic viability of the pre-selected bacterial strains

B.1. Sodium Fluoroacetate

This subsection contains the calculations and calibration curve for the compound sodium fluoroacetate that allowed to understand the viability of the strains under study. The Table B.1 shows the concentration values of the standards and the corresponding potential difference used to construct the calibration curve represented by the graph of Image B.1.

Table B.1: Concentration values and potential difference of standards for the viability assay concerning the compound sodium fluoroacetate.

mM [F^-]	Log mM	E (mV)
0.001	-3	-248.7
0.0025	-2.602	-259.8
0.005	-2.301	-277.5
0.01	-2	-294.5
0.02	-1.699	-311.9
0.1	-1	-353.6
0.2	-0.699	-370
1	0	-410.9

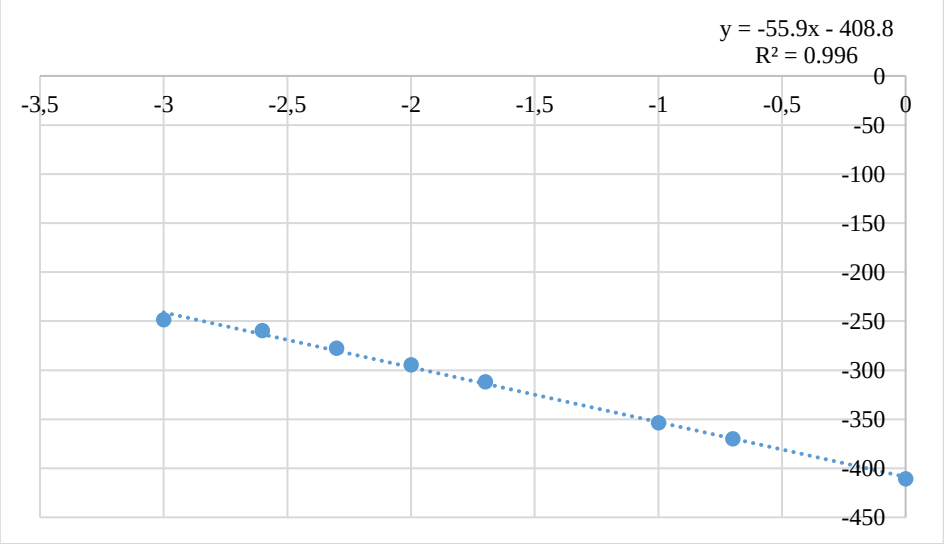

Figure B.1: Calibration curve obtained using the values in Table B.1 and the corresponding straight-line equation.

From the equation of the straight line, the concentration of [F^-] was determined. The Table B.2 shows the potential difference for each replicate of each strain and the values obtained in the calculation of free fluoride for the time of the beginning of the assay (T0).

Tabela B.2: Potential difference of each strain and the values obtained in the calculation of free fluoride for the moment T0 of the first sodium fluoroacetate assay.

	E (mV)	Log mM	mM [F-]
COL1 (1)	-266.2	-2.5510	0.0028
COL1 (2)	-246.7	-2.8998	0.0013
COL4 (1)	-268.2	-2.5152	0.0031
COL4 (2)	-245,.9	-2.9141	0.0012
COL5 (1)	-272.1	-2.4454	0.0036
COL5 (2)	-253.9	-2.7710	0.0017
COL10 (1)	-244.8	-2.9338	0.0012
COL10 (2)	-245.6	-2.9195	0.0012
COL16 (1)	-243.4	-2.9589	0.0011
COL16 (2)	-245.1	-2.9284	0.0012

Below is an example of the calculation for determining the F- concentration at T0 (start of the assay) for strain COL 1 (1).

$$Log_{10}[F-] = \frac{\left(-266.2 - (-408.8)\right)}{-55.9} \Leftrightarrow [F-] = 10^{-2.5510} \Leftrightarrow [F-] = 0.0028\, mM$$

The Table B.3 shows the potential difference for each replicate of each strain and the values obtained in the calculation of free fluoride after 8 days from the beginning of the assay (T8).

Table B.3: Potential difference of each strain and the values obtained in the calculation of free fluoride for the moment T8 of the first sodium fluoroacetate assay.

	E (mV)	Log mM	mM [F-]	[F-]Free	% Def	Med
COL1 (1)	-270.6	-2.4723	0.0034	0.0006	0.1118	0.24
COL1 (2)	-256.2	-2.7299	0.0019	0.0019	0.3725	
COL4 (1)	-299.1	-1.9624	0.0109	0.0109	2.1807	1.89
COL4 (2)	-291.6	-2.0966	0.0080	0.0080	1.6011	
COL5 (1)	-391.6	-0.3077	0.4924	0.4888	97.7605	97.55
COL5 (2)	-391.4	-0.3113	0.4883	0.4867	97.3309	

COL10 (1)	-337.7	-1.2719	0.0535	0.0535	10.6934	9.70
COL10 (2)	-332.7	-1.3614	0.0435	0.0435	8.7030	
COL16 (1)	-313.5	-1.7048	0.0197	0.0197	3.9464	3.82
COL16 (2)	-311.9	-1.7335	0.0185	0.0185	3.6947	

Below is an example of the calculation performed for the determination of free [F-], percentage of defluorination and the average of the replicates at T8 (since the start of the assay) for strain COL 1 (1).

$$Log_{10}[F-] = \frac{\left(-270.6-(-408.8)\right)}{-55.9} \Leftrightarrow [F-] = 10^{-2.4723} \Leftrightarrow [F-] = 0.0034\ mM$$

$$[F-]\ Free = 0.00337 - 0.00281 = 0.00056\ mM$$

Determination of the theoretical [F$^-$] concentration if there was complete defluorination.

Since the stoichiometry of the molecule is 1:1, then the concentration of free fluorides will be equal.

Massa Molar ($NaFC_2H_2O_2$) = 100 mg/L ---------- 1 mM

50 mg/L ---------- x mM

$$x = \frac{50 * 1}{100} = 0{,}5\ mM$$

$$\%\ Def = \frac{0.00056}{0.5} * 100 = 0.11\ \%$$

$$Med = \frac{0.11 + 0.37}{2} = 0.24\ \%$$

The Table B.4 shows the potential difference for each replicate of each strain and the values obtained in the calculation of free fluoride after 14 days from the beginning of the assay (T14).

Table B.4: Potential difference of each strain and the values obtained in the calculation of free fluoride for the moment T14 of the first sodium fluoroacetate assay.

	E (mV)	Log mM	mM [F-]	[F-]Free	% Def	Med
COL1 (1)	-282.8	-2.2540	0.0056	0.0056	1.1143	0.95

COL1 (2)	-274.2	-2.4079	0.0039	0.0039	0.7819	
COL4 (1)	-307.7	-1.8086	0.0155	0.0155	3.1077	2.77
COL4 (2)	-301.8	-1.9141	0.0122	0.0122	2.4372	
COL5 (1)	-392.2	-0.2970	0.5047	0.5047	100.9418	100.32
COL5 (2)	-391.9	-0.3023	0.4985	0.4985	99.7021	
COL10 (1)	-346.4	-1.1163	0.0765	0.0765	15.3021	15.18
COL10 (2)	-346	-1.1234	0.0753	0.0753	15.0520	
COL16 (1)	-321.4	-1.5635	0.0273	0.0273	5.4642	5.45
COL16 (2)	-321.3	-1.5653	0.0272	0.0272	5.4417	

Next, I will present the data treatment of a second trial for the same compound but with different strains.

The table B.5 shows the concentration values of the standards and the corresponding potential difference used to construct the calibration curve represented by the graph in the Image B.2.

Table B.5. Concentration values and potential difference of standards for the second viability assay concerning the compound sodium fluoroacetate.

mM [F^-]	Log mM	E (mV)
0.001	-3	-250.6
0.0025	-2.602	-260.9
0.005	-2.301	-274
0.01	-2	-291
0.02	-1.699	-308.9
0.1	-1	-350.2
0.2	-0.699	-367
1	0	-408.6

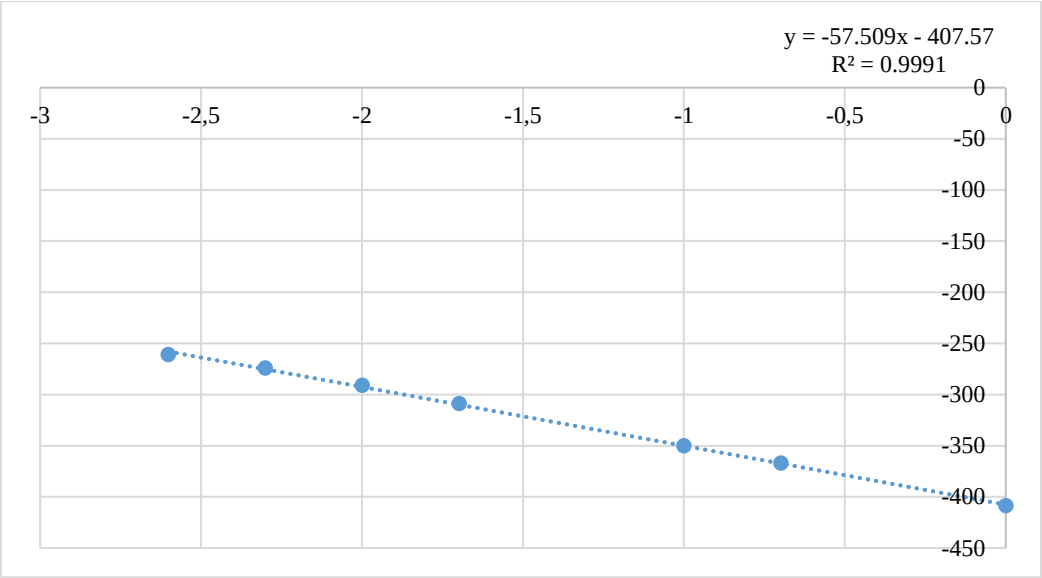

Figure B.2: Calibration curve obtained using the values in Table B.5 and the corresponding straight-line equation

The Table B.6 shows the potential difference for each replicate of each strain and the values obtained in the calculation of free fluoride for the time of the beginning of the assay (T0).

Table B.6: Potential difference of each strain and the values obtained in the calculation of free fluoride for the moment T0 of the second sodium fluoroacetate assay.

	E (mV)	Log mM	mM [F-]
19791 (1)	-257.7	-2.6060	0.0025
19791 (2)	-232.8	-3.0390	0.0009
CPN3 (1)	-232.8	-3.0390	0.0009
CPN3 (2)	-230.8	-3.0738	0.0008
1.7.L. (1)	-236	-2.9834	0.0010
1.7.L. (2)	-254.5	-2.6617	0.0022
F11 (1)	-231.2	-3.0668	0.0009
F11 (2)	-254.1	-2.6686	0.0021

The Table B.7 shows the potential difference for each replicate of each strain and the values obtained in the calculation of free fluoride after 8 days from the beginning of the assay (T8).

Table B.7: Potential difference of each strain and the values obtained in the calculation of free fluoride for the moment T7 of the second sodium fluoroacetate assay.

	E (mV)	Log mM	mM [F-]	[F-]Free	% Def	Med

19791 (1)	-279.0	-2.2357	0.0058	0.0033	0.6670	0.55
19791 (2)	-263.2	-2.5104	0.0031	0.0022	0.4347	
CPN3 (1)	-263.5	-2.5052	0.0031	0.0022	0.4421	0.43
CPN3 (2)	-262.0	-2.5313	0.0029	0.0021	0.4198	
1.7.L. (1)	-301.8	-1.8392	0.0145	0.0134	2.6885	2.08
1.7.L. (2)	-291.4	-2.0200	0.0095	0.0074	1.4740	
F11 (1)	-297.6	-1.9122	0.0122	0.0114	2.2765	2.39
F11 (2)	-302.1	-1.8340	0.0147	0.0125	2.5023	

The Table B.8 shows the potential difference for each replicate of each strain and the values obtained in the calculation of free fluoride after 15 days from the beginning of the assay (T15).

Table B.8: Potential difference of each strain and the values obtained in the calculation of free fluoride for the moment T15 of the second sodium fluoroacetate assay.

	E (mV)	Log mM	mM [F-]	[F-]Free	% Def	Med
19791 (1)	-291.2	-2.0235	0.0095	0.0070	1.3992	1.08
19791 (2)	-273.8	-2.3261	0.0047	0.0038	0.7612	
CPN3 (1)	-273.4	-2.3330	0.0046	0.0037	0.7462	0.72
CPN3 (2)	-271.4	-2.3678	0.0043	0.0034	0.6887	
1.7.L. (1)	-311.6	-1.6688	0.0214	0.0204	4.0801	3.09
1.7.L. (2)	-298.4	-1.8983	0.0126	0.0105	2.0918	
F11 (1)	-301.8	-1.8392	0.0145	0.0136	2.7248	2.84
F11 (2)	-305.7	-1.7714	0.0169	0.0148	2.9568	

Next the measured OD values after 8 and 14 days will be presented. Table B.9 allows us to show these same values, their average and standard deviation (SD).

Table B.9: OD values after 8 and 14 days, the average of these values and the associated standard deviation for the sodium fluoroacetate assay.

Strain	8 days	Median	SD	14 days	Median	SD
COL1 (1)	0.262	0.262	0	0.23	0.229	0.002
COL1 (2)	0.262			0.227		
COL4 (1)	0.253	0.243	0.014	0.146	0.143	0.005
COL4 (2)	0.233			0.139		
COL5 (1)	0.267	0.259	0.011	0.219	0.220	0.001
COL5 (2)	0.251			0.22		

COL10 (1)	0.246	0.216	0.043	0.21	0.187	0.033
COL10 (2)	0.185			0.163		
COL16 (1)	0.398	0.388	0.015	0.365	0.359	0.008
COL16 (2)	0.377			0.353		
19791 (1)	0.447	0.443	0.006	0.412	0.385	0.039
19791 (2)	0.438			0.357		
CPN3 (1)	0.397	0.406	0.013	0.381	0.393	0.016
CPN3 (2)	0.415			0.404		
1.7.L. (1)	0.596	0.436	0.227	0.538	0.398	0.198
1.7.L. (2)	0.275			0.258		
F11 (1)	0.263	0.258	0.007	0.252	0.246	0.009
F11 (2)	0.253			0.239		

Next the measured percentage of fluorine degradation values after 8 and 14 days will be presented. Table B.10 allows us to show these same values, their average and standard deviation.

Table B.10: % of defluorination values after 8 and 14 days, the average of these values and the associated standard deviation for the sodium fluoroacetate assay.

Strain	8 days	Median	SD	14 days	Median	SD
COL1 (1)	0.11	0.24	0.18	1.11	0.95	0.24
COL1 (2)	0.37			0.78		
COL4 (1)	2.18	1.89	0.41	3.11	2.77	0.47
COL4 (2)	1.60			2.44		
COL5 (1)	97.76	97.55	0.30	100.94	100.32	0.88
COL5 (2)	97.33			99.70		
COL10 (1)	10.69	9.70	1.41	15.30	15.18	0.18
COL10 (2)	8.70			15.05		
COL16 (1)	3.95	3.82	0.18	5.46	5.45	0.02
COL16 (2)	3.69			5.44		
19791 (1)	0.67	0.55	0.16	1.40	1.08	0.45
19791 (2)	0.43			0.76		
CPN3 (1)	0.44	0.43	0.02	0.75	0.72	0.04
CPN3 (2)	0.42			0.69		
1.7.L. (1)	2.69	2.08	0.86	4.08	3.09	1.41
1.7.L. (2)	1.47			2.09		

F11 (1)	2.28	2.39	0.16	2.72	2.84	0.16
F11 (2)	2.50			2.96		

The following is an example of standard deviation calculation, the OD reading for strain COL1 after 8 days.

$$SD = \sqrt{\frac{(0.11 - 0.24)^2 + (0.37 - 0.24)^2}{2}} = 0.18$$

B.2. Fluorobenzene

This subsection contains the calculations and calibration curve for the compound fluorobenzene that allowed us to understand the viability of the strains under study.

The Table B.11 shows the concentration values of the standards and the corresponding potential difference used to construct the calibration curve represented by the graph in the Image B.3.

Table B.11: Concentration values and potential difference of standards for the first viability assay concerning the compound fluorobenzene.

mM [F-]	Log mM	E (mV)
0001	-3	-249.6
0.0025	-2.602	-255.4
0.005	-2.301	-274.2
0.01	-2	-290.7
0.02	-1.699	-308.7
0.1	-1	-350
0.2	-0.699	-366.8
1	0	-407.5

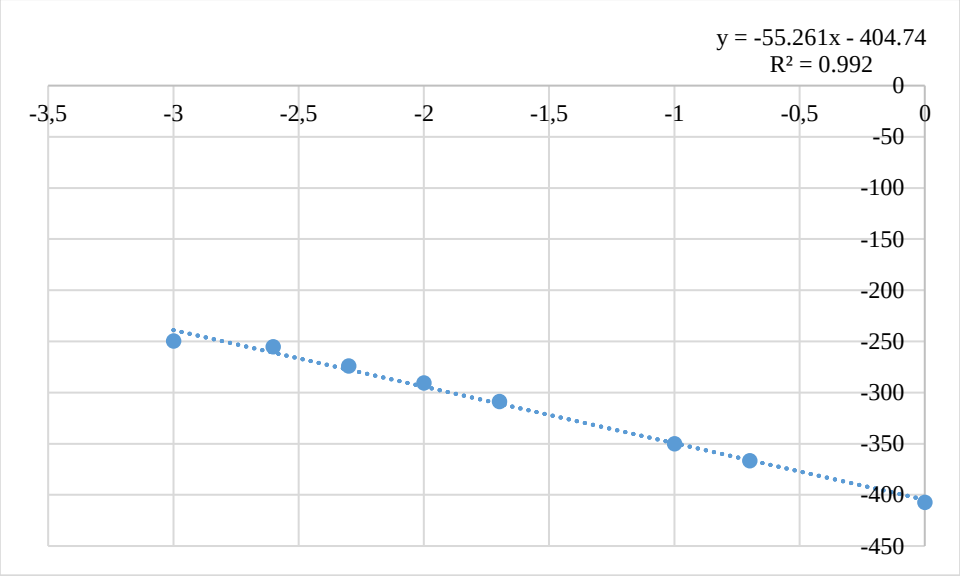

Figure B.3: Calibration curve obtained using the values in Table B.9 and the corresponding straight-line equation.

From the equation of the straight line, the concentration of [F-] was determined. The Table B.12 shows the potential difference for each replicate of each strain and the values obtained in the calculation of free fluoride for the time of the beginning of the assay (T0).

Table B.12: Potential difference of each strain and the values obtained in the calculation of free fluoride for the moment T0 of the first fluorobenzene assay.

	E (mV)	Log mM	mM [F-]
F11 (1)	-231.3	-3.15345	0.000702
F11 (2)	-288.3	-2.11709	0.007637
COL 5 (1)	-243.1	-2.93891	0.001151
COL 5 (2)	-233.2	-3.11891	0.000760

Below is an example of the calculation for determining the [F-] concentration at T0 (start of the assay) for strain F11 (1).

$$Log_{10}[F-] = \frac{\left(-231.3-(-404.74)\right)}{-55} \Leftrightarrow [F-] = 10^{-3.1535} \Leftrightarrow [F-] = 0.0007\ mM$$

The Table B.13 shows the potential difference for each replicate of each strain and the values obtained in the calculation of free fluoride after 8 days from the beginning of the assay (T8).

Table B.13: Potential difference of each strain and the values obtained in the calculation of free fluoride for the moment T8 of the first fluorobenzene assay.

	E (mV)	Log mM	mM [F-]	[F-]Free	% Def	Med
F11 (1)	-389.4	-0.27891	0.52613	0.52543	101.0433	102.319
F11 (2)	-390.3	-0.26255	0.54633	0.53869	103.5947	

Below is an example of the calculation performed for the determination of free [F-], percentage of defluorination and the average of the replicates at T8 (since the start of the assay) for strain F11 (1).

$$Log_{10}[F-] = \frac{\left(-389.4-(-404.74)\right)}{-55} \Leftrightarrow [F-] = 10^{0.2789} \Leftrightarrow [F-] = 0.52613\ mM$$

$$[F-]\ Free = 0.52543 - 0.0028 = 0.0006\ mM$$

Determination of the theoretical [F$^-$] concentration if there was complete defluorination.

Since the stoichiometry of the molecule is 1:1, then the concentration of free fluorides will be equal.

Massa Molar (C_6H_5F) = 96.103 mg/L ---------- 1 mM

50 mg/L ---------- x mM

$$x = \frac{50 * 1}{96.103} = 0.52\ mM$$

$$\%\ Def = \frac{0.0006}{0.52} * 100 = 101.04\ \%$$

$$Med = \frac{101.04 + 103.59}{2} = 102.32\ \%$$

The Table B.14 shows the potential difference for each replicate of each strain and the values obtained in the calculation of free fluoride after 14 days from the beginning of the assay (T14).

Table B.14: Potential difference of each strain and the values obtained in the calculation of free fluoride for the moment T14 of the first fluorobenzene assay.

	E (mV)	Log mM	mM [F-]	[F-]Free	% Def	Med

COL5 (1)	-392.2	-3.09345	0.00081	-0.00034	-0.06628	-0.03465
COL5 (2)	-391.9	-3.12800	0.00074	-0.00002	-0.00303	

Next, I will present the data treatment of a second trial for the same compound but with different strains.

The Table B.15 shows the concentration values of the standards and the corresponding potential difference used to construct the calibration curve represented by the graph in the Image B.4.

Table B.15: Concentration values and potential difference of standards for the second viability assay concerning the compound fluorobenzene.

mM [F-]	Log mM	E (mV)
0.001	-3	-248.9
0.0025	-2.602	-259.6
0.005	-2.301	-274.4
0.01	-2	-291.1
0.02	-1.699	-309.1
0.1	-1	-350.5
0.2	-0.699	-366.2
1	0	-406.4

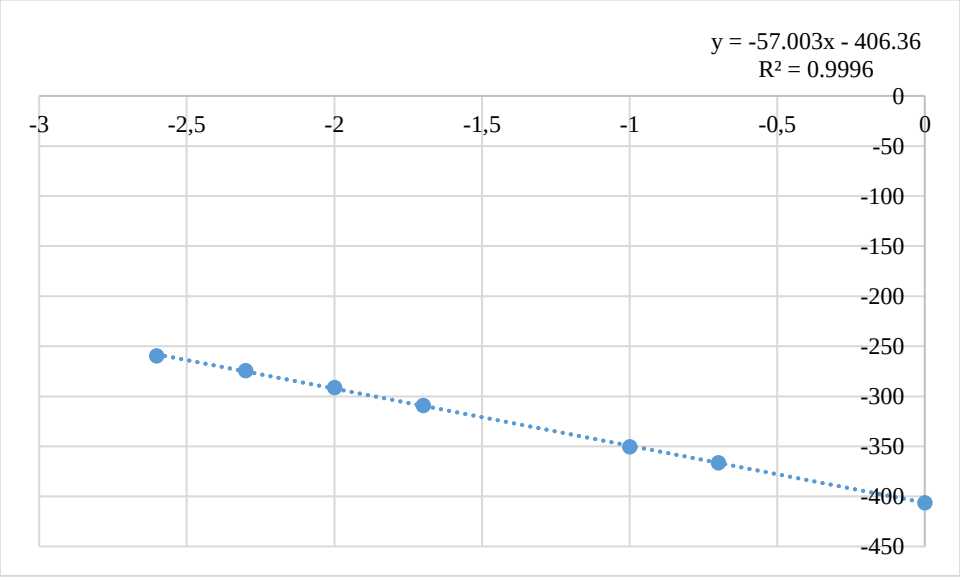

Figure B.4: Calibration curve obtained using the values in Table B.13 and the corresponding straight-line equation

The Table B.16 shows the potential difference for each replicate of each strain and the values obtained in the calculation of free fluoride for the time of the beginning of the assay (T0).

Table B.16: Potential difference of each strain and the values obtained in the calculation of free fluoride for the moment T0 of the second fluorobenzene assay.

	E (mV)	Log mM	mM [F-]
19791 (1)	-236.2	-2.9851	0.0010
19791 (2)	-254.2	-2.6693	0.0021
CPN3 (1)	-252.2	-2.7044	0.0020
CPN3 (2)	-235.1	-3.0044	0.0010
1.7.L. (1)	-262.5	-2.5237	0.0030
1.7.L. (2)	-239.5	-2.9272	0.0012

The Table B.17 shows the potential difference for each replicate of each strain and the values obtained in the calculation of free fluoride after 8 days from the beginning of the assay (T8).

Table B.17: Potential difference of each strain and the values obtained in the calculation of free fluoride for the moment T8 of the second fluorobenzene assay.

	E (mV)	Log mM	mM [F-]	[F-]Free	% Def	Med
19791 (1)	-254.7	-2.6606	0.0022	0.0012	0.2212	0.03
19791 (2)	-241.0	-2.9009	0.0013	-0.0009	-0.1702	
CPN3 (1)	-262.2	-2.5290	0.0030	0.0010	0.1890	0.17
CPN3 (2)	-249.7	-2.7483	0.0018	0.0008	0.1530	
1.7.L. (1)	-264.7	-2.4851	0.0033	0.0003	0.0535	0.02
1.7.L. (2)	-237.9	-2.9553	0.0011	-0.0001	-0.0142	

The Table B.18 shows the potential difference for each replicate of each strain and the values obtained in the calculation of free fluoride after 14 days from the beginning of the assay (T14).

Table B.18: Potential difference of each strain and the values obtained in the calculation of free fluoride for the moment T14 of the second fluorobenzene assay.

	E (mV)	Log mM	mM [F-]	[F-]Free	% Def	Med
19791 (1)	-259.4	-2.5781	0.0026	0.0016	0.3090	0.06
19791 (2)	-239	-2.9360	0.0012	-0.0010	-0.1889	

CPN3 (1)	-264.8	-2.4834	0.0033	0.0013	0.2520	0.23
CPN3 (2)	-253.7	-2.6781	0.0021	0.0011	0.2132	
1.7.L. (1)	-266.3	-2.4571	0.0035	0.0005	0.0955	0.04
1.7.L. (2)	-238.8	-2.9395	0.0011	0.0000	-0.0063	

Next the measured OD values after 8 and 14 days will be presented. Table B.19 allows to show these same values, their average and standard deviation.

Table B.19: OD values after 8 and 14 days, the average of these values and the associated standard deviation for the fluorobenzene assay.

Strain	8 days	Median	SD	14 days	Median	SD
COL5 (1)	-	-	-	-	-	-
COL5 (2)	-	-	-	-	-	-
F11 (1)	-	-	-	-	-	-
F11 (2)	-	-	-	-	-	-
CPN3 (1)	0.365	0.367	0.003	0.364	0.358	0.009
CPN3 (2)	0.369			0.351		
1.7.L. (1)	0.311	0.319	0.011	0.301	0.294	0.011
1.7.L. (2)	0.327			0.286		
19791 (1)	0.283	0.272	0.016	0.218	0.231	0.018
19791 (2)	0.260			0.244		

Next the measured percentage of fluorine degradation values after 8 and 14 days will be presented. Table B.20 allows us to show these same values, their average and standard deviation.

Table B.20: % of defluorination values after 8 and 14 days, the average of these values and the associated standard deviation for the fluorobenzene assay.

Strain	8 days	Median	SD	14 days	Median	SD
COL5 (1)	0	0	0	0	0	0
COL5 (2)	0			0		
F11 (1)	100	100	0	100	100	0
F11 (2)	100			100		
CPN3 (1)	0.19	0.17	0.03	0.25	0.23	0.03
CPN3 (2)	0.15			0.21		

1.7.L. (1)	0.05	0.02	0.05	0.09	0.04	0.07
1.7.L. (2)	0			0		
19791 (1)	0.22	0.03	0.28	0.31	0.06	0.35
19791 (2)	-0.17			0		

The following is an example of standard deviation calculation, the OD reading for strain 19791 after 8 days.

$$SD = \sqrt{\frac{(0.283 - 0.272)^2 + (0.260 - 0.272)^2}{2}} = 0.016$$

B.3. Paroxetine

This subsection contains the calculations and calibration curve for the compound paroxetine that allowed us to understand the viability of the strains under study. The Table B.21 shows the concentration values of the standards and the corresponding potential difference used to construct the calibration curve represented by the graph in the Image B.5.

Table B.21: Concentration values and potential difference of standards for the viability assay concerning the compound paroxetine.

mM [F^-]	Log mM	E (mV)
0.001	-3	-252.9
0.0025	-2.602	-261.1
0.005	-2.301	-274.2
0.01	-2	-291.5
0.02	-1.699	-309.8
0.1	-1	-350.8
0.2	-0.699	-367.8
1	0	-409.3

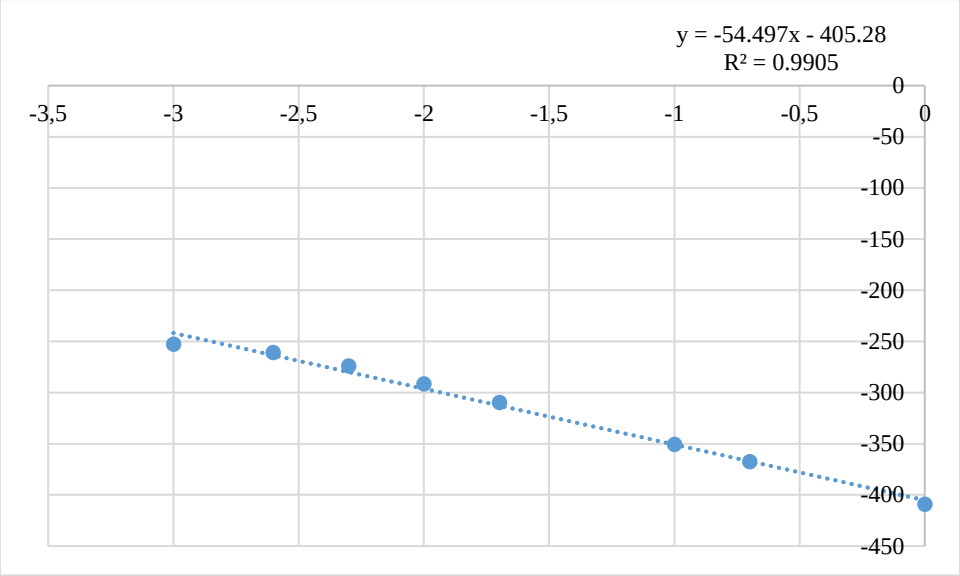

Figure B.5: Calibration curve obtained using the values in Table B.16 and the corresponding straight-line equation

From the equation of the straight line, the concentration of [F-] was determined. The Table B.22 shows the potential difference for each replicate of each strain and the values obtained in the calculation of free fluoride for the time of the beginning of the assay (T0).

Table B.22: Potential difference of each strain and the values obtained in the calculation of free fluoride for the moment T0 of the paroxetine assay.

	E (mV)	Log mM	mM [F-]
DPS1 (1)	-255.6	-2.7468	0.0018
DPS1 (2)	-238.3	-3.0642	0.0009
DPS4 (1)	-236.6	-3.0954	0.0008
DPS4 (2)	-236.3	-3.1009	0.0008
DPS5 (1)	-237.6	-3.0771	0.0008
DPS5 (2)	-254.9	-2.7596	0.0017
DPS8 (1)	-256.9	-2.7229	0.0019
DPS8 (2)	-257.6	-2.7101	0.0019
DPS10 (1)	-255.3	-2.7523	0.0018
DPS10 (2)	-238.2	-3.0661	0.0009

Below is an example of the calculation for determining the [F-] concentration at T0 (start of the assay) for strain DPS1 (1).

$$Log_{10}[F-] = \frac{(-255.6 - (-405.3))}{-54.5} \Leftrightarrow [F-] = 10^{-2.7468} \Leftrightarrow [F-] = 0.0018\ mM$$

The Table B.23 shows the potential difference for each replicate of each strain and the values obtained in the calculation of free fluoride after 8 days from the beginning of the assay (T8).

Table B.23: Potential difference of each strain and the values obtained in the calculation of free fluoride for the moment T8 of the paroxetine assay.

	E (mV)	Log mM	mM [F-]	[F-]Free	% Def	Med
DPS1 (1)	-259.6	-2.6734	0.0021	0.0003	10.8500	6.873
DPS1 (2)	-240.6	-3.0220	0.0010	0.0001	2.8955	
DPS4 (1)	-235.3	-3.1193	0.0008	0.0000	-1.4113	0.206
DPS4 (2)	-237.9	-3.0716	0.0008	0.0001	1.8235	
DPS5 (1)	-240.1	-3.0312	0.0009	0.0001	3.0687	3.022
DPS5 (2)	-256.1	-2.7376	0.0018	0.0001	2.9754	
DPS8 (1)	-258.3	-2.6972	0.0020	0.0001	3.7935	-30.166
DPS8 (2)	263.6	-12.2734	0.0000	-0.0019	-64.1261	
DPS10 (1)	-257.2	-2.7174	0.0019	0.0001	4.8636	4.206
DPS10 (2)	-241	-3.0147	0.0010	0.0001	3.5481	

Below is an example of the calculation performed for the determination of free [F-], percentage of defluorination and the average of the replicates at T8 (since the start of the assay) for strain F11 (1).

$$Log_{10}[F-] = \frac{(-259.6 - (-405.3))}{-54.5} \Leftrightarrow [F-] = 10^{-2.6734} \Leftrightarrow [F-] = 0.0021\ mM$$

$$[F-]\ Free = 0.0021 - 0.0018 = 0.0003\ mM$$

Determination of the theoretical [F$^-$] concentration if there was complete defluorination.

Since the stoichiometry of the molecule is 1:1, then the concentration of free fluorides will be equal.

Massa Molar ($C_{19}H_{20}FNO_3$) = 329.37 mg/L ---------- 1 mM

1 mg/L ---------- x mM

$$x = \frac{1 * 1}{329.37} = 0.0034\ mM$$

$$\%\ Def = \frac{0.0003}{0.0034} * 100 = 10.85\ \%$$

$$Med = \frac{10.85 + 2.90}{2} = 6.9\ \%$$

The Table B.24 shows the potential difference for each replicate of each strain and the values obtained in the calculation of free fluoride after 21 days from the beginning of the assay (T21).

Table B.24: Potential difference of each strain and the values obtained in the calculation of free fluoride for the moment T21 of the paroxetine assay.

	E (mV)	Log mM	mM [F-]	[F-]Free	% Def	Med
DPS1 (1)	-260.7	-2.6532	0.0022	0.0004	14.1695	12.5391
DPS1 (2)	-246	-2.9229	0.0012	0.0003	10.9087	
DPS4 (1)	-239.5	-3.0422	0.0009	0.0001	3.4420	2.7511
DPS4 (2)	-238.1	-3.0679	0.0009	0.0001	2.0602	
DPS5 (1)	-246.5	-2.9138	0.0012	0.0004	12.5741	11.5540
DPS5 (2)	-258.9	-2.6862	0.0021	0.0003	10.5338	
DPS8 (1)	-258.2	-2.6991	0.0020	0.0001	3.5151	11.7125
DPS8 (2)	-264	-2.5927	0.0026	0.0006	19.9100	
DPS10 (1)	-259.8	-2.6697	0.0021	0.0004	12.1844	10.4783
DPS10 (2)	-244.6	-2.9486	0.0011	0.0003	8.7722	

Next the measured OD values after 8 and 21 days will be presented. Table B.25 allows to show these same values, their average and standard deviation.

Table B.25: OD values after 8 and 21 days, the average of these values and the associated standard deviation for the paroxetine assay.

Strain	8 days	Median	SD	21 days	Median	SD
DPS1 (1)	0.640	0.637	0.005	0.582	0.641	0.083
DPS1 (2)	0.633			0.699		
DPS4 (1)	0.232	0.180	0.074	0.198	0.158	0.057
DPS4 (2)	0.127			0.117		
DPS5 (1)	0.574	0.573	0.001	0.736	0.716	0.029

DPS5 (2)	0.572			0.695		
DPS8 (1)	0.480	0.498	0.025	0.436	0.437	0.001
DPS8 (2)	0.515			0.438		
DPS10 (1)	0.535	0.499	0.051	0.552	0.533	0.026
DPS10 (2)	0.463			0.515		

Next the measured percentage of fluorine degradation values after 8 and 21 days will be presented. Table B.26 allows us to show these same values, their average and standard deviation.

Table B.26: % of defluorination values after 8 and 21 days, the average of these values and the associated standard deviation for the paroxetine assay.

Strain	8 days	Median	SD	21 days	Median	SD
DPS1 (1)	10.85	6.87	5.62	14.17	12.54	2.31
DPS1 (2)	2.90			10.90		
DPS4 (1)	0	0.91	1.29	3.44	2.75	0.98
DPS4 (2)	1.82			2.06		
DPS5 (1)	3.07	3.02	0.07	12.57	11.55	1.44
DPS5 (2)	2.98			10.53		
DPS8 (1)	3.79	11.15	10.40	3.52	11.71	11.59
DPS8 (2)	18.50			19.91		
DPS10 (1)	4.86	4.21	0.93	12.18	10.48	2.41
DPS10 (2)	3.55			8.77		

The following is an example of standard deviation calculation, the OD reading for strain DPS10 after 8 days.

$$SD = \sqrt{\frac{(0.535 - 0.499)^2 + (0.463 - 0.499)^2}{2}} = 0.051$$

B.4. Epoxiconazole

This subsection contains the calculations and calibration curve for the compound epoxiconazole that allowed us to understand the viability of the strains under study. The Table B.27 shows the concentration values of the standards and the corresponding potential difference used to construct the calibration curve represented by the graph in the Image B.6.

Table B.27: Concentration values and potential difference of standards for the viability assay concerning the compound epoxiconazole.

mM [F-]	Log mM	E (mV)
0.001	-3	-251.2
0.0025	-2.602	-259.9
0.005	-2.301	-272.5
0.01	-2	-289.1
0.02	-1.699	-306.7
0.1	-1	-348
0.2	-0.699	-365.1
1	0	-406.3

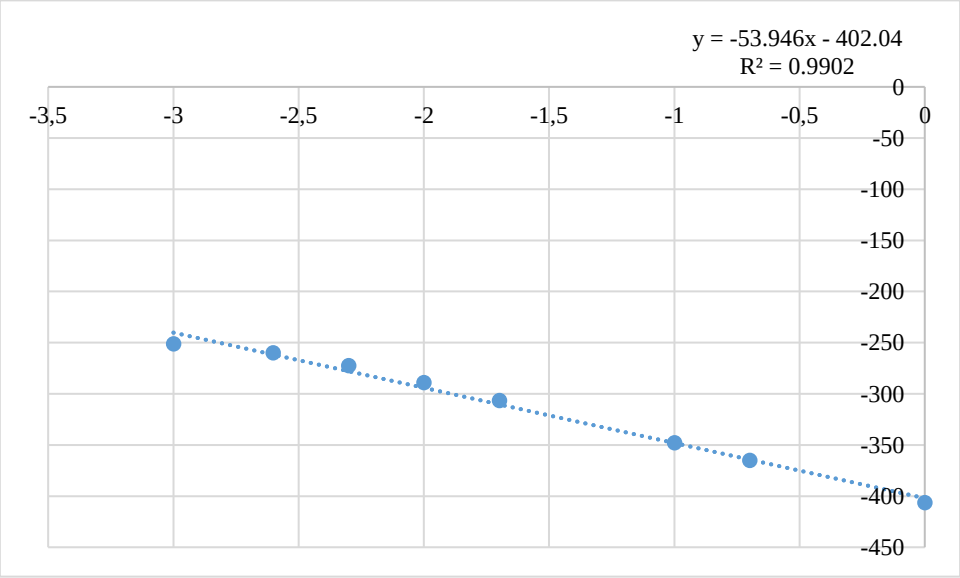

Figure B.6: Calibration curve obtained using the values in Table B.20 and the corresponding straight-line equation

From the equation of the straight line, the concentration of [F-] was determined. The Table B.28 shows the potential difference for each replicate of each strain and the

values obtained in the calculation of free fluoride for the time of the beginning of the assay (T0).

Table B.28: Potential difference of each strain and the values obtained in the calculation of free fluoride for the moment T0 of the epoxiconazole assay.

	E (mV)	Log mM	mM [F-]
8EE (1)	-256.6	-2.6960	0.0020
8EE (2)	-254.1	-2.7424	0.0018
5AE (1)	-235.4	-3.0890	0.0008
5AE (2)	-253.5	-2.7535	0.0018
3EE (1)	-233.4	-3.1261	0.0007
3EE (2)	-246	-2.8925	0.0013

Below is an example of the calculation for determining the [F-] concentration at T0 (start of the assay) for strain 8EE (1).

$$Log_{10}[F-] = \frac{\left(-256.6-(-402.04)\right)}{-53.9} \Leftrightarrow [F-] = 10^{-2.6960} \Leftrightarrow [F-] = 0.0020\,mM$$

The Table B.29 shows the potential difference for each replicate of each strain and the values obtained in the calculation of free fluoride after 14 days from the beginning of the assay (T14).

Table B.29: Potential difference of each strain and the values obtained in the calculation of free fluoride for the moment T14 of the epoxiconazole assay.

	E (mV)	Log mM	mM [F-]	[F-]Free	% Def	Med
8EE (1)	-260.1	-2.6311	0.0023	0.0003	2.1630	1.40
8EE (2)	-255.3	-2.7201	0.0019	0.0001	0.6341	
5AE (1)	-237.4	-3.0519	0.0009	0.0001	0.4840	1.16
5AE (2)	-256.9	-2.6905	0.0020	0.0003	1.8367	
3EE (1)	-239.3	-3.0167	0.0010	0.0002	1.4281	4.47
3EE (2)	-260.8	-2.6182	0.0024	0.0011	7.5210	

Below is an example of the calculation performed for the determination of free [F-], percentage of defluorination and the average of the replicates at T14 (since the start of the assay) for strain F11 (1).

$$Log_{10}[F-] = \frac{\left(-260.1-(-402.04)\right)}{-53.9} \Leftrightarrow [F-] = 10^{-2.6311} \Leftrightarrow [F-] = 0.0023\,mM$$

$$[F-]\ Free = 0.0023 - 0.0020 = 0.0003\ mM$$

Determination of the theoretical [F⁻] concentration if there was complete defluorination.

Massa Molar ($C_{17}H_{13}ClFN_3O$) = 329.76 mg/L ---------- 1 mM

5 mg/L ---------- x mM

Since the stoichiometry of the molecule is 1:1, then the concentration of free fluorides will be equal.

$$x = \frac{5 * 1}{329.76} = 0.015\ mM$$

$$\%\ Def = \frac{0.0003}{0.015} * 100 = 2.16\ \%$$

$$Med = \frac{2.16 + 0.63}{2} = 1.40\ \%$$

The Table B.30 shows the potential difference for each replicate of each strain and the values obtained in the calculation of free fluoride after 21 days from the beginning of the assay (T21).

Table B.30: Potential difference of each strain and the values obtained in the calculation of free fluoride for the moment T21 of the epoxiconazole assay.

	E (mV)	Log mM	mM [F-]	[F-]Free	% Def	Med
8EE (1)	-261.5	-2.6052	0.0025	0.0005	3.1228	2.72
8EE (2)	-258.2	-2.6664	0.0022	0.0003	2.3074	
5AE (1)	-250	-2.8184	0.0015	0.0007	4.6971	4.23
5AE (2)	-260	-2.6330	0.0023	0.0006	3.7603	
3EE (1)	-268.1	-2.4829	0.0033	0.0025	16.9441	12.87
3EE (2)	-262.6	-2.5848	0.0026	0.0013	8.8035	

Next the measured OD values after 14 and 21 days will be presented. Table B.31 allows to show these same values, their average and standard deviation.

Table B.31: OD values after 14 and 21 days, the average of these values and the associated standard deviation for the epoxiconazole assay.

Strain	14 days	Median	SD	21 days	Median	SD
8EE (1)	0.371	0.383	0.0170	0.364	0.372	0.0113

8EE (2)	0.395			0.380		
5AE (1)	0.459	0.475	0.0219	0.438	0.451	0.0184
5AE (2)	0.490			0.464		
3EE (1)	0.516	0.4795	0.0516	0.500	0.464	0.0509
3EE (2)	0.443			0.428		

Next the measured percentage of fluorine degradation values after 14 and 21 days will be presented. Table B.32 allows us to show these same values, their average and standard deviation.

Table B.32: % of defluorination values after 14 and 21 days, the average of these values and the associated standard deviation for the epoxiconazole assay.

Strain	14 days	Median	SD	21 days	Median	SD
8EE (1)	2.16	1.40	1.081	3.12	2.72	0.577
8EE (2)	0.63			2.31		
5AE (1)	0.48	1.16	0.957	4.70	4.23	0.662
5AE (2)	1.84			3.76		
3EE (1)	1.43	4.47	4.308	16.94	12.87	5.756
3EE (2)	7.52			8.80		

The following is an example of standard deviation calculation, the OD reading for strain 3EE after 8 days.

$$SD = \sqrt{\frac{(0.516 - 0.480)^2 + (0.443 - 0.480)^2}{2}} = 0.0516$$

C. Hybrid technology deployment

C.1. Nanotechnology treatment

In this section the treatments of the nanophotocatalysis results will be presented. Table C.1 presents the concentration values of the H_2O standards and the measured potential difference, allowing the calibration curve in Figure C.1 to be constructed. This calibration curve allowed understanding the feasibility of the technology in the degradation of perfluorohexanoic acid and trifloxystrobin compounds of concentration 1 mgL^{-1}.

Table C.1: Concentration values and potential difference of standards for the relative to the nanophotocatalytic treatment.

mM [H_2O]	Log mM	E (mV)
0.001	-3	-256.5
0.0025	-2.602	-257
0.005	-2.301	-264.6
0.01	-2	-277.3
0.02	-1.699	-296
0.1	-1	-340.4
0.2	-0.699	-363.5
1	0	-405.1

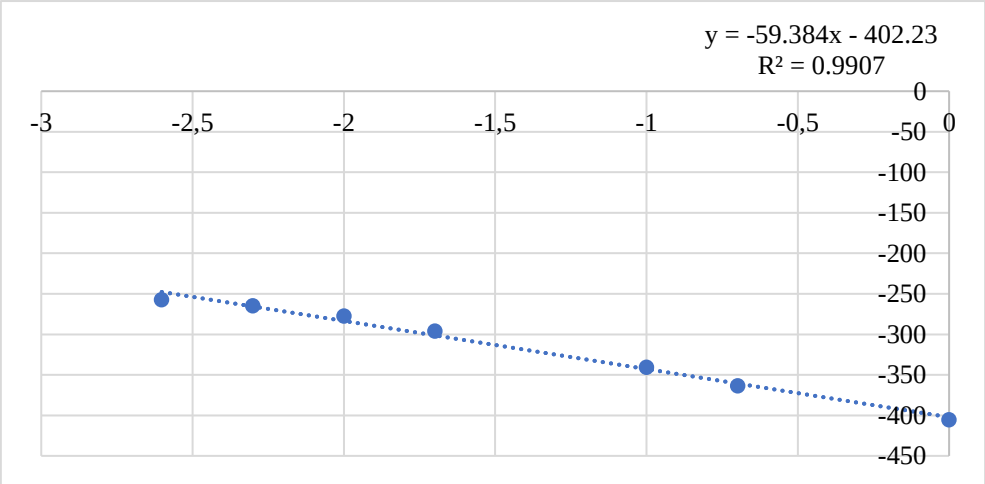

Figure C.1: Calibration curve obtained using the values in Table C.1 and the corresponding straight-line equation.

Nanoparticle Zinc Oxide - ZnO

The samples were taken 30 minutes before adding the nanoparticles to check for interference. Table C.2 shows the measured potential difference and the values obtained in the calculation of free fluoride at the beginning of the test and 6 hours later for the ZnO nanoparticle in the control samples.

Table C.2: Potential difference and the values obtained in the calculation of free fluoride at the beginning of the assay and 6 hours later for the ZnO nanoparticle in the control samples.

Time	E (mV)	Log mM	mM F-
0h	-250.3	-2.5584	0
6h	-261.1	-2.3766	0.0042

Below is an example of the calculation for determining the [F-] concentration at the start of the assay.

$$Log_{10}[F-] = \frac{\left(-250.3 - (-402.23)\right)}{-59.384} \Leftrightarrow [F-] = 10^{-2.5584} \Leftrightarrow [F-] = 0.0020\, mM$$

Next, the calculations necessary for the determination of free fluoride from perfluorohexanoic acid of concentration 1 mgL^{-1} are shown in Table C.3.

Table C.3: Potential difference, values obtained in the calculation of free fluoride and % defluorination at the beginning of the test and 6 hours later by the ZnO nanoparticle on the perfluorohexanoic acid compound.

Time	E (mV)	Log mM	mM F-	F- Lib	% def
0h	-245.3	-2.6426	0	0	0
6h	-255.4	-2.4726	0.0034	-0.0008	-2.38

Below is an example of the calculation performed for the determination of free [F-], percentage of defluorination after 6 hours since the start of the assay.

$$Log_{10}[F-] = \frac{\left(-255.4 - (-402.23)\right)}{-59.384} \Leftrightarrow [F-] = 10^{-2.4726} \Leftrightarrow [F-] = 0.0034\, mM$$

$$[F-]\, Free = 0.0042 - 0.0034 = -0.0008\, mM$$

Determination of the theoretical [F^-] concentration if there was complete defluorination.

Massa Molar ($C_6HF_{11}O_2$) = 314.054 mg/L ---------- 1 mM

1 mg/L ---------- x mM

Since the stoichiometry of the molecule is 1:11, then the concentration of free fluorides will be 11 times higher.

$$x = \frac{1 * 1}{314.054} = 0.003184\, mM$$

$$0.003184 * 11 = 0.03503\, mM$$

$$\%\, Def = \frac{-0.0008}{0.03503} * 100 = -2.38\,\%$$

Next, the calculations necessary for the determination of free fluoride from trifloxystrobin of concentration 1 mgL^{-1} are shown in Table C.4.

Table C.4: Potential difference, values obtained in the calculation of free fluoride and % defluorination at the beginning of the test and 6 hours later by the ZnO nanoparticle on the trifloxystrobin compound.

Time	E (mV)	Log mM	mM F-	F- Lib	% def
0h	-243.2	-2.6780	0	0	0
6h	-271.2	-2.2065	0.0062	0.0020	27.42

Below is an example of the calculation performed for the determination of free [F-], percentage of defluorination after 6 hours since the start of the assay.

$$Log_{10}[F-] = \frac{\left(-271.2-(-402.23)\right)}{-59.384} \Leftrightarrow [F-] = 10^{-2.2065} \Leftrightarrow [F-] = 0.0062\ mM$$

$$[F-]\ Free = 0.0042 - 0.0062 = 0.0020\ mM$$

Determination of the theoretical [F^-] concentration if there was complete defluorination.

Massa Molar ($C_{20}H_{19}F_3N_2O_4$) = 408.37 mg/L ---------- 1 mM

1 mg/L ---------- x mM

Since the stoichiometry of the molecule is 1:3, then the concentration of free fluorides will be 3 times higher.

$$x = \frac{1 * 1}{408.37} = 0.002449\ mM$$

$$0.002449 * 3 = 0.00734\ mM$$

$$\%\ Def = \frac{0.0020}{0.00734} * 100 = 27.42\ \%$$

Nanoparticle Titanium Dioxide – TiO_2

The samples were taken 30 minutes before adding the nanoparticles to check for interference. Table C.5 shows the measured potential difference and the values obtained in the calculation of free fluoride at the beginning of the test and 6 hours later for the TiO_2 nanoparticle in the control samples.

Table C.5: Potential difference and the values obtained in the calculation of free fluoride at the beginning of the assay and 6 hours later for the TiO_2 nanoparticle in the control samples.

Time	E (mV)	Log mM	mM F-
0h	-250.8	-2.5500	0

6h	-250.1	-2.5618	0.0027

Below is an example of the calculation for determining the [F-] concentration at the start of the assay.

$$Log_{10}[F-] = \frac{(-250.8 - (-402.23))}{-59.384} \Leftrightarrow [F-] = 10^{-2.5500} \Leftrightarrow [F-] = 0.0027\ mM$$

Next, the calculations necessary for the determination of free fluoride from perfluorohexanoic acid of concentration 1 mgL^{-1} are shown in Table C.6.

Table C.6: Potential difference, values obtained in the calculation of free fluoride and % defluorination at the beginning of the test and 6 hours later by the TiO_2 nanoparticle on the perfluorohexanoic acid compound.

Time	E (mV)	Log mM	mM F-	F- Lib	% def
0h	-246.9	-2.6157	0	0	0
6h	-255.4	-2.4726	0.0034	0.0006	1.79

Below is an example of the calculation performed for the determination of free [F-], percentage of defluorination after 6 hours since the start of the assay.

$$Log_{10}[F-] = \frac{(-255.4 - (-402.23))}{-59.384} \Leftrightarrow [F-] = 10^{-2.4726} \Leftrightarrow [F-] = 0.0034\ mM$$

$$[F-]\ Free = 0.0027 - 0.0034 = 0.0006\ mM$$

Determination of the theoretical [F^-] concentration if there was complete defluorination.

Massa Molar ($C_6HF_{11}O_2$) = 314.054 mg/L ---------- 1 mM

1 mg/L ---------- x mM

Since the stoichiometry of the molecule is 1:11, then the concentration of free fluorides will be 11 times higher.

$$x = \frac{1 * 1}{314.054} = 0.003184\ mM$$

$$0.003184 * 11 = 0.03503\ mM$$

$$\%\ Def = \frac{0.0006}{0.03503} * 100 = 1.79\ \%$$

Next, the calculations necessary for the determination of free fluoride from trifloxystrobin of concentration 1 mgL^{-1} are shown in Table C.7.

Table C.7: Potential difference, values obtained in the calculation of free fluoride and % defluorination at the beginning of the test and 6 hours later by the TiO_2 nanoparticle on the trifloxystrobin compound.

Time	E (mV)	Log mM	mM F-	F- Lib	% def
0h	-243.2	-2.6780	0	0	0
6h	-246	-2.6308	0.0023	-0.0004	-5.49

Below is an example of the calculation performed for the determination of free [F-], percentage of defluorination after 6 hours since the start of the assay.

$$Log_{10}[F-] = \frac{\left(-246-(-402.23)\right)}{-59.384} \Leftrightarrow [F-] = 10^{-2.6308} \Leftrightarrow [F-] = 0.0023\ mM$$

$$[F-]\ Free = 0.0027 - 0.0023 = -0.0004\ mM$$

Determination of the theoretical [F^-] concentration if there was complete defluorination.

Massa Molar ($C_{20}H_{19}F_3N_2O_4$) = 408.37 mg/L ---------- 1 mM

1 mg/L ---------- x mM

Since the stoichiometry of the molecule is 1:3, then the concentration of free fluorides will be 3 times higher.

$$x = \frac{1 * 1}{408.37} = 0.002449\ mM$$

$$0{,}002449 * 3 = 0.00734\ mM$$

$$\%\ Def = \frac{-0.0004}{0.00734} * 100 = -5.49\ \%$$

C.2. Bioremediation treatment

In this section the treatments of the bioremediation results will be presented. Table C.8 presents the concentration values of the sodium fluoride standards and the measured potential difference, allowing the calibration curve in Figure C.2 to be constructed. This calibration curve allowed understanding the feasibility of the technology in the degradation of perfluorohexanoic acid and trifloxystrobin compounds of concentration 1 mgL^{-1}.

Table C.8: Concentration values and potential difference of standards for the relative to the bioremediation treatment.

[F-]	Log mM	E (mV)
0.001	-3	-255.9
0.0025	-2.602	-261.8
0.005	-2.301	-274.4
0.01	-2	-291.3
0.02	-1.699	-309.2
0.1	-1	-350.5
0.2	-0.699	-367.8
1	0	-409.3

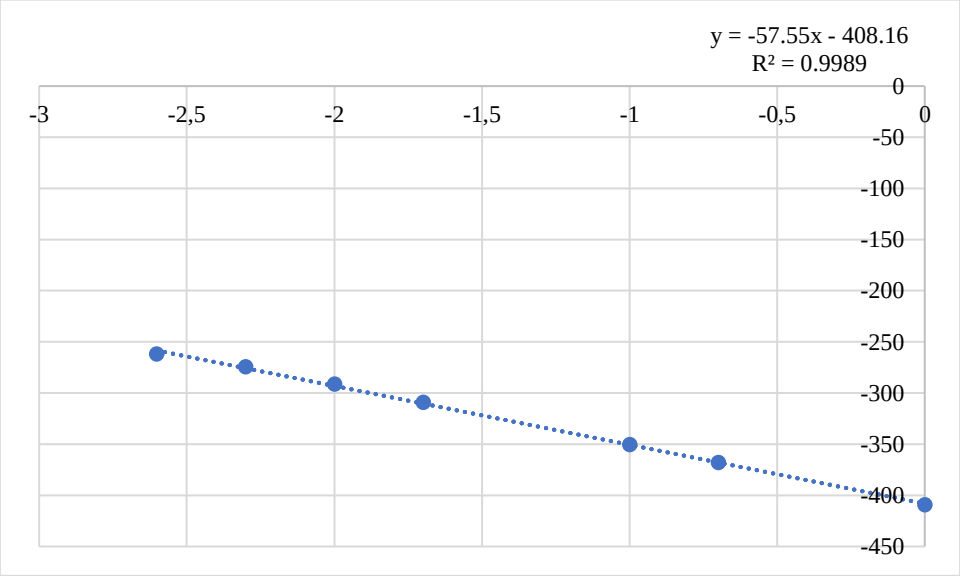

Figure C.2: Calibration curve obtained using the values in Table C.8 and the corresponding straight-line equation.

Perfluorohexanoic acid

In this section the treatment of the results related to the degradation test of the perfluorohexanoic acid compound using the consortium will be presented. Table C.9 shows the potential difference for each replicate and the values obtained in the calculation of free fluoride for the moment of the beginning of the assay (T0).

Table C.9: Potential difference for each replicate and the values obtained in the calculation of free fluoride for the time of trial start (T0) in the bioremediation trial for the perfluorohexanoic acid compound.

	E (mV)	Log mM	mM [F-]
1	-243.5	-2.8612	0.0014

2	-262.6	-2.5293	0.0030
3	-262.8	-2.5258	0.0030

Below is an example of the calculation for determining the [F-] concentration at T0 (start of the assay) for replicate 1

$$Log_{10}[F-] = \frac{(-243.5-(-408.16))}{-57.55} \Leftrightarrow [F-] = 10^{-2.8612} \Leftrightarrow [F-] = 0.0014\ mM$$

The Table C.10 shows the potential difference for each replicate of each strain and the values obtained in the calculation of free fluoride after 7 days from the beginning of the assay (T7).

Table C.10: Potential difference for each replicate and the values obtained in the calculation of free fluoride, and % defluorination for the time (T7) in the bioremediation trial for the perfluorohexanoic acid compound.

	E (mV)	Log mM	mM [F-]	[F-]Free	% Def	Med
1	-243.8	-2.8560	0.0014	1.66E-05	0.05	0.05
2	-261.7	-2.5449	0.0029	-1.05E-04	-0.30	
3	-263.9	-2.5067	0.0031	1.34E-04	0.38	

Below is an example of the calculation performed for the determination of free [F-], percentage of defluorination and the average of the replicates at T7 (since the start of the assay) for replicate 1.

$$Log_{10}[F-] = \frac{(-243.8-(-408.16))}{-57.55} \Leftrightarrow [F-] = 10^{-2.8560} \Leftrightarrow [F-] = 0.0014\ mM$$

$$[F-]\ Free = 0.001377 - 0.001393 = 1.66 * 10^{-5} mM$$

Determination of the theoretical [F$^-$] concentration if there was complete defluorination.

Massa Molar ($C_6HF_{11}O_2$) = 314.054 mg/L ---------- 1 mM

1 mg/L ---------- x mM

Since the stoichiometry of the molecule is 1:11, then the concentration of free fluorides will be 11 times higher.

$$x = \frac{1 * 1}{314.054} = 0.003184\ mM$$

$$0.003184 * 11 = 0.03503\ mM$$

$$\%\ Def = \frac{1.66 * 10^{-5}}{0.03503} * 100 = 0.05\ \%$$

$$Med = \frac{0.05 + (-0.30) + 0.38}{3} = 0.05\ \%$$

The Table C.11 shows the potential difference for each replicate and the values obtained in the calculation of free fluoride after 14 days from the beginning of the assay (T14).

Table C.11: Potential difference for each replicate and the values obtained in the calculation of free fluoride, and % defluorination for the time (T14) in the bioremediation trial for the perfluorohexanoic acid compound.

	E (mV)	Log mM	mM [F-]	[F-]Free	% Def	Med
1	-241.4	-2.89765	0.001265744	-0.000128	-0.36	0.11
2	-262.1	-2.53797	0.002897564	4.6E-05	0.13	
3	-264.2	-2.50148	0.003151541	3.760E-05	0.11	

The Table C.12 shows the potential difference for each replicate and the values obtained in the calculation of free fluoride after 20 days from the beginning of the assay (T20).

Table C.12: Potential difference for each replicate and the values obtained in the calculation of free fluoride, and % defluorination for the time (T20) in the bioremediation trial for the perfluorohexanoic acid compound.

	E (mV)	Log mM	mM [F-]	[F-]Free	% Def	Med
1	-239.4	-2.93241	0.001168	-9.73E-05	-0.28	0.11
2	-262.8	-2.5258	0.002980	8.23E-05	0.23	
3	-264.5	-2.49626	0.003190	3.81E-05	0.11	

Next the measured OD values after 7, 14 and 20 days will be presented. Table C.13 allows to show these same values, their average and standard deviation.

Table C.13: OD values after 7, 14 and 20 days, the average of these values and the associated standard deviation for the bioremediation assay for the perfluorohexanoic acid compound.

	7 d	M	SD	14 d	Me	SD	20 d	Me	SD
1	0.533	0.683	0.093	0.539	0.837	0.174	0.544	0.859	0.184
2	0.683			0.837			0.866		
3	0.704			0.844			0.859		

Next the measured percentage of fluorine degradation values after 7, 14 and 20 days will be presented. Table C.14 allows us to show these same values, their average and standard deviation.

Table C.14: % of defluorination values after 7, 14 and 20 days, the average of these values and the associated standard deviation for the bioremediation assay for the perfluorohexanoic acid compound.

	7 d	M	SD	14 d	Me	SD	20 d	Me	SD
1	0.05	0.05	0.34	-0.36	0.11	0.28	-0.28	0.11	0.267
2	-0.3			0.13			0.23		
3	0.38			0.11			0.11		

Trifloxystrobin

In this section the treatment of the results related to the degradation test of the trifloxystrobin compound using the consortium will be presented. Table C.15 shows the potential difference for each replicate and the values obtained in the calculation of free fluoride for the moment of the beginning of the assay (T0).

Table C.15: Potential difference for each replicate and the values obtained in the calculation of free fluoride for the time of trial start (T0) in the bioremediation trial for the trifloxystrobin compound.

	E (mV)	Log mM	mM [F-]
1	-263	-2.5223	0.0030
2	-238.8	-2.9428	0.0011
3	-241.4	-2.8977	0.0013

Below is an example of the calculation for determining the [F-] concentration at T0 (start of the assay) for replicate 1

$$Log_{10}[F-] = \frac{\left(-263-(-408.16)\right)}{-57.55} \Leftrightarrow [F-] = 10^{-2.5223} \Leftrightarrow [F-] = 0.0030\ mM$$

The Table C.16 shows the potential difference for each replicate of each strain and the values obtained in the calculation of free fluoride after 7 days from the beginning of the assay (T7).

Table C.16: Potential difference for each replicate and the values obtained in the calculation of free fluoride, and % defluorination for the time (T7) in the bioremediation trial for the trifloxystrobin compound.

	E (mV)	Log mM	mM [F-]	[F-]Free	% Def	Med

1	-262.6	-2.5293	0.0030	-4.77E-05	-0.65	-0.65
2	-243.8	-2.8560	0.0014	2.53E-04	3.44	
3	-239.8	-2.9255	0.0012	-7.85E-05	-1.07	

Below is an example of the calculation performed for the determination of free [F-], percentage of defluorination and the average of the replicates at T7 (since the start of the assay) for replicate 1.

$$Log_{10}[F-] = \frac{(-262.6 - (-408.16))}{-57.55} \Leftrightarrow [F-] = 10^{-2.5293} \Leftrightarrow [F-] = 0.0030\ mM$$

$$[F-]\ Free = 0.002956 - 0.003004 = -4.77 * 10^{-5} mM$$

Determination of the theoretical [F$^-$] concentration if there was complete defluorination.

Massa Molar ($C_{20}H_{19}F_3N_2O_4$) = 408.37 mg/L ---------- 1 mM

1 mg/L ---------- x mM

Since the stoichiometry of the molecule is 1:3, then the concentration of free fluorides will be 3 times higher.

$$x = \frac{1 * 1}{408.37} = 0.002449\ mM$$

$$0.002449 * 3 = 0.00734\ mM$$

$$\%\ Def = \frac{-4.77 * 10^{-5}}{0.00734} * 100 = -0.65\ \%$$

$$Med = \frac{3.44 + (-0.65) + (-1.07)}{3} = -0.65\ \%$$

The Table C.17 shows the potential difference for each replicate and the values obtained in the calculation of free fluoride after 14 days from the beginning of the assay (T14).

Table C.17: Potential difference for each replicate and the values obtained in the calculation of free fluoride, and % defluorination for the time (T14) in the bioremediation trial for the trifloxystrobin compound.

	E (mV)	Log mM	mM [F-]	[F-]Free	% Def	Med
1	-263.9	-2.50669	0.003113939	0.000157826	2.15	-0.32

2	-241	-2.9046	0.001245648	-0.00014766	-2.01	
3	-239.3	-2.93414	0.00116374	-2.3515E-05	-0.32	

The Table C.18 shows the potential difference for each replicate and the values obtained in the calculation of free fluoride after 20 days from the beginning of the assay (T20).

Table C.18: Potential difference for each replicate and the values obtained in the calculation of free fluoride, and % defluorination for the time (T20) in the bioremediation trial for the trifloxystrobin compound.

	E (mV)	**Log mM**	**mM [F-]**	**[F-]Free**	**% Def**	**Med**
1	-265.4	-2.48063	0.003307	0.000193	2.62	-0.92
2	-239.6	-2.92893	0.001178	-6.79E-05	-0.92	
3	-237.3	-2.9689	0.001074	-8.95E-05	-1.22	

Next the measured OD values after 7, 14 and 20 days will be presented. Table C.17 allows to show these same values, their average and standard deviation.

Table C.19: OD values after 7, 14 and 20 the average of these values and the associated standard deviation for the hybrid technology assay for the trifloxystrobin compound.

	7 d	**M**	**SD**	**14 d**	**Me**	**SD**	**20 d**	**Me**	**SD**
1	0.659	0.524	0.079	0.809	0.513	0.172	0.854	0.541	0.183
2	0.524			0.509			0.533		
3	0.522			0.513			0.541		

Next the measured percentage of fluorine degradation values after 7, 14 and 20 days will be presented. Table C.20 allows us to show these same values, their average and standard deviation.

Table C.20: % of defluorination values after 7, 14 and 20 the average of these values and the associated standard deviation for the hybrid technology assay for the trifloxystrobin compound.

	7 d	**Me**	**SD**	**14 d**	**Me**	**SD**	**20 d**	**Me**	**SD**
1	-0.65	-0.65	2.49	2.15	-0.32	2.09	2.62	-0.92	2.136
2	3.44			-2.01			-0.92		
3	-1.07			-0.32			-1.22		

C.3. Implementation of hybrid technology

This section will present the treatments of the results obtained in the assays in which the two technologies were copied. Table C.21 presents the concentration values of the standards and the measured potential difference, allowing the construction of the calibration curve in Figure C.3. This calibration curve allowed for an understanding of the viability of the technology in the degradation of the compound trifloxystrobin of concentration 1 mgL-1.

Table C.21: Concentration values and potential difference of standards for the relative to the hybrid technology.

[F-]	Log mM	E (mV)
0.001	-3	-248.7
0.0025	-2.602	-259.8
0.005	-2.301	-277.5
0.01	-2	-294.5
0.02	-1.699	-311.9
0.1	-1	-353.6
0.2	-0.699	-370
1	0	-410.9

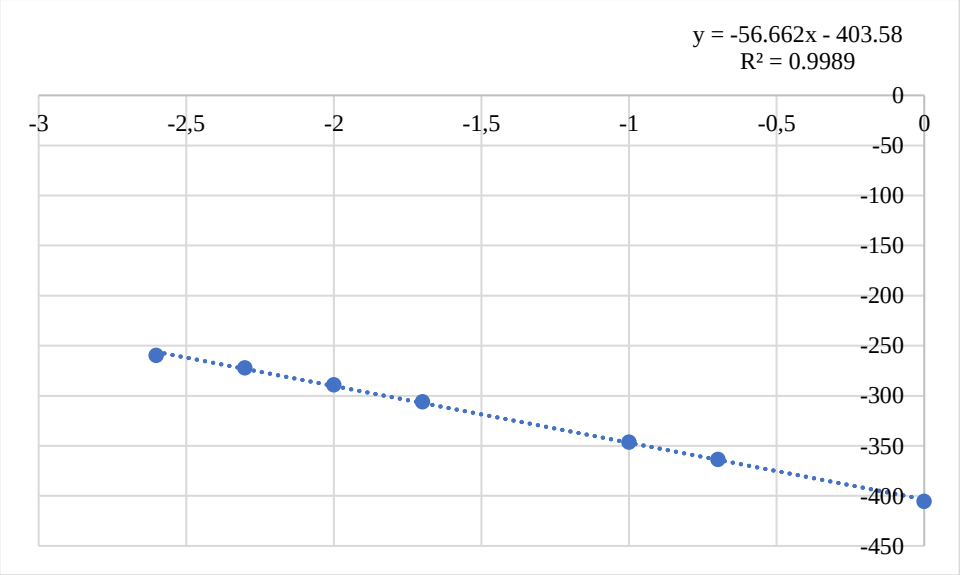

Figure C.3: Calibration curve obtained using the values in Table C.19 and the corresponding straight-line equation.

In this section the treatment of the results related to the degradation test of the trifloxystrobin compound using the hybrid technology will be presented. Table C.22

shows the potential difference for each replicate and the values obtained in the calculation of free fluoride for the moment of the beginning of the assay (T0).

Table C.22: Potential difference for each replicate and the values obtained in the calculation of free fluoride for the time of test start (T0) in the hybrid assay.

	E (mV)	Log mM	mM [F-]
1	-243.4	-2.8269	0.0015
2	-254.2	-2.6363	0.0023
3	-255.1	-2.6205	0.0024

Below is an example of the calculation for determining the [F-] concentration at T0 (start of the assay) for replicate 1.

$$Log_{10}[F-] = \frac{\left(-243.4-(-403.58)\right)}{-56.662} \Leftrightarrow [F-] = 10^{-2.8269} \Leftrightarrow [F-] = 0.0015\,mM$$

The Table C.23 shows the potential difference for each replicate of each strain and the values obtained in the calculation of free fluoride after 7 days from the beginning of the assay (T7).

Table C.23: Potential difference for each replicate and the values obtained in the calculation of free fluoride, and % of defluorination for the time (T7) in the hybrid assay.

	E (mV)	Log mM	mM [F-]	[F-]Free	% Def	Med
1	-241.6	-2.8587	0.0014	-0.0001	-1.4302	1.91
2	-257.4	-2.5799	0.0026	0.0003	4.3673	
3	-256.5	-2.5957	0.0025	0.0001	1.9096	

Below is an example of the calculation performed for the determination of free [F-], percentage of defluorination and the average of the replicates at T7 (since the start of the assay) for replicate 1.

$$Log_{10}[F-] = \frac{\left(-241.6-(-403.58)\right)}{-56.662} \Leftrightarrow [F-] = 10^{-2.8587} \Leftrightarrow [F-] = 0.0014\,mM$$

$$[F-]\,Free = 0.0014 - 0.0015 = -0.0001\,mM$$

Determination of the theoretical [F^-] concentration if there was complete defluorination.

Massa Molar ($C_{20}H_{19}F_3N_2O_4$) = 408.37 mg/L ---------- 1 mM

1 mg/L ---------- x mM

Since the stoichiometry of the molecule is 1:3, then the concentration of free fluorides will be 3 times higher.

$$x = \frac{1 * 1}{408.37} = 0.002449\ mM$$

$$0.002449 * 3 = 0.00734\ mM$$

$$\%\ Def = \frac{-0.0001}{0.00734} * 100 =* 1.43\ \%$$

$$Med = \frac{4.36 + (-1.43) + 1.91}{3} = 1.91\ \%$$

The Table C.24 shows the potential difference for each replicate and the values obtained in the calculation of free fluoride after 14 days from the beginning of the assay (T14).

Table C.24: Potential difference for each replicate and the values obtained in the calculation of free fluoride, and % of defluorination for the time (T14) in the hybrid assay.

	E (mV)	Log mM	mM [F-]	[F-]Free	% Def	Med
1	-240.8	-2.8728	0.0013	-0.0001	-2.0331	1.57
2	-255.4	-2.6152	0.0024	0.0001	1.5716	
3	-257.6	-2.5763	0.0027	0.0003	3.4881	

The Table C.25 shows the potential difference for each replicate and the values obtained in the calculation of free fluoride after 20 days from the beginning of the assay (T20).

Table C.25: Potential difference for each replicate and the values obtained in the calculation of free fluoride, and % of defluorination for the time (T20) in the hybrid assay.

	E (mV)	Log mM	mM [F-]	[F-]Free	% Def	Med
1	-237.5	-2.9311	0.0012	-0.0003	-4.3226	2.94
2	-256.4	-2.5975	0.0025	0.0002	2.9410	
3	-258.4	-2.5622	0.0027	0.0003	4.6813	

Next the measured OD values after 7, 14 and 20 days will be presented. Table C.26 allows to show these same values, their average and standard deviation.

Table C.26: OD values after 7, 14 and 20 days, the average of these values and the associated standard deviation for the hybrid assay.

	7 d	M	SD	14 d	Me	SD	20 d	Me	SD
1	0,579	0.689	0.074	0,641	0.683	0.0025	0,64	0.631	0.013
2	0,72			0,685			0,615		
3	0,689			0,683			0,631		

Next the measured percentage of fluorine degradation values after 7, 14 and 20 days will be presented. Table C.27 allows us to show these same values, their average and standard deviation.

Table C.27: % of defluorination values after 7, 14 and 20 days, the average of these values and the associated standard deviation for the hybrid assay.

	7 d	Me	SD	14 d	Me	SD	20 d	Me	SD
1	-1,430	1.910	2.91	-2,033	1.572	2.80	-4,323	2.941	4.78
2	4,367			1,572			2,941		
3	1,910			3,488			4,681		

Next, the treatment of the data referring to the tests performed to verify if there was non-biological degradation of the compost and if the consortium resisted under the given conditions will be presented.

Table C.28 presents the concentration values of the standards and the measured potential difference, allowing the construction of the calibration curve in Figure C.4.

Table C.28: Concentration values and potential difference of the standards compared to the assay to check for biological degradation and resistance of the consortium in the water samples.

[F-]	Log mM	E (mV)
0.001	-3	-251
0.0025	-2.602	-254.1
0.005	-2.301	-261
0.01	-2	-274.8
0.02	-1.699	-293.1
0.1	-1	-338.3
0.2	-0.699	-360.8
1	0	-406

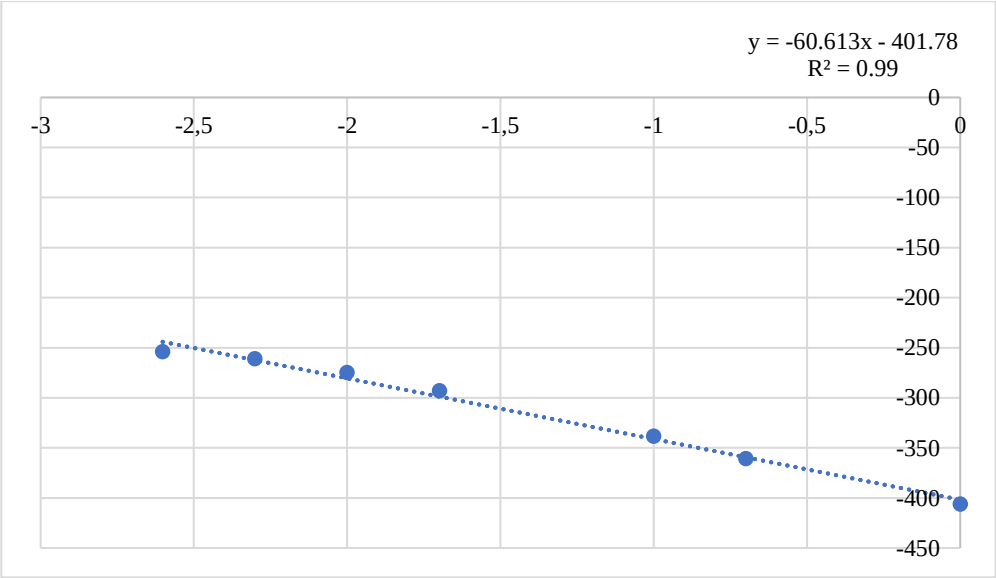

Figure C.4: Calibration curve obtained using the values in Table C.19 and the corresponding straight-line equation.

From the equation of the straight line, the concentration of [F-] was determined. The Table C.29 shows the potential difference for each replicate of each assay and the values obtained in the calculation of free fluoride for the time of the beginning of the assay (T0). The abbreviation AB points to the test where only the water was analyzed, and the abbreviation M points to the test where the consortium was tested in the water sample.

Table C.29: Potential difference for each replicate of each assay (consortium resistance and non-biological degradation) and the values obtained in the calculation of free fluoride for the moment of the beginning of the assay (T0).

	E (mV)	Log mM	mM [F-]
AB (1)	-294.9	-1.7633	0.0172
AB (2)	-289.5	-1.8524	0.0140
M (1)	-279.3	-2.0207	0.0095
M (2)	-271.5	-2.1494	0.0071

Below is an example of the calculation for determining the [F-] concentration at T0 (start of the assay) for the assay AB (1).

$$Log_{10}[F-] = \frac{\left(-294.9 - (-401.78)\right)}{-60.613} \Leftrightarrow [F-] = 10^{-1.7633} \Leftrightarrow [F-] = 0.0172\ mM$$

The Table C.30 shows the potential difference for each replicate of each strain and the values obtained in the calculation of free fluoride after 8 days from the beginning of the assay (T8).

Table C.30: Potential difference for each replicate of each assay (consortium resistance and non-biological degradation), the values obtained in the calculation of free fluoride and % of fluorination for the moment (T8).

	E (mV)	Log mM	mM [F-]	[F-]Free	% Def	Med
AB (1)	-282.5	-1.9679	0.0108	-0.0065	-88.1872	-76.03
AB (2)	-278.8	-2.0289	0.0094	-0.0047	-63.8674	
M (1)	-258	-2.3721	0.0042	-0.0053	-72.0033	-63.01
M (2)	-249.9	-2.5057	0.0031	-0.0040	-54.0255	

Below is an example of the calculation performed for the determination of free [F-], percentage of defluorination and the average of the replicates at T8 (since the start of the assay) for the assay AB (1).

$$Log_{10}[F-] = \frac{\left(-282.5 - (-401.78)\right)}{-60.613} \Leftrightarrow [F-] = 10^{-1.9679} \Leftrightarrow [F-] = 0.0108\, mM$$

$$[F-]\, Free = 0.0108 - 0.0172 = -0.0065\, mM$$

Determination of the theoretical [F$^-$] concentration if there was complete defluorination.

Massa Molar ($C_{20}H_{19}F_3N_2O_4$) = 408.37 mg/L ---------- 1 mM

1 mg/L ---------- x mM

Since the stoichiometry of the molecule is 1:3, then the concentration of free fluorides will be 3 times higher.

$$x = \frac{1 * 1}{408.37} = 0.002449\, mM$$

$$0.002449 * 3 = 0.00734\, mM$$

$$\%\, Def = \frac{-0.0065}{0.00734} * 100 = -88.19\,\%$$

$$Med = \frac{-88.19 + (-63.87)}{2} = -76.03\,\%$$

The Table C.31 shows the potential difference for each replicate of each strain and the values obtained in the calculation of free fluoride after 14 days from the beginning of the assay (T14).

Table C.31: Potential difference for each replicate of each assay (consortium resistance and non-biological degradation), the values obtained in the calculation of free fluoride and % of fluorination for the moment (T14).

	E (mV)	Log mM	mM [F-]	[F-]Free	% Def	Med
AB (1)	-274	-2.1081	0.0078	-0.0094	-128.6332	-114
AB (2)	-270.2	-2.1708	0.0067	-0.0073	-99.3594	
M (1)	-256.7	-2.3935	0.0040	-0.0055	-74.7878	-65.58
M (2)	-248.4	-2.5305	0.0029	-0.0041	-56.3785	

The Table C.32 shows the potential difference for each replicate of each strain and the values obtained in the calculation of free fluoride after 21 days from the beginning of the assay (T21).

Table C.32: Potential difference for each replicate of each assay (consortium resistance and non-biological degradation), the values obtained in the calculation of free fluoride and % of fluorination for the moment (T21).

	E (mV)	Log mM	mM [F-]	[F-]Free	% Def	Med
AB (1)	-269	-2.1906	0.0064	-0.0108	-146.9914	-126.37
AB (2)	-268.3	-2.2022	0.0063	-0.0078	-105.7558	
M (1)	-252.5	-2.4628	0.0034	-0.0061	-82.8993	-69.49
M (2)	-248.6	-2.5272	0.0030	-0.0041	-56.0725	

Next, in the Table C.33 the OD values of the two assays after 8, 14 and 21 days will be presented.

Table C.33: OD values for the assay of consortium resistance and non-biological degradation after 8, 14 and 21 days.

	8 days	14 days	21 days
AB (1)	0	0	0
AB (2)	0	0	0
M (1)	0,45	0,405	0,448
M (2)	0,424	0,404	0,397